



TECHNISCHE
UNIVERSITÄT
WIEN
Vienna University of Technology

Dissertation

Advanced analytical approaches to characterize ion mobility and structural changes in polyimides

carried out for the purpose of obtaining the degree of
Doctor of Technical Sciences (Dr. techn.)

at

Technische Universität Wien
Faculty of Technical Chemistry

under the supervision of

Univ.Prof. Dipl.-Ing. Dr. techn. Andreas Limbeck

and

Dipl.-Ing. Dr. techn. Patrick Knaack

defended by

DI Birgit Achleitner

Mat.Nr.: 0926519

Wien, August 2024

Abstract

High-performance polymers are usually indicated by their extraordinary material properties like high heat and oxidative resistance, chemical inertness, high dimensional stability and corrosion resistance. Because of their ability to maintain their mechanical and physical properties over a wide temperature range, they are widely used in applications that involve high temperature and extreme environment. Polyimides are one important class of high-performance polymers, characterized by an imide group as a building block of the polymer backbone. Since they can be processed as films, fibers, porous membranes, etc. they have found extensive implementations in the automotive, aerospace and electronics industry. Due to their low dielectric constant and very good electrical insulation properties, they are particularly interesting for electronics and electrical engineering applications and are extensively used as isolation and protective medium. Their purpose is to ensure reliable operation under harsh conditions, for instance in the presence of high temperatures, humidity or corrosive gases. To prevent device failure and improve the reliability of microelectronic devices, two interdependent questions regarding the use of polyimides arise: (1) the uptake and diffusion behaviour of corrosive species within polymers, especially polyimides are of great interest and (2) techniques to obtain structural information about the polymer and monitor alterations both laterally- and depth-resolved are needed for thorough investigations.

In this work, we aimed to implement LIBS (Laser induced breakdown spectroscopy) and LA-ICP-MS (Laser ablation inductively coupled plasma mass spectrometry) based measurement protocols to investigate the migration pattern of harmful substances like Cl and K while gaining information about the polymer structure. Especially the usage of LIBS for polymer analysis could be a promising strategy to perform elemental as well as structural analysis since characteristic regions in the LIBS spectrum can be used to gain molecular information.

In order to keep the system as simple as possible and limit the number of influencing parameters, industry relevant polyimides were synthesized and used as a model substance. First, the capabilities of LIBS to monitor possible structural alterations were tested and the imidization reaction was chosen as an illustrative example. This reaction is especially important because the shaping of polyimides is typically done using a soluble precursor which is cyclodehydrated in a thermal or chemical process called imidiza-

tion. The degree of imidization is one parameter, in general obtained by IR (infrared) spectroscopy representing the conversion of the amic acid group into the imide and it is closely related to the final properties of the polymer. Using LIBS, the determination of the imidization degree as a bulk parameter was successfully implemented and similar results compared to IR spectroscopy were obtained. Additionally, depth resolved polymerization studies of layered polymer structures were conducted enabling a deeper insight into the reaction process and the optimization of curing parameters during production. Furthermore, the robustness of the procedure was demonstrated in the presence of additives and by analyzing industry-relevant polymer samples. Subsequently, the investigations were continued using an in-situ measurement setup to study the reaction process within polymer thin films in more detail. With this approach, sample preparation time was minimized and the reaction progress could be tracked continuously on the same sample. Furthermore, the implemented LIBS method was transferred to other instrumental setups to ensure independence from hardware conditions like the laser wavelength.

In order to investigate failure mechanisms, the uptake and distribution of harmful substances is equally important as changes in polymer structure. Determining the degree of imidization based on LIBS was an important step in this direction. Subsequently, the methodology was optimized and applied in order to quantify the chlorine (Cl) and potassium (K) uptake in polyimides as examples for corrosion-inducing substances in an electronic device. Therefore, commercially available polyimide films were exposed to various aqueous solutions and voltage in a migration cell to simulate environmental stress testing. Especially halogens, such as chlorine pose a challenge in elemental analysis. As a result, different approaches to obtain maximum sensitivity were employed: (1) by reducing the ambient pressure during LIBS measurements and (2) by implementing a LA-ICP-MS measurement protocol. Both imaging and depth-profiling experiments of Cl and K distribution profiles within the stressed polyimide samples were conducted and revealed an even distribution of both elements over the sampled area. The penetration profiles were dependent on the exposure conditions and Cl uptake only occurred after a certain time period. Compared to the initial LIBS experiments, where a limit of detection (LOD) of 0.71 m% was calculated for Cl, a clear improvement in sensitivity (LOD = 0.015 m%) and depth resolution (approx. 200 nm) was achieved by implementing a LA-ICP-MS method although imaging experiments were not feasible due to severe problems regarding the sample transport. As an alternative, LIBS measurements under reduced pressure still enabled imaging while obtaining an LOD of 0.12 m% for Cl.

In combination, the newly developed analytical approaches using LIBS and LA-ICP-MS proved to be a powerful toolbox to investigate migration patterns and track the imidization reaction within a high-performance polymer.

Kurzfassung

Hochleistungspolymere zeichnen sich in der Regel durch ihre außergewöhnlichen Materialeigenschaften wie hohe Wärme- und Oxidationsbeständigkeit, chemische Inertheit, hohe Dimensionsstabilität und Korrosionsbeständigkeit aus. Da sie in der Lage sind, ihre mechanischen und physikalischen Eigenschaften über einen weiten Temperaturbereich beizubehalten, werden sie häufig in Anwendungen eingesetzt, die hohe Temperaturen und extreme Umweltbedingungen erfordern. Polyimide sind eine wichtige Klasse von Hochleistungspolymeren, die sich durch eine Imidgruppe in der Polymerkette auszeichnen. Da sie als Folien, Fasern, poröse Membranen usw. verarbeitet werden können, haben sie in der Automobil-, Luft- und Raumfahrt- sowie in der Elektronikindustrie breite Anwendung gefunden. Aufgrund ihrer niedrigen Dielektrizitätskonstante und ihrer sehr guten elektrischen Isolationseigenschaften sind sie für Anwendungen in der Elektronik und Elektrotechnik besonders interessant und werden in großem Umfang als Isolier- und Schutzfilme eingesetzt. Ihre Aufgabe ist es einen zuverlässigen Betrieb auch unter harschen Bedingungen zu gewährleisten, beispielsweise bei hohen Temperaturen oder dem Vorhandensein von Feuchte und/oder korrosiven Gasen. Um Korrosion zu verhindern und die Zuverlässigkeit von mikroelektronischen Geräten zu verbessern, ergeben sich in Bezug auf die Verwendung von Polyimiden zwei voneinander abhängige Fragestellungen: (1) die Aufnahme und das Diffusionsverhalten von korrosiven Spezies innerhalb von Polymeren, insbesondere Polyimiden, sind von großem Interesse und (2) Untersuchungsmethoden zur lateral aufgelösten Bestimmung von Polymerveränderungen sind erforderlich, insbesondere über die gesamte Dicke der aufgetragenen Schutzfilme.

Das Ziel dieser Arbeit war es, LIBS (Laserinduzierte Plasmaspektroskopie) und LA-ICP-MS (Laser Ablation Massenspektrometrie mit induktiv gekoppeltem Plasma) basierte Messprotokolle zu implementieren, um einerseits das Migrationsverhalten von schädlichen Substanzen wie Chlor (Cl) und Kalium (K) innerhalb eines Polymerfilms zu untersuchen und gleichzeitig Informationen über Veränderungen in der Polyimidstruktur zu gewinnen. Besonders der Einsatz von LIBS für die Polymeranalyse könnte eine vielversprechende Strategie sein, um sowohl elementare als auch strukturelle Analysen durchzuführen, denn charakteristische Bereiche im LIBS Spektrum können genutzt

werden, um molekulare Informationen zu gewinnen.

Um das zu untersuchende System so einfach wie möglich zu halten und die Anzahl der Einflussparameter zu begrenzen, wurden industrienaher Polyimide im Labor synthetisiert und als Modellsystem für die Methodenentwicklung verwendet. Die Imidierungsreaktion wurde als illustratives Beispiel ausgewählt um das Potential von LIBS zur Analyse struktureller Veränderungen im Polyimid zu testen. Diese Reaktion ist von besonderem Interesse, da die Formgebung von Polyimiden typischerweise unter Verwendung eines löslichen Vorproduktes erfolgt, welches in einem thermischen oder chemischen Prozess namens Imidierung cyclodehydriert wird. Der Grad der Imidierung ist ein Parameter, der im Allgemeinen durch IR (Infrarot) -Spektroskopie ermittelt wird und die prozentuelle Umwandlung des Vorproduktes in das Imid darstellt. Dieser Wert ist außerdem eng mit den finalen Eigenschaften des Polymers verbunden. Mit der Implementierung von LIBS waren neben der Bestimmung des Imidierungsgrades als Summenparameter auch tiefenaufgelöste Polymerisationsstudien von geschichteten Polymerstrukturen erfolgreich möglich. Zudem wurde die Robustheit des Verfahrens in Anwesenheit von Additiven und durch die Untersuchung von kommerziellen Polymerproben demonstriert.

Anschließend wurden die Untersuchungen mit einem in-situ-Messaufbau fortgesetzt, um den Reaktionsprozess innerhalb dünner Polymerfilme genauer zu untersuchen. Mit diesem Ansatz wurde die Probenvorbereitungszeit minimiert und zeitabhängige Imidierungsstudien konnten kontinuierlich an derselben Probe durchgeführt werden.

Des Weiteren wurde die neu entwickelte LIBS-Methode auf andere Geräte übertragen, um die Unabhängigkeit von Hardware-Bedingungen wie der Laserwellenlänge zu gewährleisten.

Um bestimmte Fehlermechanismen zu untersuchen, sind neben Informationen zur Polymerstruktur auch Untersuchungen über die Aufnahme und Verteilung schädlicher Substanzen notwendig. Die Bestimmung des Imidierungsgrades mittels LIBS war ein wichtiger Schritt in diese Richtung. Deshalb wurde die Methode zusätzlich zur Quantifizierung von Chlor (Cl) und Kalium (K) in Polymeren als wichtige Beispiele für korrosionsauslösende Substanzen in der Elektronikindustrie optimiert.

Für diese Untersuchungen wurden handelsübliche Polyimidfilme, die verschiedenen wässrigen Lösungen und Spannungen in einem Migrationsexperiment ausgesetzt waren, verwendet, um Migrationsprofile und laterale Verteilungen für K und Cl zu untersuchen. Besonders Halogene wie Chlor stellen eine Herausforderung in der Elementaranalyse dar, weshalb mehrere Ansätze zur Erzielung maximaler Empfindlichkeit verfolgt wurden: (1) durch Reduktion des Umgebungsdrucks während der LIBS-Messungen und (2) durch Implementierung eines LA-ICP-MS-Messprotokolls als Alternativverfahren.

Mit Hilfe von Imaging Experimenten wurde eine gleichmäßige Verteilung der beiden Analyten K und Cl auf der beprobten Fläche des Polymers deutlich. Anders die Verteilung über den Filmquerschnitt: hier war das Migrationsprofil von den experimentellen Parametern des Migrationstests abhängig und besonders Cl wurde erst nach einer bestimmten Versuchsdauer aufgenommen. Im Vergleich zu den ursprünglichen LIBS Messungen mit einer Nachweisgrenze von 0.71 m% Cl konnte die Sensitivität (LOD = 0.015 m%) und Tiefenauflösung (200 nm) durch die Entwicklung einer LA-ICP-MS Methode deutlich verbessert werden. Aufgrund des Auswaschverhaltens der Probe waren allerdings keine Imaging Experimente mehr möglich. Eine Alternative dazu, stellten LIBS Messungen unter verringertem Druck dar: mit einem nach wie vor verbesserten LOD von 0.12 m% für Cl war auch Imaging der gestressten Polymerfilme erfolgreich durchführbar.

Somit konnte in dieser Arbeit gezeigt werden, dass sowohl die Aufnahme und Verteilung schädlicher Substanzen als auch strukturelle Veränderungen von Polymiden mittels LIBS und/oder LA-ICP-MS zugänglich sind. Die neu entwickelten analytischen Ansätze stellen somit ein leistungsstarkes Werkzeug zur Untersuchung von Migrationsmustern und zur Verfolgung des Imidisierungsgrades in einem Hochleistungspolymer dar.

Acknowledgements

First, I would like to thank my academic supervisor, Andreas Limbeck who paved the way back to university for me. I highly appreciate all the helpful discussions, his technical expertise and detailed feedback which contributed to this work.

Sincere appreciation goes to Patrick Knaack as my co-supervisor, who was immensely helpful in all polymer and synthesis related topics.

I would also thank Pavel Pořízka and Herbert Hutter for providing the written assessment of my doctoral thesis.

My deepest gratitude goes to Silvia Larisegger as the FFG project leader for providing the main link between TU Wien and Infineon. Besides enabling a successful collaboration, I am much obliged for the friendly atmosphere and her tireless support and commitment. Special thanks go to everybody at KAI and Infineon who contributed to my work, taking interest in our monthly telephone conference and providing technical release for each conference contribution and publication.

Further I would like to thank my colleagues and project mates who made this time truly special. It was a pleasure working with you and we became a great team, always offering support and more importantly times to relax and laugh together. I especially enjoyed all of our company trips and conference stays. They not only brought us closer as a group, but are a reservoir of funny stories, interesting encounters and new experiences.

Last but not least, I would like to thank my family and friends, who support me in all my endeavors and truly make me feel at home.

Contents

Abstract	iii
Kurzfassung	v
Acknowledgements	ix
Abbreviations	xiii
1 Introduction	1
2 Goals and analytical challenges	5
3 Fundamentals	7
3.1 Polyimides - a class of high-performance polymers	7
3.1.1 Properties of polyimides	8
3.1.2 Synthesis and characterization of polyimides	10
3.2 Polyimides as protective layers	13
4 Methodological Background	15
4.1 Basic principles of LIBS	15
4.1.1 Fundamentals	16
4.1.2 Instrumentation	17
4.1.3 LIBS analysis of polymers	18
4.1.4 Introduction to Chemometrics	19
4.2 Basic principles of LA-ICP-MS	21
4.2.1 Fundamentals	22
4.2.2 Instrumentation	23
5 Experimental Details	25
5.1 Reagents	25
5.2 Synthesis and characterization of sample polyimides	26
5.2.1 Thermal behaviour	28
5.2.2 Determination of the polymer chain length	29

5.3	Migration cell experiments	29
5.3.1	Introduction to the measurement setup	30
5.3.2	Sample list	31
5.3.3	Preparation of in-house calibration standards	31
5.4	Instrumental setup	32
5.4.1	Laser assisted material analysis	33
5.4.2	Polymer characterization	37
6	Monitoring the imidization reaction of polyimides using LIBS	39
6.1	Method development	40
6.1.1	Sample preparation	40
6.1.2	IR as a reference method	42
6.1.3	LIBS method development	45
6.1.4	Comparison of both techniques	50
6.2	Application examples	52
6.2.1	Imaging and depth-profiling of artificial samples	52
6.2.2	Investigation of industry samples	55
6.3	In-situ monitoring of the imidization reaction	59
6.4	Transferability of the proposed LIBS method	62
7	Polymer films exposed to migration cell experiments	65
7.1	LIBS investigations of exposed polymer films	65
7.1.1	J200	66
7.1.2	imageGEO193	68
7.2	Increasing sensitivity to detect ion migration	74
7.2.1	Depth-profiling using LA-ICP-MS	75
7.2.2	LIBS under reduced pressure	78
7.3	Detection of polymer alterations	83
8	Summary and Outlook	87
	Bibliography	91
	Curriculum Vitae	99
	Dissemination	101

Abbreviations

6FDA	4,4'-(Hexafluoroisopropylidene) diphthalic anhydride
6FDAM	2,2-Bis(4-aminophenyl)hexafluoropropane
ANN	artificial neural networks
ATR	attenuated total reflexion
BPDA	3,3',4,4'-biphenyltetracarboxylic dianhydride
BTDA	3,3', 4,4'-benzophenonetetracarboxylic dianhydride
CA	contact angle
CCD	charge coupled device
CMOS	complementary metal oxide semiconductor
DCI	dual concentric injector
DLS	dynamic light scattering
DMAc	N,N-dimethylacetamide
DMF	N,N-dimethylformamide
DMSO	dimethyl sulfoxide
DSC	dynamic scanning calorimetry
FT-IR	Fourier transform infrared
GPC	gel permeation chromatography
HDPE	high density polyethylene
HPP	high performance polymer
ICCD	intensified charge-coupled device
ICP	inductively coupled plasma
ICP-MS	inductively coupled plasma mass spectrometry
ID	degree of imidization
IR	infrared
k-NN	k-nearest neighbors
KCl	potassium chloride
KED	kinetic energy discrimination
LA	laser ablation
LA-ICP-MS	laser ablation ICP-MS
LDA	linear discriminant analysis
LDPE	low density polyethylene

LIBS	laser induced breakdown spectroscopy
LOD	limit of detection
MPD	m-phenylene diamine
M/Z	mass-to-charge-ratio
NaCl	sodium chloride
Nd:YAG	Neodymium-doped yttrium aluminium garnet (Nd:Y ₃ Al ₅ O ₁₂)
NMP	N-methyl-2-pyrrolidon
NMR	nuclear magnetic resonance
ODA	4,4'-oxy-dianiline
OPA	3,3',4,4'-oxydiphthalic anhydride
PAA	poly(amic acid)
PBA	polybutylacrylate
PC	principal component
PCA	principal component analysis
PEI	polyetherimide
PI	polyimide
PLS-DA	partial least squares discriminant analysis
PMDA	pyromellitic dianhydride
PMMA	polymethylmethacrylate
POM	polyoxymethylene
PP	polypropylene
PPD	p-phenylene diamine
PS	polystyrene
PSU	polysulfone
PVC	polyvinylchloride
RF	random forest
S/N	signal-to-noise-ratio
SIMCA	soft independent modelling of class analogy
SVM	support vector machines
T-MDSC	temperature modulated DSC
T _d	thermal decomposition temperature
T _g	glass transition temperature
TGA	thermogravimetric analysis
TOF	time-of-flight
UHMW PE	ultra high molecular weight polyethylene
UV	ultraviolet
XPS	X-ray photoelectron spectroscopy
XRD	X-ray diffraction

1 Introduction

In our modern world, polymers and polymer composites have become one of the most widely used materials with applications in many different fields from packaging, construction, automotive as well as household and agriculture. [1] The wide variety of materials in use can be classified according to their chemical structure or their thermal behavior (e.g. thermoplastics, thermosets and elastomers). According to their temperature resistance as well as chemical and mechanical stability, they can also be divided into standard (commodity), engineering or high performance polymers (HPP). In contrast to commodity or engineering polymers, HPP are characterized by superior material properties like high heat and oxidative resistance, chemical inertness and high dimensional stability. Because they can withstand extremely harsh conditions like corrosive environments, high temperature and pressure conditions while maintaining their mechanical and physical properties, they play an important role in the automotive, electric and electronic industry as well as in aerospace, industrial and medical applications. Figure 1.1 presents a classification of polymers according to their temperature, chemical and mechanical stability. [2]

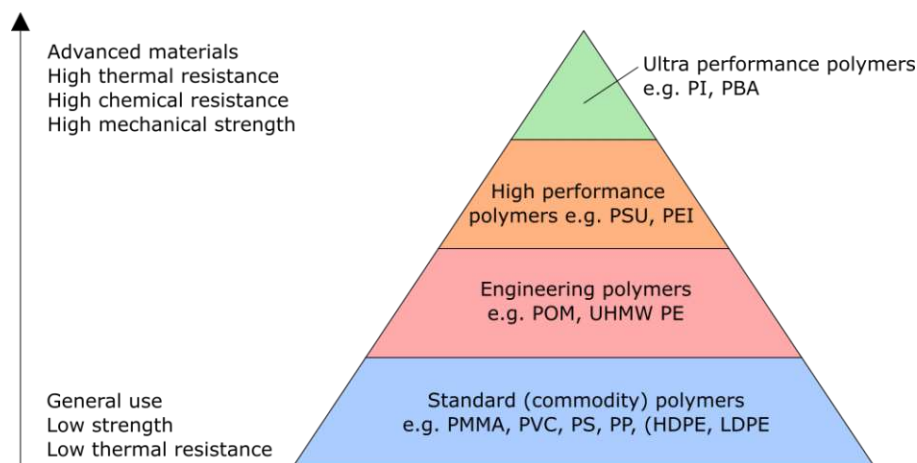


Figure 1.1: Classification of polymer materials according to their chemical and physical characteristics [2]

Polyimides are one important class of high-performance polymers. They exhibit an exceptional combination of properties: thermal stability $> 500\text{ }^{\circ}\text{C}$, mechanical toughness, chemical resistance against solvents and moisture and low dielectric constant. They are usually fabricated from diamines and dianhydrides, which form an imide bond in the polymers backbone (see figure 1.2). Nowadays a huge variety of monomers has been used to synthesize polyimides, tailoring the materials properties to the respective area of application. Because they can be processed as film, fibers and fiber composites, porous membranes, etc., polyimides have found extensive application in most high-tech fields from sensors, membranes, electronic displays, optoelectronic devices, batteries, anticorrosion coatings for steel as well as biomedical applications. [3–7]

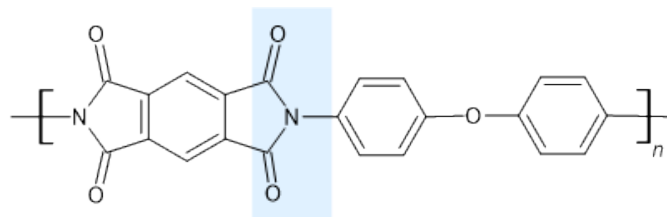


Figure 1.2: Structure of Kapton[®], a common polyimide used in industry applications with the characteristic imide bond highlighted in blue

The production of polyimides was pioneered by workers at DuPontTM in the 1950ies by implementing a two-step process which is still in use today: first, a soluble precursor is synthesized called the poly (amic)acid which can still be processed and molded into the desired shape. Afterwards the precursor is thermally or chemically cured and the imide bond forms. This reaction, which is called imidization stiffens the polymer backbone considerably, leading to a thermo-oxidatively stable, linear polymer with a high glass transition temperature (T_g). [8–12]

Due to their outstanding characteristics, polyimides have been increasingly used by the electronics industry in the form of thin films, coatings or encapsulation materials. Electronic devices are very complex systems, consisting of a variety of different materials. They have to meet many requirements since the environments where they are used vary and can be quite extreme due to high voltages, temperature fluctuations and high humidity. Therefore, a multitude of different reactions and processes may occur in the device. The purpose of the polyimide in this applications is to protect the underlying material or components from the environment, preventing corrosion and supporting structural integrity. [13]

Considering the rapid development of many high-tech fields and materials, especially

in the electronics industry, each step in the production process requires methods and tools for chemical analysis. Further, it is necessary to assess material behavior during its use, ageing and degradation to guarantee reliability during the entire lifetime of the product. To satisfy all the mentioned aspects around polymers or polymer-containing products, there is already a wide variety of polymer characterisation techniques available in modern analytical chemistry. Although many methods are routinely applied in an industrial applications, modern analysis development is needed for up-to-date characterization and production processes, especially to assess specific information for dedicated sample types and scenarios.

In the case of polyimides used in the electronics industry this involves new methods to ensure constant material properties, accompany material processing and test or investigate material failure.

Furthermore, spatially resolved analysis methods are particularly interesting because polyimide is often used as a protective coating. Therefore, local information over the entire thickness of the layer is relevant and techniques with depth-profiling capabilities are needed. Ideally, this technique would provide information about structural changes within the polymer, due to deviations during the manufacturing process or ageing as well as the distribution of harmful substances leading to corrosion facilitating multi-element investigations.

2 Goals and analytical challenges

The aim of this work was to develop analytical techniques to support material processing in the electronics industry as well as investigate and understand certain failure mechanisms within an electronic device. Special attention was given to the role of the polyimide thin film, which often acts as a protective layer within these devices. Understanding the role of polyimide in case of a defect requires not only information about its structure but also about the presence and movement of harmful substances, often metals or salts in the form of ions. The migration of harmful substances might also be spatially concentrated, making spatial resolved analysis an important feature. For polyimide thin films, which are usually several micrometers thick, depth-profiling over the entire thickness of the film is particularly interesting.

In order to investigate certain failure mechanisms and the contribution of the polyimide film, a special migration cell setup was developed in a previous project and used for serial examination of polymer films. [14,15] Therefore, a particular challenge was to establish analytical techniques to investigate these special samples in the simplest and fastest way possible.

LIBS (Laser induced breakdown spectroscopy) is a prominent technique for elemental analysis, exhibiting mapping and depth-profiling capabilities. Additionally, specific parts of the LIBS spectrum can be used to obtain molecular information about organic substances. Therefore, LIBS has the potential to become a viable tool in quality assurance or failure analysis of polyimide samples. To satisfy the requirements for a comprehensive polyimide analysis regarding structural changes in combination with the migration of harmful substances, the two tasks were initially considered separately:

- **Monitoring of the reaction process of polyimides using LIBS:** LIBS has been successfully applied for polymer analysis [16–19], especially for the discrimination and classification of polymers and to detect polymer degradation [20–25]. For this task, the capabilities of LIBS to monitor possible structural changes within a polyimide network had to be tested anew and a method to quantify changes had to be implemented.

Changes in the polyimide structure might occur both during thermal curing and

in subsequent production steps (e.g. surface treatment) or due to ageing. Since the production of polyimides takes place in a two-step process and the imidization is done during the manufacturing process of an electronic device, this reaction was used as a representative example. Also, the imidization reaction is reversible, which would also open up the possibility of detecting degradation due to hydrolysis. Therefore, the scope was to implement a LIBS method to determine the degree of imidization, which describes the percent conversion of the amic acid group into the imide bond. Traditionally, this is done using IR spectroscopy but using LIBS, also depth-resolved analysis would be possible. Therefore, a new LIBS measuring method had to be developed and tested.

- **Investigation of ion migration within polyimide films:** The uptake and migration of harmful substances throughout the polyimide barrier, especially chlorine containing salts poses a substantial risk for the lifetime of electronic devices. Therefore, the localization and quantification of harmful substances is essential for failure analysis. LIBS is a multi-element measurement method, but some of the elements in question, such as chlorine, pose substantial difficulties due to their weak transition probability in the LIBS spectral range from 200 - 900 nm. Analyzing the stronger chlorine emission in the ultraviolet (UV) would require a vacuum setup and a UV sensitive spectrometer. Therefore, detection limits are rather high and are situated in the promille (mg/g) range [26–28]. Thus, it is necessary to optimize the measurement method in terms of sensitivity, potentially by changing the measurement atmosphere. Alternatively, a different detection method could be considered: LA-ICP-MS inherently has lower detection limits as LIBS and both methods could be used simultaneously. However, using ICP-MS the elements in question, chlorine and potassium, suffer from polyatomic interferences, and in the case of chlorine, a high ionization energy is required. Therefore, comprehensive method development is necessary as well.

By combining the findings from both questions, a thorough investigation of polyimide films based on laser assisted methods like LIBS and LA-ICP-MS should be possible. However, in the case of commercial polymer films, it is possible that the effectiveness of LIBS or LA-ICP-MS may not be sufficient to investigate potential failure mechanisms. In such cases, alternative analytical techniques, especially in the field of polymer analysis, should be tested to complete the picture.

3 Fundamentals

In this chapter, the fundamental aspects concerning polyimides including the most important characteristics for their application in the electronics industry are presented. This also includes a short summary of prominent monomers and an overview of synthesis and characterisation strategies. Finally, a short introduction to the usage of polyimides as protective layers in an electronic device is given emphasising aspects of reliability and failure mechanisms.

3.1 Polyimides - a class of high-performance polymers

Polyimides are a type of high performance polymer, characterized by an imide group as a building block of the polymer backbone. They are usually formed from diamines or diisocyanates and dianhydride. Depending on the starting material they are further divided into aromatic, semi-aromatic and aliphatic polyimides. [3,29] The first synthesis of polyimides was reported in 1908 by Bogert and Renshaw [30] but the production was pioneered by workers at DuPontTM in the 1950ies [8–12]. Since then, a huge variety of polyimides synthesized from a number of different monomers has been produced. Because the field has developed so broadly, polyimides can cover an extremely broad property range, e.g. from extremely temperature stable ($T_g > 300$ °C) to melt-processible. Therefore, this chapter will focus on the properties and synthesis of aromatic polyimides. A short outline of frequently used monomers for the synthesis of aromatic polyimides is shown in figure 3.1 [29].

Due to their chemical structure, consisting of a rigid imide and aromatic rings, polyimides are known for their excellent mechanical characteristics, high chemical resistance and low dielectric constant. They have found extensive use in most high-tech fields including automotive, aerospace and electronic applications. [4,6,7] Hence, the characteristics and manufacturing process are explained in detail in the following sections.

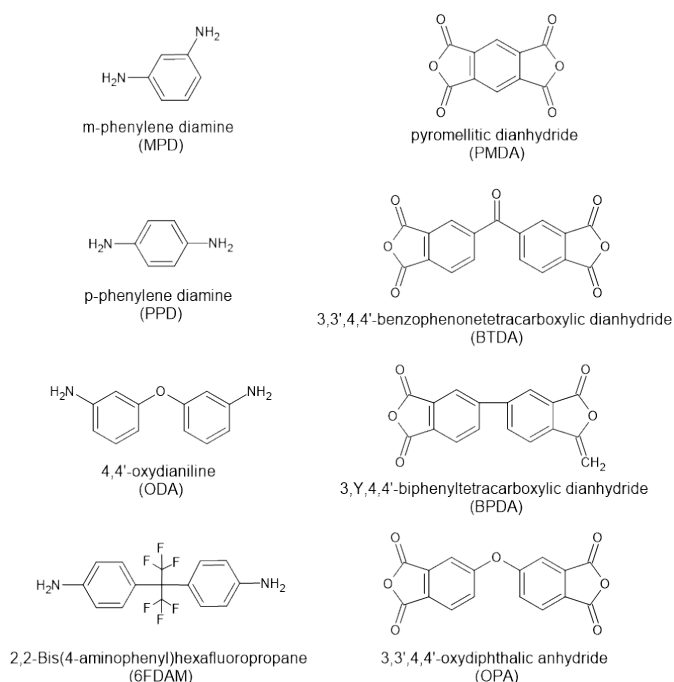


Figure 3.1: Frequently used diamines and dianhydrides for industrial polyimides

3.1.1 Properties of polyimides

Important properties of polyimides, especially for the electronics industry are thermal stability and water sorption.

Thermal stability

High-temperature applications are an important area of use for polyimides as modern PI thin films might reach a thermal decomposition temperature (T_d) of > 500 °C. [31,32] As a result, understanding the factors influencing thermal stability of polyimides is important and extensive research has been conducted in this area. Dynamic scanning calorimetry (DSC) and thermogravimetric analysis (TGA) were the most frequently used techniques to assess thermal and thermooxidative degradation. But also the analysis of compositional changes using mass spectrometry, particularly in combination with separation techniques, solid-state nuclear magnetic resonance (NMR) spectroscopy, X-ray photoelectron spectroscopy (XPS) or Fourier transform infrared (FT-IR) spectroscopy has been carried out. Besides the backbone structure of the polyimide, its secondary structure, density, chain packing, proximity of functional groups and other conformational aspects have to be considered when predicting thermal stability. [33,34]

Systematic investigations on the effect of monomer structure revealed, that polyimides based on 4,4'-(Hexafluoroisopropylidene) diphthalic anhydride (6FDA) as a dianhydride

led to the most heat-resistant derivatives mostly due to the fluorine substitution and non-rigid nature of the structure of the monomer. [33] But in general, the diamine structure seemed to have a greater effect on the thermals stability because it is presumably the site of greatest electron density and therefore a likely point of oxidation. As a result, electron-deficient diamines lead to more oxidatively stable polyimides than electron-rich diamines as illustrated in figure 3.2. [33,35,36]

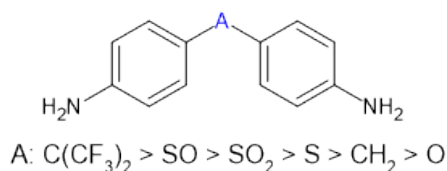


Figure 3.2: Stability trend of a series of dianilines [33,35,36]

However, certain structural attributes like charge transfer along the polymer backbone can influence stability contrary to this statement. Nevertheless, general trends which serve as a useful guideline for selecting monomer pairs have been established. [33,35–37] Nowadays, even high thermal resistance PI films with glass transition temperatures $T_g > 300$ even 400 °C and $T_d > 500$ °C have been fabricated by introducing heterocyclic rings into the polymer chain and/or the addition of nanocomposites. [32]

Water sorption

One drawback of polyimides, when used as protective layers is their ability to absorb up to 3.5 m% of water, which is significant for electronic, composite or adhesive applications. In general, low permeation of water vapor is required in these fields because the sorbed water may not only affect performance but also causes metal corrosion, adhesion failure and degradation of dielectric properties. [13,38] Although the structure of the polyimide backbone changes depending on the monomers used, there are specific sites that seem prone for water molecule binding (see figure 3.3). [39]

Since the correlation of water uptake and relative humidity is almost linear and increasing water uptake might enable ion diffusion and lead to corrosion phenomena, the factors influencing water absorption were thoroughly investigated in literature. To predict water absorption, polyimide specific characteristics like the density, the chemical affinity of the polymer backbone and chain flexibility need to be considered. For example, for polyimides synthesized from pyromellitic dianhydride (PMDA) or 3,3',4,4'-benzophenonetetracarboxylic dianhydride (BTDA) as dianhydrides and m-phenylene diamine (MPD) or 4,4'-oxy-dianiline (ODA) as diamines, the coefficients of water diffusion measured at 298.15 K and 308.15 K varied in the range of $1.566 \cdot 10^{-15}$ to 8.652

* $10^{-15} \text{ m}^2\text{s}^{-1}$ and were dependent on the T_g and the free volume of the synthesized polyimide. [38] Also, a reduction of the water uptake could be achieved by the usage of fluorine-containing groups in the polymer backbone decreasing the moisture absorption to 1-1.5 m%. However, the opposite effect was also reported when incorporating 6FDA: the water sorption was increased to 5.08 m% due to an amorphous structure and poor packing order. [13,40]

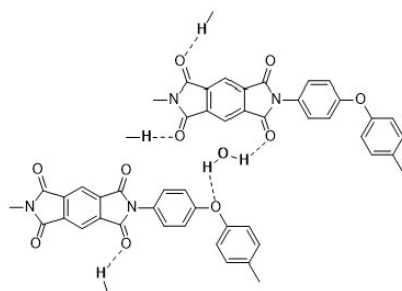


Figure 3.3: Water molecule binding sites in polyimides [39]

Similar to investigating the temperature resistance, predicting the water absorption of polyimides is not straightforward and many different features have to be considered.

3.1.2 Synthesis and characterization of polyimides

The first synthesis of an aromatic polyimide was carried out in 1908 [30], but it was not until the late 1950ies that commercial, high-molecular weight polyimides were synthesized. The procedure was pioneered by workers at DuPontTM and continues to be the most common method for their synthesis until this day. In the classic 2-step process, a dianhydride is added to a solution of diamine in a dipolar aprotic solvent, such as N,N-dimethylformamide (DMF), N-Methyl-2-pyrrolidone (NMP) or N,N-dimethylacetamide (DMAc) at ambient conditions. The generated poly (amic)acid is then cyclodehydrated in a thermal process or by treatment with chemical dehydrating agents. Because polyimides are generally non-soluble and will degrade at high temperatures, the polymer is usually processed in the form of the poly (amic)acid, which is then imidized in place. [8–12,41] A schematic drawing of the 2-step synthesis of an aromatic polyimide is shown in 3.4. High-molecular weight poly (amic)acids can be obtained from many different combinations of diamines and dianhydrides. The propagation reaction is reversible but dipolar aprotic solvents decrease the rate of the reverse reaction because of the formation of strong hydrogen bonds. It was also noted, that the highest molecular weight PAA were obtained by adding solid dianhydride to a diamine solution, therefore avoiding competing reactions of dianhydrides with water or impurities in the solvent. Additionally, the dissolution

of the dianhydride is slower than the rate of polymerisation, also contributing to a high-molecular weight product. The formation of PAA occurs rapidly and is favoured by low temperatures, typically between -20 and 70 °C. Despite its high molecular weight, PAA remains soluble and can be further processed in this form, e.g. by casting a film, forming a coating or spinning a fiber. [41]

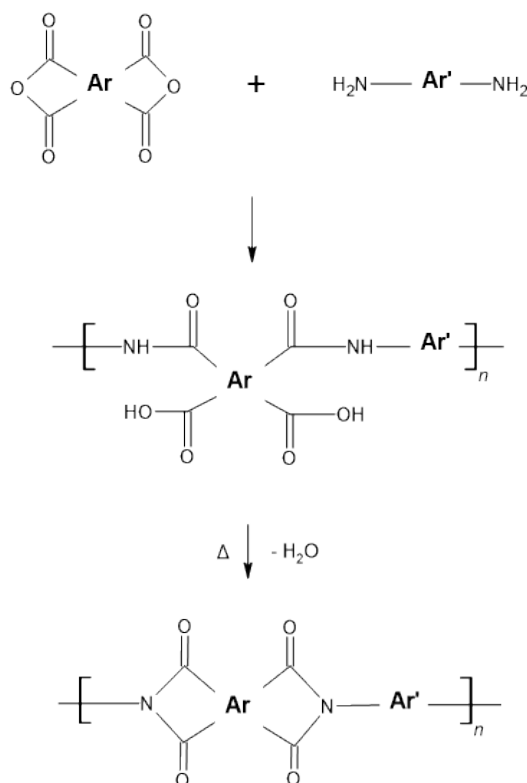


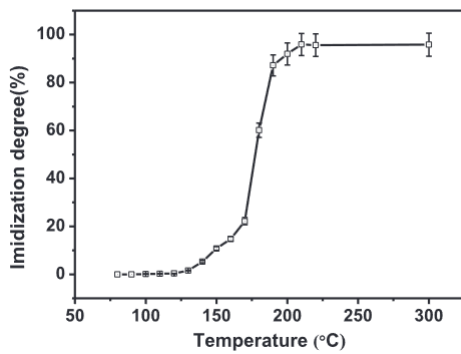
Figure 3.4: Schematic of a general reaction scheme of aromatic polyimides

The thermal process that converts the poly (amic)acid into the polyimide is called imidization. This usually involves a drying step, followed by either stepwise heating from 100 - 400 °C or an isothermal temperature program. Similar to the synthesis of the PAA, the thermal imidization is a complex step and the properties of the product depend on the drying temperature and rate as well as the imidization temperature and temperature program. [42–46]

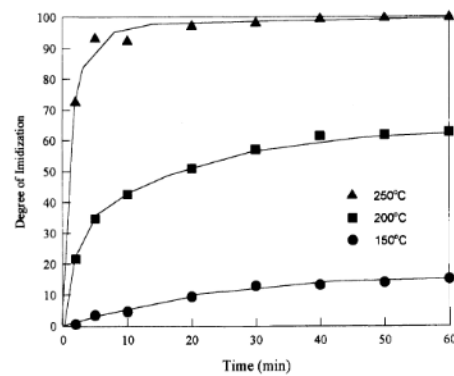
As a result, the curing of polyimides has been studied extensively in the last decades. FT-IR is a popular technique to monitor the reaction process and calculate the degree of imidization since it is a fast and simple analysis method. The degree of imidization describes the percent conversion of the amic acid group into imide. To calculate the degree of imidization based on IR spectroscopy, the ratio of the IR absorption intensity of a characteristic imide band and an internal standard corresponding to the

C=C stretching of benzene which does not change during imidization is formed. The calculation also assumes, that PI films are 100% imidized when the calculated ratio is constant at high processing temperatures. Therefore, the degree of imidization of PIs after different imidization procedures represents a relative value and the value might decrease or increase above the chosen maximum temperature due to polymer chain orientation. [42,47,48]

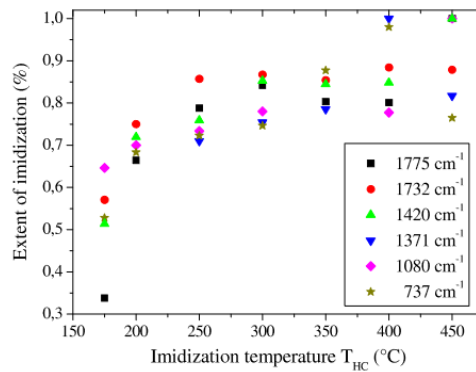
Signal trends for the degree of imidization based on different temperature programs and imide-based IR absorption bands are depicted in figure 3.5.



(a) Imidization degree of a polyimide based on PMDA-ODA as a function of the temperature [49]



(b) Degree of imidization of CBDA-BAPP after isothermal imidization [42]



(c) Degree of imidization calculated from different absorption bands for a BPDA-PDA polyimide [47]

Figure 3.5: Signal trends for the imidization degree based on literature

Besides FT-IR, DSC and TGA have been employed to study the thermal behavior during cyclization [44,50] and X-ray Diffraction (XRD) has been used to investigate the polymer chain orientation [43–45].

3.2 Polyimides as protective layers

Due to their outstanding material properties, polyimides are widely used in high-demanding applications like the automotive, aerospace or electronics industry. In these fields, the polymer properties like temperature stability, water sorption and others, must be thoroughly optimized and tested to fulfill the intended purpose. In the semiconductor industry, polyimides serve as coatings, insulation or encapsulation material and must ensure reliable operation under harsh conditions. If temperature, humidity or corrosive gases lead to changes in the material behavior, complete failure of the component or device might arise.

Electronic devices are made up of many layers of different materials and reliability can be tested in many ways. It is usually associated with a kind of environmental stressing to accelerate the time to failure. Highly accelerated stress testing (HAST) chambers are commercially available and commonly used in electronic packaging testing. [51] However, other, non-standardized setups can be used to investigate material behavior. Due to the complexity of material systems in electronic devices, simplified test structures can be used, e.g. containing of a protective polyimide coating on a semiconductor substrate.

One well-known phenomenon in the electronics industry is electrochemical migration, where ions migrate through a non-metallic medium driven by an electric field eventually leading to a short circuit in the device. [52] The most important factors in this case are contaminations, moisture, large temperature variations and applied voltage. Contaminations, which can derive from the surrounding materials, the manufacturing process and the operation environment will furthermore affect water sorption and conductivity of the water film. Even little amounts of chlorine containing salts originating from the manufacturing process or the environment (e.g. NaCl or KCl) can cause material alteration and device failure. [53] In order to investigate the uptake of harmful substances in more detail, an in-house built migration setup was implemented in previous projects and used for serial testing of polyimide films with a focus on the migration of Cl and K. (a detailed description of the setup is provided in chapter 5.3)

4 Methodological Background

Laser induced breakdown spectroscopy (LIBS) and Laser ablation - inductively coupled plasma - mass spectrometry (LA-ICP-MS) are two techniques to obtain the elemental composition of a solid sample. Both methods have in common, that a high-energy laser pulse is focused on the sample surface, leading to material ablation and the induction of a localized plasma. Within the plasma, the ablated material is partially atomized, ionized and excited, enabling LIBS experiments by collecting the emitted radiation. When the plasma cools down, the atomized sample material condensates and the formed aerosol can be transported to an ICP-MS instrument describing the basis principle of a LA-ICP-MS. [54–56]

Due to their unique characteristics like high sensitivity, wide elemental coverage, fast sample throughput and minimal sample preparation these methods are especially attractive for material characterization. Furthermore, both techniques offer the possibility of laterally resolved analysis. Since a small amount of material is removed during the laser impingement, also depth profiling is applicable. The combination of both procedures enables the examination of the sample composition (respectively the uptake of harmful substances or changes in homogeneity) over the entire geometry.

Therefore, LIBS as well as LA-ICP-MS were employed as the main tools within this work and will be described in more detail in the following sections. Besides the fundamental processes and instrumentation, strategies for data evaluation have become more and more important and will be discussed as well in chapter 4.1.4.

4.1 Basic principles of LIBS

Over the past decades, LIBS has become a widely known and powerful analytical method made possible by the invention of the laser in the 1960ies and the pioneering work of D.A. Kremers and L.J. Radziensky in the early 1980ies on the utilization of emission from a laser-induced plasma for chemical analysis. Since then, LIBS research and its analytical applications have been growing rapidly and numerous books and review papers have been published. [54, 55, 57–59]

For solid sample analysis, LIBS typically achieves detection limits in the ppm (mg/kg) range for alkaline and earth alkaline metals and the per mill range (mg/g) for non-metals.

With a dynamic range of around 3 orders of magnitude, also trace and minor components can be analyzed. In the context of this work, LIBS promised to be an interesting tool as it allows non-targeted analysis of a sample material. Since the whole emission spectrum is recorded during analysis it can be considered as an elemental fingerprint of a sample enabling identification and classification applications. Additionally, LIBS allows spatially resolved investigations and besides elemental analysis, characteristic regions of the LIBS spectrum can be used to gain molecular information which is particularly interesting for polymer studies.

4.1.1 Fundamentals

During the LIBS analysis of a solid sample, a high-energy laser pulse (up to 100 mJ) is focused on the sample surface. Due to the absorption of the photons, the temperature of the material in the focus spot rises rapidly, leading to the ejection of sample vapor, fragments and particles. Then the ongoing laser pulse further heats the ablated material turning it into a plasma where the constituents are thermally atomized, excited and ionized and radiation which is characteristic of its chemical components is emitted. Quantification of the sample material is possible since the intensity of the emission lines is related to the particular analyte concentration. As soon as the laser pulse ends, the plasma will cool down and expand into the surrounding medium initiating an outward facing shockwave contributing to a quick decay of the plasma. During the cooling and expansion of the plasma plume, condensation of the material leads to the formation of micro- and nanodroplets/particles which will partially fall back onto the sample surface where a small crater was left behind due to the laser-matter interaction. [54, 59]

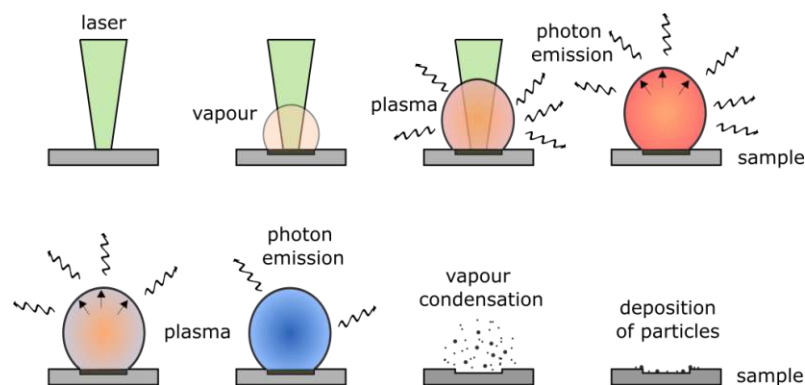


Figure 4.1: Schematic overview of the laser-matter interaction during a LIBS measurement

Due to the very short plasma lifetime, the delay and the width of the sampled emission spectrum has to be timed and optimized based on the analyte species (atoms, ions

or molecules) to be recorded. Early in the plasma lifetime, the emitted light mainly comes from excited ions and electrons in the form of continuous Bremsstrahlung. When the plasma cools down, the recombination of electrons and ions will produce excited atoms and the continuous background decreases. During this time window, elemental analysis with an ideal signal-to-noise ratio (S/N) can be performed. Later on, collision and recombination will generate excited molecules and molecular emission bands might be recorded. The time evolution of the described processes is illustrated in figure 4.2. Based on the LIBS instrumentation, especially the laser and the measurement conditions, the specified values on the time scale shift accordingly. [59]

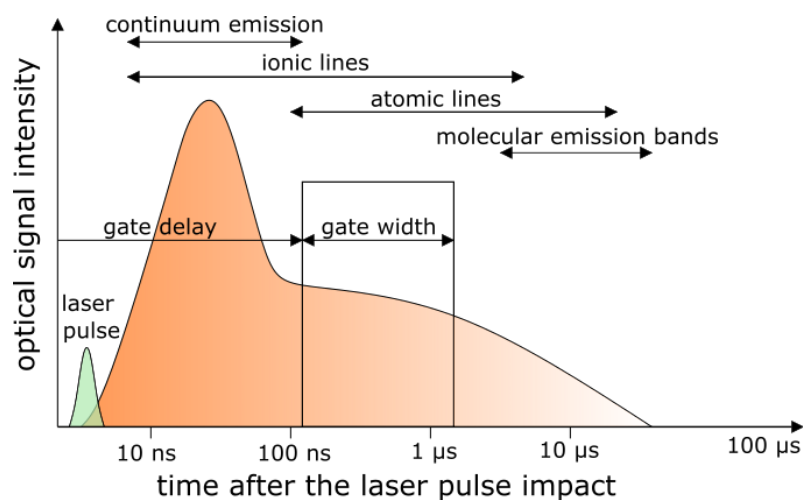


Figure 4.2: Time evolution of the light emission of a laser-induced plasma with a nanosecond laser pulse

4.1.2 Instrumentation

The main components necessary for a LIBS instrument are a pulsed laser for sample ablation and plasma ignition, an optical system to focus the laser onto the sample surface, a sample holder mounted on a xy-stage, optics to collect the emitted light and a spectrometer to provide the spectral analysis of the sampled emissions. A schematic of a LIBS instrument is provided in figure 4.3.

Laser sources with various wavelengths (from the near-IR to the UV) and femtosecond or nanosecond pulse durations are available for LIBS instruments and the type of laser source strongly influences the efficiency of the signal generation. In general, wavelengths from the visible to near-IR and ns-duration laser pulses are preferred for LIBS experiments due to higher pulse energy and plasma shielding effects which improve sensitivity. [59,60]

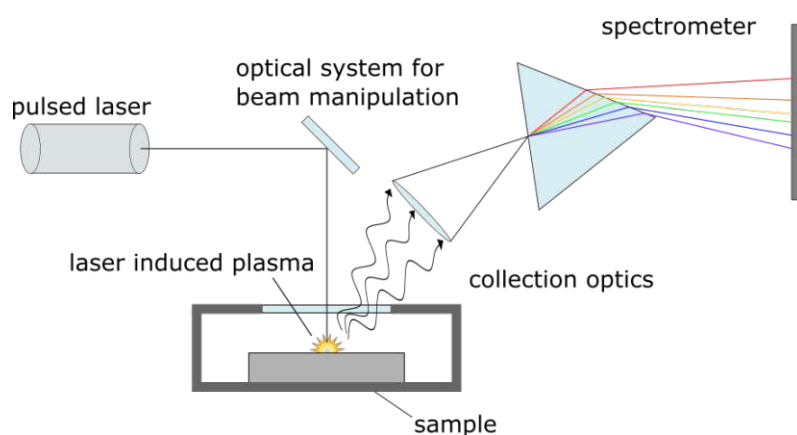


Figure 4.3: Schematic of LIBS instrument

The two main parts of the optical system of a LIBS instrument are used to guide and focus the laser beam onto the sample and to collect the emitted light from the laser induced plasma. The light collection optics direct a fraction of the emitted light to the spectrometer often via an optical fiber. Most common spectrometers in LIBS are equipped with charge-coupled device (CCD) or complementary metal-oxide semiconductor (CMOS) detectors. Broadband LIBS spectra can cover an adjustable wavelength range from the UV to the near-IR depending on the instrumental setup and spectrometers used, thus enabling simultaneous multi-element analysis. [59]

4.1.3 LIBS analysis of polymers

Although LIBS is considered to be an analytical tool to determine the elemental composition of a sample, it has been successfully used for polymer analysis [16–19], especially for discrimination and classification studies [20–23] as well as for the investigation of polymer degradation [24, 25]. LIBS spectra of polymers are dominated by the atomic emission of the main components, namely C, H, O and N but molecular information about the sample under investigation can be provided. The emission bands of molecular fragments, e.g. C_2 and CN, originate from either incomplete atomization or recombination processes in the laser-induced plasma. Figure 4.4 shows a representative LIBS spectrum of a polymer with all typical features.

Although similar elemental composition of different elements results in almost identical LIBS spectra, chemometric approaches have been developed to allow polymer discrimination and classification tasks from simply exploiting different elemental ratios to techniques like principal component analysis (PCA), random forest classifiers (RF) or artificial neural networks (ANN). Additionally, inorganic polymer additives, impurities and contaminations can be used for identification and classification as the whole emission

spectrum is recorded during analysis. [17,61]

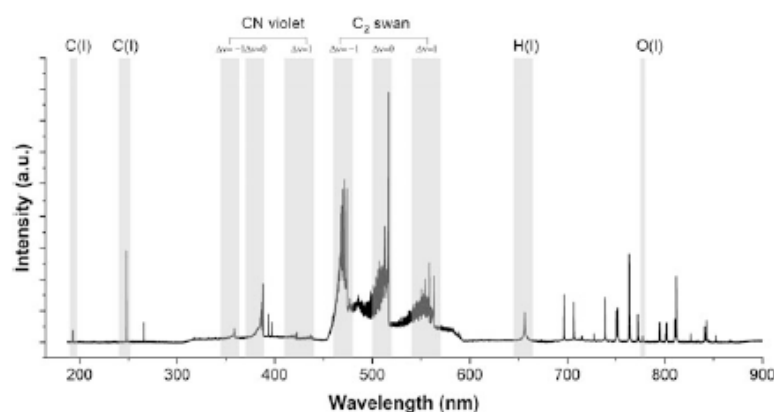


Figure 4.4: Representative LIBS spectrum of a polymer sample [17]

Besides, the determination of metal contents and distributions within a polymer has also been of great interest in material sciences (e.g. originating from additives) as well as environmental (e.g. heavy metals) and life science applications. The mapping of different polymer types is another LIBS application within this field [62, 63], as well as degradation studies of polymers by monitoring the C₂ swan band or the uptake of O within the polymer matrix [24, 25]. Concluding, even investigations regarding the molecular structure of organic compounds were undertaken by analysing organic molecules containing different amounts of aromatic rings [18, 22, 23, 64].

4.1.4 Introduction to Chemometrics

In contrast to many other analytical techniques where only one signal is detected, LIBS is a spectroscopic method and in a general instrumental setup a broadband emission spectrum is recorded. Depending on the type and number of spectrometer used, a spectral range from approximately 200 to 900 nm is accessible. This allows non-targeted analysis since no prior knowledge about the sample composition is necessary and each detected intensity can be used as an input variable for data evaluation. Additionally, modern instruments enable the acquisition of large amounts of data in a very short period of time. As a result, chemometrics have become an important tool in the data evaluation strategy of LIBS experiments and this chapter aims in at providing a short introduction to the topic.

The basis of all chemometric methods is the multivariate space. The analyzed wavelengths define the coordinate system and the detected signal intensities determine the exact position whereby each LIBS spectrum can be regarded as a point in this multidimensional space. Ideally, samples with similar chemical composition would be located

nearby in a particular region and the analysis of the p -dimensional space would allow sample discrimination and classification. Also, the best basis for the chemometric evaluation of LIBS spectra lies in the quality and quantity of the available data and these aspects should be considered during the design and performance of experiments.

The usual data processing steps involve data preprocessing, variable selection and the application of the chemometric method itself. Data preprocessing might include background correction, noise removal as well as spectral normalization to reduce signal fluctuations due to changing measurement conditions (e.g. laser energy, sample inhomogeneity, roughness). [60, 65, 66]. Typical normalization strategies in LIBS data processing are 'Normalization to the total emission intensity' or 'Normalization to an internal standard' as well as 'Normalization to the standard normal variate' [58]

Because LIBS is a non-targeted analysis, variable selection is done to reduce the dimensionality of the data set and the total amount of measurements needed. Feature selection makes sure that only emission signals which contain useful information are selected for further evaluation. From extracting certain emission lines present in the spectrum to dimensionality reduction by principal component analysis (PCA), a huge variety of different approaches has been reported. [58, 67] Subsequently, feature-wise centering and scaling of the data matrix might be necessary to avoid that features with greater scales dominate the analysis.

Regarding the application of chemometric methods, PCA was applied in the course of this work as a tool for exploratory data analysis. It provides as graphical representation of the multivariate space and relationships within the data. PCA represents the data by rotating the p -dimensional space in such a way that the greatest variance stored in the matrix becomes captured. A graphical representation is shown in 4.5. The individual dimensions in this new coordinate system are called principal components (PC) and are sorted in descending order regarding the represented variance. By projecting the data points onto a 2-dimensional space, visual examination of the data structure becomes possible, revealing data clusters or outliers. Additionally, the relationship between clusters and the selected variables can be investigated increasing the chemical understanding of the recorded data.

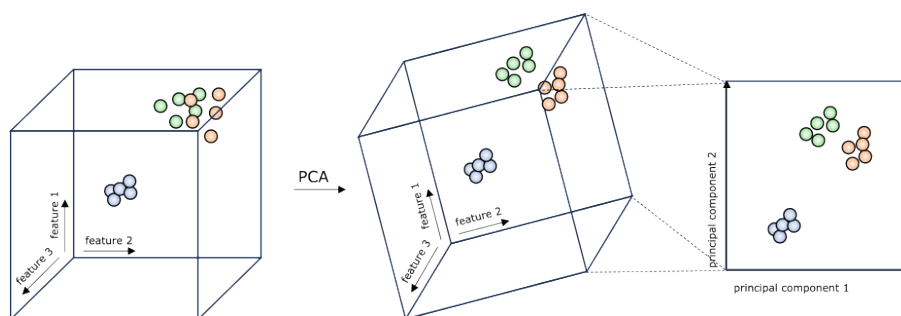


Figure 4.5: Graphical representation of PCA

Furthermore, a variety of different chemometric methods is available. For unsupervised methods like PCA or cluster analysis, the only information known is the data matrix. For supervised methods, the class information is known in addition and a classification algorithm can be built. Constructing a classification model comprises of two steps: learning based on a subset of the data and classification/validation with an untouched data set. Supervised classification methods commonly employed are linear discriminant analysis (LDA), partial least squares discriminant analysis (PLS-DA), k-nearest neighbors (k-NN), support vector machines (SVM), random forests (RF), soft independent modelling of class analogy (SIMCA) and artificial neural networks (ANN). [58]

4.2 Basic principles of LA-ICP-MS

LA-ICP-MS has been used to determine the elemental composition of a solid sample for more than 35 years, since Alan Gray first demonstrated that a laser ablation system could be coupled to an ICP-MS in 1985. Today, this technique is widely used for spatially resolved measurements and isotopic analysis in various fields.

Using LA-ICP-MS for solid sample analysis, detection limits down to the sub-ng/g range can be achieved which makes it ideally suited for trace element analysis. However, some analytes are difficult to measure due to high ionization energies, isotopic abundances and isobaric or polyatomic interferences. This is especially true for the elemental composition of polymers, consisting of N,O,H and C because the ICP is operated under ambient conditions. Therefore, the major and minor constituents of the atmosphere are either not accessible or lack sensitivity due to high background signals. [68] But when it comes to determining the uptake and distribution of traces especially halogens and metals in a polymer matrix, LA-ICP-MS offers higher sensitivity and improvements in spatial resolution compared to LIBS.

4.2.1 Fundamentals

LA-ICP-MS, similar to LIBS uses a high-energy laser pulse to obtain the elemental composition of a solid sample. Therefore, the same fundamental processes of laser-matter interaction take place from material ablation to plasma induction and condensation of a particle aerosol. A detailed description of the plasma evolution can be found in the according LIBS fundamentals section, see chapter 4.1.1. But in contrast to LIBS, LA-ICP-MS analyzes the formed aerosol which consists of sample vapor, particles and agglomerates. In order to do that, the generated aerosol is transported into an ICP via a carrier gas stream. In the ICP the vaporization, atomization and ionization takes place. Subsequently the ions are extracted and analyzed in a mass spectrometer where they are separated by their mass-to-charge (M/Z) ratio and detected.

A disadvantage of all laser based sampling techniques is the occurrence of elemental fractionation, which is a non-stoichiometric effect arising during sampling, aerosol transportation and within the plasma. It is caused by the different thermal behavior of elements and the resulting particle size distribution, which may lead to insufficient ionization in the ICP. Appropriate laser and ICP operating conditions are key to reducing the effect of elemental fractionation. [56,69,70]

Besides elemental fractionation, spectral interferences generated by polyatomic ions are a major issue in ICP-MS, limiting the selectivity and sensitivity of the method. Popular spectral interferences like, e.g. $^{38}\text{Ar}^1\text{H}^+$ ($^{39}\text{K}^+$), $^{40}\text{Ar}^+$ ($^{40}\text{Ca}^+$), $^{40}\text{Ar}^{16}\text{O}^+$ ($^{56}\text{Fe}^+$), $^{40}\text{Ar}^{40}\text{Ar}^+$ ($^{80}\text{Se}^+$), arrive from the plasma gas and the surrounding atmosphere. To overcome this issue, either sufficient resolution or collision/reaction cells are used. These cells are positioned prior to the mass analyzer and are filled with helium, a helium/hydrogen mixture or a reaction gas like oxygen. The ions then collide or react with the gas molecules and are converted to harmless species. Commercial collision cells discriminate by kinetic energy (KED) to distinguish between the collision product and the analyte ion. By adjusting the collision cell potential, the collision-product ions generated in the cell are rejected due to their lower kinetic energy as a result of the collision process. The analyte ions are transmitted. [68]

An advantage of LA as a solid sampling technique is a distinct reduction of polyatomic species in the plasma, because of the absence of a solvent in the sample aerosol. Thus, the abundance of molecular ions based on O, N or H is lower than in solution based methods. [71] Nevertheless, for the detection of certain elements, measurements in KED mode might still be favourable.

4.2.2 Instrumentation

The general instrumental setup of LA-ICP-MS has not changed significantly over the past years. The key components are a laser source for sample ablation and an optical system to guide the laser onto the sample. The sample is placed in a moveable ablation chamber with an aerosol transport line that connects it with the ICP-MS, which serves as a detection system. A schematic representation of a LA-ICP-MS instrument is depicted in figure 4.6.

Today, lasers used for LA-ICP-MS mainly operate in the UV wavelength range (266, 213 and 193 nm) due to the advantages in the ablation behavior. These advantages are related to an increased coupling of the laser energy into the sample, resulting in reduced thermal alteration of the material under observation. Furthermore, the application of femtosecond laser pulses also improves selective vaporization due to minimized thermal effects and produces an aerosol with a narrower size distribution. Still, these lasers are more expensive and maintenance intensive, which is why nanosecond lasers are more widespread. [56,70,72]

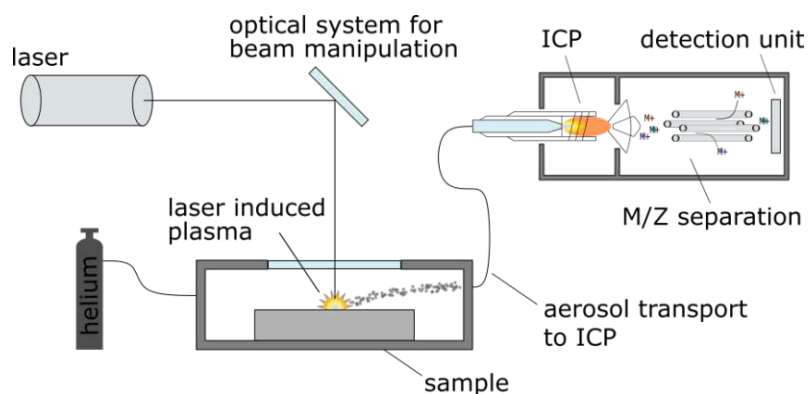


Figure 4.6: Schematic of LA-ICP-MS instrumentation

Besides laser wavelength and pulse duration, improvements in depth-profiling and imaging have been made by flat-top energy profiles, either with appropriate imaging optics for Nd:YAG lasers or the usage of excimer lasers. This ensures an even energy distribution throughout the ablation spot, resulting in uniform sample removal. [69,70]

The ablation atmosphere also influences the particle formation during laser ablation, which is why Helium is mainly used as a transportation gas. [71]

Commercially available ICP-MS instruments are equipped with quadrupole, sector field- or time-of-flight (TOF) mass analyzers. Based on the sampling conditions, individual benefits and drawbacks arise, e.g. sensitivity, mass resolution, sequential/simultaneous measurement. Quadrupole systems allow fast, but sequential scanning over the mass spectrum which might limit the number of masses e.g. analytes detectable if fast transient

4 Methodological Background

signals are produced. Also, due to the sequential measurement principle, data points acquired within one replicate do not originate directly from the aerosol cloud. Sector field mass analyzers also operate in a sequential mode but offer improved resolution to compensate for spectral interferences, usually accompanied by a significant loss in sensitivity. On the other hand, TOF instruments permit simultaneous sampling but lack sensitivity for nonrestrictive trace analysis. [56,69]

5 Experimental Details

In the course of this work, different analytical techniques were approached to investigate polyimide samples with an emphasis on laser assisted material analysis in the form of LIBS and LA-ICP-MS. The materials investigated were ranging from self-synthesized polyimides to commercially available thin films. Furthermore, polyimides were subjected to thermal treatment or exposed to high voltage and aqueous solutions containing different salts. Therefore, this chapter gives an overview of the various types of samples analyzed as well as technical details about the equipment used to characterize ion mobility and structural changes within the polymers.

In the first part, the synthesis and characterization of a polyimide based on pyromellitic dianhydride (PMDA) and 4,4'-oxy-dianiline (ODA) is described. These samples were used to manufacture model polymer thin films without industrial additives aiming to implement a novel characterization method for the degree of imidization based on LIBS.

In the second part, the ageing procedure of commercially available polyimide thin films using a migration cell setup is depicted and an overview of tested samples and a quantification strategy is given.

Finally, the technical specifications of state-of-the-art and novel characterization techniques for the prepared polyimide samples is listed, providing an overview of different LIBS and LA-ICP-MS setups as well as additional polymer characterization methods.

5.1 Reagents

Synthesis and characterization of sample polyimides

Silicon wafer with a gold top layer ($10 \times 10 \text{ mm}^2$) were provided by Infineon Austria AG (Villach, Austria) and used as a substrate material. Polyimides were synthesized from pyromellitic dianhydride (PMDA) from TCI Deutschland GmbH (Eschborn, Germany) and 4,4'-oxy-dianiline (ODA, 97%) from Sigma-Aldrich (Buchs, Switzerland). N-Methyl-2-pyrrolidon (NMP, anhydrous, 99.5%) served as solvent and was purchased from Sigma-Aldrich (Buchs, Switzerland). All reagents were used as received and no prior purification was done before synthesis. Furthermore, two different polymer additives were obtained: butylated hydroxytoluene from Merck (Darmstadt, Germany) and 2,4-dibromophenol from Honeywell Fluka (Schwerte, Germany). Nitrogen (5.0) was

used during thermal imidization and obtained from Messer Austria.

Migration cell experiments

Commercially available polyimides were provided as fully imidized films (film thickness approx. 12 μm), attached on a gold coated silicon wafer and cut in 30 x 30 mm² pieces by Infineon Austria AG (Villach, Austria). Additionally, a general-purpose polyimide thin film Du PontTM Kapton[®] HN with a thickness of approx. 12 μm was purchased from GoodFellow (Huntington, England). The electrolyte solution used for migration cell testing was composed from ACS grade KCl (VWR Chemicals, Radnor, USA) and deionized water.

LIBS and LA-ICP-MS measurements

Gases used for LIBS and LA-ICP-MS measurements (Argon 5.0 and Helium 5.0) were supplied by Messer Austria. For quantification, calibration standards were prepared from P84 obtained from HP Polymer GmbH (Lenzing, Austria) and potassium trifluoromethanesulfonate (98%, Alfa Aesar, Ward Hill, USA) and 4-Chlorobenzoic acid (Sigma Aldrich, Buchs, Switzerland). N-Methyl-2-pyrrolidone (NMP, p.a.) served as solvent and was purchased from Merck (Darmstadt, Germany). Silicon wafer (10 x 10 mm²) were used as substrate material for the preparation of the standards and were provided by Infineon Austria AG (Villach, Austria). KCl (p.a.) from Merck (Darmstadt, Germany) was used for the preparation of pressed powder pellets.

5.2 Synthesis and characterization of sample polyimides

To test the capabilities of LIBS for structural investigations within polyimides, the imidization step was chosen as a characteristic reaction. In order to keep the system as simple as possible, a commercial available polyimide was synthesized as a model substance. Polyimides based on the reactants PMDA and ODA were chosen and prepared via a 2-step process, illustrated in figure 5.1.

The chemicals and the initial weights used for this work are listed in the following table 5.1. PMDA and ODA were each used in a 1:1 mole ratio to obtain the maximum chain length and the solid content was adjusted between 5 and 15 % to ensure easy processing.

In order to synthesize the poly(amic acid) precursor, ODA was first dissolved in NMP at room temperature under argon atmosphere. Then PMDA was slowly added to the ODA/NMP solution while stirring under inert conditions for 24 h. Soon after the addition of both reagents, the solution turned yellow-brownish and the viscosity increased based

on the solid content of the solution.

To prepare polyimide thin films, the precursor solution was dispersed onto a gold coated silicon wafer and subjected to thermal imidization. The conversion from poly(amic acid) into the polyimide was done in a tube furnace under nitrogen gas flow. Based on the research question, different temperature programs were selected for curing, with imidization temperatures between 160 and 400 °C.

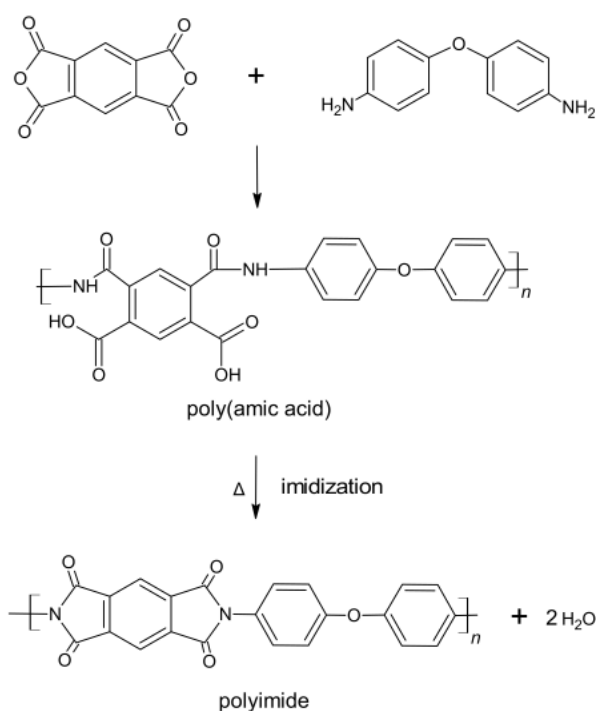


Figure 5.1: Reaction scheme for the synthesis of polyimides from pyromellitic dianhydride (PMDA) and 4,4'-oxy-dianiline (ODA)

batch	PMDA	ODA	amount	NMP
1	0.522 g	0.479 g	2.4 mmol	10 ml
2	0.522 g	0.479 g	2.4 mmol	10 ml
3	1.565 g	1.437 g	7.2 mmol	30 ml
4	6.544 g	6.010 g	30 mmol	120 ml

Table 5.1: Reagents and initial weights used for polyimide synthesis, PMDA and ODA were used in a 1:1 mole ratio

Batch 1 and 2 were mainly used for polyimide characterization based on DSC/TGA and gel permeation chromatography (GPC) and the optimization of the sample preparation steps. Batch 3 was employed for the preliminary tests for the determination of the degree of imidization based on IR spectroscopy and LIBS as described later in chapter 6. Batch 4

was the final batch within this work and was utilized for the determination of the chain length based on dynamic light scattering (DLS) and the final test specimen for the method development to determine the degree of imidization using LIBS (see chapter 6).

5.2.1 Thermal behaviour

After synthesis of the poly(amic acid), the polymer precursor was characterized by DSC/TGA. The simultaneous thermogravimetry was done using a STA 449 F1 Jupiter[®] from Netzsch with a temperature range from room temperature to 400 °C and a heating ramp of 10 °C/K. About 10 mg of the PAA sample were put in an aluminium pan and nitrogen gas was purged (20 mL/ min) during the measurement.

Exemplary signal trends are depicted in figure 5.2. The blue curve shows the change in heat capacity as heat flow in mW/mg (left y-axis), while the red curve depicts the mass loss in m% (right y-axis) during the measurement. Generally, the heat flow should contain information about thermal curing, evaporation, crystallisation, thermal decomposition, etc. In the case of a polyimide precursor, it involves dehydration with cyclization and evaporation of solvent [49, 50]. Figure 5.2 shows the endothermic heat flow due to the imidization and solvent evaporation which was predominant over the temperature range of 150 - 220 °C/K. The peaks below 150°C might be due to the presence of moisture. Due to the broad endothermic heat flow peak no glass transition could be recognized.

The mass loss trend followed the course of the DSC measurements, with the main mass loss between 100 - 200 °C representing the removal of the reaction byproduct (i.e. water) and residual solvent.

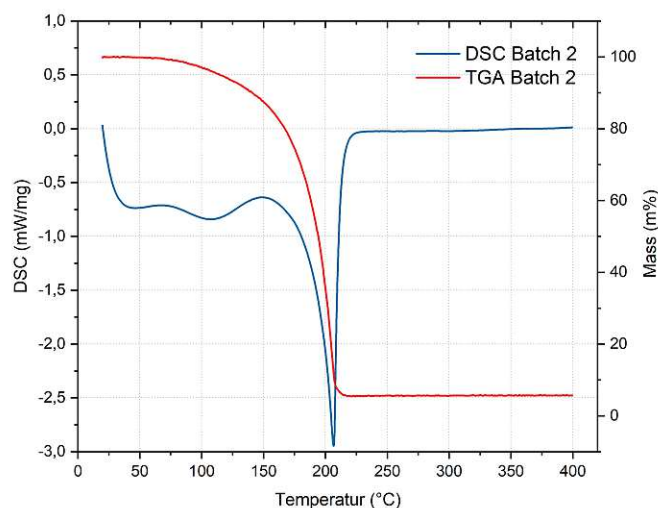


Figure 5.2: Signal trends from DSC/TGA measurements of PAA from batch 2 from 15.09.2021

5.2.2 Determination of the polymer chain length

Attempts to determine the molecular weight of the poly(amic acid) using GPC turned out to be unsuccessful due to limited solubility of the precursors in dimethyl sulfoxide (DMSO) and the polarity of the available GPC columns.

Therefore, DLS was chosen to determine the molecular weight of the polyimide precursor. Prior to the measurements, the poly(amic acid) (batch 4 from 20230619) was diluted in NMP with the following concentrations: 5, 8, 10, 15 and 20 mg/ml. Then, the analysis was conducted using an AVL/CGS-3 compact goniometer system from ALV-GmbH (Langen, Germany) equipped with a 22mW He-Ne Laser with a wavelength of 633 nm. The measurements were conducted in batch mode and the intensity of the scattered light was recorded at 13 different angles ranging from 30 - 150 °. The baseline was determined using toluene that had been filtered through a 0.2 µm PTFE filter to remove dust and other particulate matter. The light scattering data were processed using AVL-Correlator Software (V 3.0) and a value of $dn/dc = 0.192$ ml/g was chosen for calculations [73,74]. Figure 5.3 shows the Zimm plot of the conducted measurements, which resulted in a molecular weight $M_w(c) = 13\,600$ g/mol.

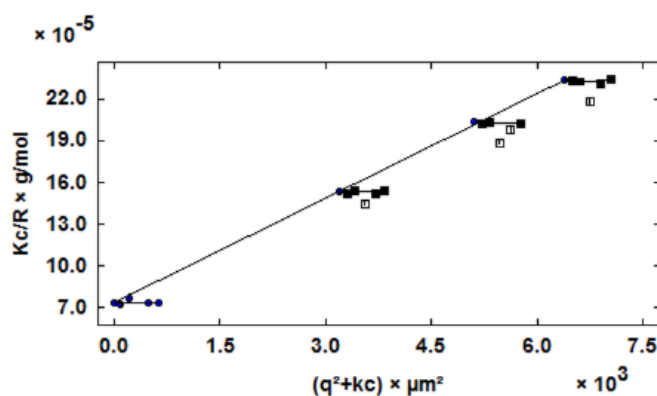


Figure 5.3: Zimm plot

5.3 Migration cell experiments

Polyimides have to meet many requirements during their lifetime in the electronics industry. Because they are used as protective layers or encapsulation material they are subjected to harsh environments including high voltages and high humidity. To investigate the role of the polyimide in the case of defects or device failure, stress testing in various forms is performed in industry. To assess the outcome of the stress test, the presence and distribution of harmful substances, often metals or salts is of great interest.

In order to investigate ion migration and their relationship with structural changes in

polyimide films, commercially available polymers were stressed using a migration cell developed at the Institute of Chemical Technologies and Analytics in the research group for Electrochemical Methods and Corrosion. [14,15] The experiments and modeling based on current profiles and breakthrough times were carried out in the same project as part of a post-doctoral fellowship and were made available for this work. Nevertheless, a brief explanation of the structure of the migration cell and a sample list are provided in the following sections. Subsequently to the electrochemical stress testing, the aim of this work was to detect the migrating species within the polyimide film, record migration profiles and distribution maps as well as implement a quantification method based on LIBS or LA-ICP-MS.

5.3.1 Introduction to the measurement setup

The migration cell experiments were conducted using two different instrumental setups: either using a double or single sided configuration according to figure 5.4. In both cases, 0.5 M KCl served as an ion source and different commercially available polyimide thin films were employed. In general, free-standing films were tested in the double sided setup, while the single sided configuration was utilized for polymer films attached to a support like a silicon wafer. During one measurement run, a certain migration voltage was applied (0 - 800 V) and the potential difference over the membrane was recorded using Ag/AgCl electrodes in the double sided setup. The stressed polymer films were subjected to LA-ICP-MS or LIBS analysis to determine the uptake and distribution of ions afterwards. Since KCl was used as electrolyte during the migration test, K and Cl were the analytes of interest for elemental analysis.

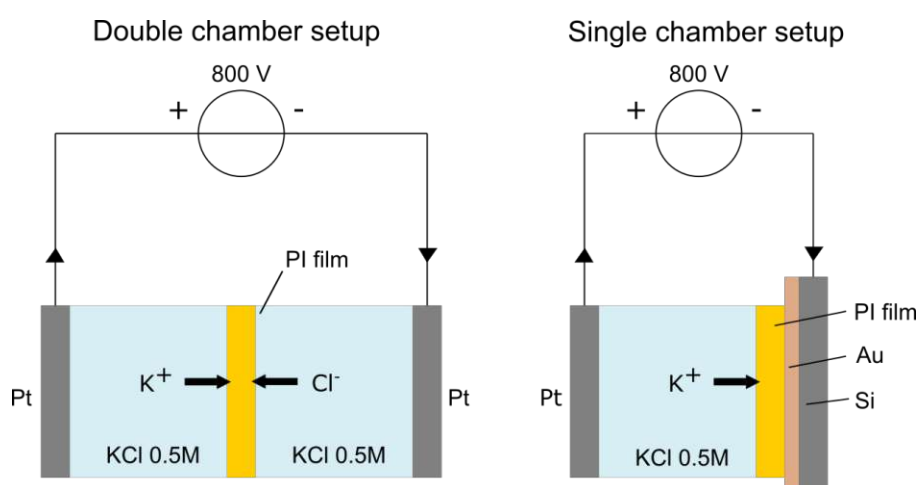


Figure 5.4: Migration cell schemes of the double and single sided configuration [14,15]

5.3.2 Sample list

Several commercially available polyimide films were used for migration cell experiments. PI1 is a general-purpose polyimide film used for a wide range of applications ranging from fiber optics to insulation tubings [75,76], while PI2 is based on a photosensitive precursor commonly used in the electronics industry.

All samples were named according to the following scheme:

PItype-mig-setup-electrolyte-exposure/date

with PItype either being PI1 or PI2, setup indicating the double or single sided configuration, electrolyte stating the type of salt dissolved in distilled water followed by either the exposure time after breakthrough or if the experiment was stopped right after breakthrough the experiment date.

sample name	setup	exposure time after breakthrough	date
PI2-mig-double-KCl-20220429	double sided	0 h	20220429
PI2-mig-double-KCl-20220719	double sided	0 h	20220719
PI2-mig-double-KCl-20230119	double sided	0 h	20230119
PI2-mig-double-KCl-20230203	double sided	0 h	20230203
PI2-mig-double-KCl-20230406	double sided	0 h	20230406
PI2-mig-double-KCl-20230719	double sided	0 h	20230719
PI1-mig-double-KCl-0h	double sided	0 h	20231120
PI1-mig-double-KCl-2h	double sided	2 h	20231120
PI1-mig-double-KCl-4h	double sided	4 h	20231120
PI1-mig-double-KCl-8h	double sided	8 h	20231120
PI1-mig-double-KCl-16h	double sided	16 h	20231120
PI2-mig-double-KCl-0h	double sided	0 h	20221104
PI2-mig-double-KCl-2h	double sided	0 h	20221104
PI2-mig-double-KCl-4h	double sided	0 h	20221104
PI2-mig-single-KCl-0h	single sided	0 h	20231120
PI2-mig-single-KCl-2h	single sided	2 h	20231120
PI2-mig-single-KCl-4h	single sided	4 h	20231120

Table 5.2: List of samples provided from migration cell experiments

5.3.3 Preparation of in-house calibration standards

Besides the localization and distribution analysis of harmful substances within stressed polyimide films, the quantification of the ingested elements was equally important.

Therefore, in-house prepared calibration standards based on a soluble polyimide were doped with K- and Cl-containing organic salts. First, a 10 m% solution of the polyimide powder in NMP was produced, as well as a stock solution of Potassium trifluoromethane sulfonate and 4-Chlorobenzoic acid in NMP. Then aliquots of the stock solution were added to the dissolved polyimide to obtain standards with the nominal concentrations listed in table 5.3. All weights were noted and used to calculate the actual concentrations listed in table 5.3 as well.

Afterwards, 10 μ l of the respective standard solution were cast of a silicon wafer and the solvent was evaporated by thermal treatment on a hot plate at 120 °C for 20 min.

c(Cl) [m%]		c(K) [m%]	
set value	actual value	set value	actual value
2.0	1.5	0.50	0.37
0.50	0.40	0.20	0.17
0.20	0.16	0.05	0.04
0.05	0.04	0.02	0.02

Table 5.3: Nominal and actual concentration of K and Cl calibration standards

In addition, pressed powder pellets with higher concentrations were produced for the determination of Cl. Therefore, P84 powder was mixed with KCl to obtain Cl concentrations of 2, 5 and 10 m%. Then, the powder mix was ground in the vibrating mill for 30 s and pressed into round pellets.

5.4 Instrumental setup

The aim of this work was to implement characterization techniques to track the uptake and distribution of ions within stressed polyimide films as well as the exposure of structural changes within the polymer network. The main tools used for this task were laser-based measurement methods, like LIBS and LA-ICP-MS which were complemented by standard methods for polymer characterization, like IR or CA if necessary. The following sections give an overview of the equipment used and list important configurations and technical details.

All measurements at this stage were conducted on polyimide thin films, either self-synthesized model polymers or commercially available polyimides. All free standing films were attached onto a silicon wafer as substrate if necessary.

5.4.1 Laser assisted material analysis

Several different laser systems, optical spectrometer and ICP-MS instruments were available for LIBS and/or LA-ICP-MS measurements. An overview of all components and their possible interconnections is shown in the following diagram.

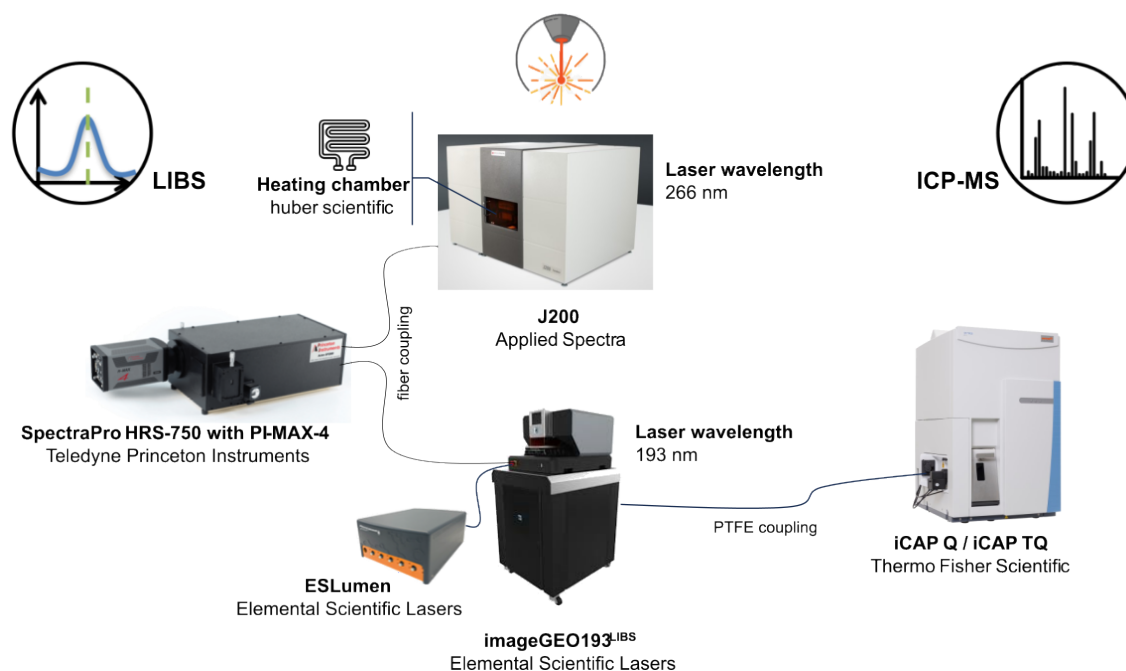


Figure 5.5: Overview of the instrumental setup

As can be seen in figure 5.5, two laser systems with different wavelengths (266 nm and 193 nm) were available to conduct experiments. Both systems were equipped with a broadband spectrometer and could be connected to an additional HR spectrometer via a glass fiber for LIBS measurements. Moreover, an in-house designed heating chamber was available for in-situ experiments at elevated temperatures or under reduced pressure using the J200 system. Both lasers can also be set up for LA-ICP-MS, but only the imageGEO193^{LIBS} was connected to an iCAP Qc or iCAP TQ due to improved aerosol transport properties. More details on the particular instruments is provided in the following sections.

LIBS J200 system

LIBS experiments were carried out using a commercially available LIBS J200 system (Applied Spectra, Inc., Fremont, CA). A frequency quadrupled Nd:YAG laser operating at a wavelength of 266 nm with a 5 ns pulse duration was used for ablation and excitation. Emitted radiation after each laser pulse was cumulated using a collection optic connected

to optical fibers. The collected light was analyzed using a Czerny-Turner spectrometer with 6 channels covering a total wavelength range from 188 to 1.048 nm. LIBS data was recorded using Axiom 2.0 software provided by the manufacturer of the instrument.

Laser wavelength	266 nm
Laser repetition rate	20 Hz
Laser beam diameter	100 μm
Laser beam geometry	circular
Atmosphere	1 l/min Argon or Helium
Spectrometer	Czerny-Turner
Detector	6 channel CCD
Gate delay	0.1 - 1 μs
Gate width	1.05 ms
Covered wavelength range	188 - 1048 nm

Table 5.4: J200 instrument configuration

Heating chamber for in-situ LIBS experiments

For in-situ experiments, a self-built heating and vacuum ablation chamber (by huber scientific, <https://sofc.at/>) was available for the J200 LIBS instrument. A photo of the opened chamber with a description of the individual components can be seen in figure 5.6.

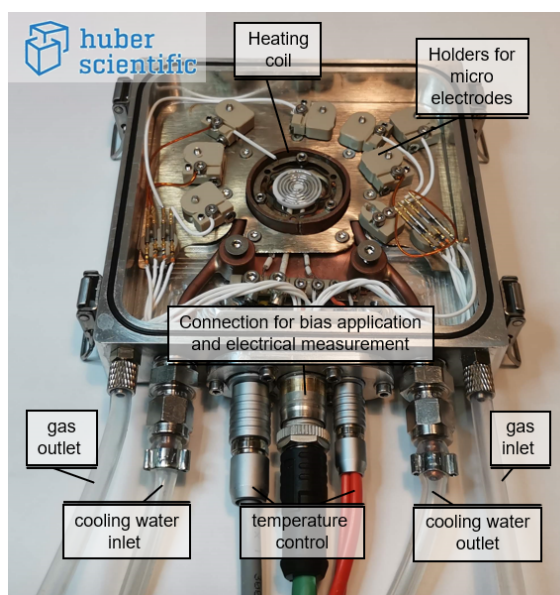


Figure 5.6: Heating chamber (designed by huber scientific) for in-situ LIBS experiments

This vacuum-tight sample chamber can be installed into the LIBS instrument, and was placed instead of the commercial sample holder facilitating sample geometries up to 30 x 30 mm² and allowing experiments at elevated temperatures and under reduced pressure. Precisely, temperatures up to 750 °C and pressures from mbar vacuum to 1 bar overpressure were available. Furthermore, the chamber is connected to the instruments gas supply, facilitating measurements under inert atmosphere (He and Ar). Additionally, 8 individually placeable microcontacts were available for the application of bias (0 - 500 V) and the recording of electro(-chemical) measurements. However, the application of a bias was not carried out in the course of this work.

HR Spectrometer with ICCD camera

An additional spectrograph (SpectraPro HRS-750, Teledyne Princeton Instruments, Acton, MA, USA), equipped with a high-speed gated camera (PI-MAX-4, Teledyne Princeton Instruments, Acton, MA, USA) was connected via an optical fiber to either laser respectively LIBS system (imageGEO193^{LIBS} and J200). The data was recorded using Lightfield (v 6.13) software provided by the manufacturer of the instrument.

Spectrograph	SpectraPro HRS-750
Camera	PI-MAX-4
Accessible wavelength range	350 - 900 nm
Motorized slit	10 - 3000 μm slit width
Gratings (on interchangeable turret)	150 g/mm 600 g/mm 1800 g/mm
Intensifier gain	1 - 100 x

Table 5.5: Optical spectrometer configuration

Laser ablation imageGEO193^{LIBS} system

Laser ablation and LIBS experiments were performed with an imageGEO193^{LIBS} laser system (Elemental Scientific Lasers, Bozeman, MT, USA) operating at a wavelength of 193 nm and equipped with a 'TwoVol3' ablation chamber. The ablation cup was provided with two fiber mounts capable of collecting the light that is emitted from the laser-induced plasma.

One fiber mount was used to connect the system to an 'ESLumen' (Elemental Scientific Lasers, Bozeman, MT, USA), a 5-channel Czerny-Turner spectrometer with CMOS detectors feasible for broadband LIBS spectra acquisition from 188 - 1097 nm and a spectral

resolution of 0.1 nm. The other fiber mount was either blocked or connected to an additional optical spectrometer equipped with an ICCD camera (Spectra HRS-750Pro with a PI-MAX-4 camera, both Teledyne Princeton Instruments, Acton, MA, USA, see chapter 5.4.1).

For LA-ICP-MS measurements, the system was coupled to one of the ICP-MS systems available using PTFE tubing.

The data evaluation of LIBS and LA-ICP-MS measurements was done using Iolite (v 4.9.1) provided by the manufacturer of the instrument [77].

Laser wavelength	193 nm
Laser repetition rate	up to 100 Hz
Laser beam diameter	100 - 150 μm
Laser beam geometry	rectangular
Atmosphere	0.8 l/min Helium
Spectrometer	Czerny-Turner
Detector	5 channel CMOS
Gate delay	0.1 μs
Gate width	3 ms
Covered wavelength range	188 - 1097 nm

Table 5.6: imageGEO193^{LIBS} system configuration for LIBS analysis

ICP-MS systems

LA-ICP-MS measurements were carried out using either an iCAP Qc or an iCap TQ instruments (both from Thermo Fisher Scientific, Bremen, Germany) based on availability and measurement requirements. The ICP-MS systems were coupled to the laser ablation device (imageGEO193^{LIBS}, Elemental Scientific Lasers, Bozeman, MT, USA) using PTFE tubing and a 'Dual Concentric Injector (DCI)' interface (Elemental Scientific Lasers, Bozeman, MT, USA) with a helium flow rate of 800 ml/min.

The data was recorded using Qtegra (v 2.10) software provided by the manufacturer of the instrument.

5.4.2 Polymer characterization

To uncover structural changes within the polymer network, additional characterization techniques were employed in this work.

FT-IR measurements have been conducted using a Spectrum 65 (Perkin Elmer, Waltman, MA, USA) in attenuated total reflection (ATR) mode. The instrument was equipped with the MKII Golden Gate Single Reflection ATR System (Specac, Orpington, UK). Applying the instruments software ('Spektrum'), a mathematical background correction was applied to all spectra directly after each measurement.

Contact angle measurements have been performed on the drop shape analyzer DSA30 (KRÜSS GmbH, Hamburg, Germany) using the 'Advance' software provided by the manufacturer in 'sessile drop' mode.

6 Monitoring the imidization reaction of polyimides using LIBS

In order to investigate certain failure mechanisms in the electronics industry and the role of the polyimide film as a protective layer, information about structural changes is necessary. The first task of this work was to test the capabilities of LIBS for structural investigations of the polyimide network. As already described in detail in chapter 3.1, most polyimides are manufactured from a soluble precursor named the poly(amic acid) and are converted into the final imide via a subsequent thermal (or chemical) process step. A schematic of the imidization reaction is illustrated in figure 6.1. Since the thermal curing process defines the final material properties and hydrolysis might occur during stress testing, the imidization was chosen as a representative example.

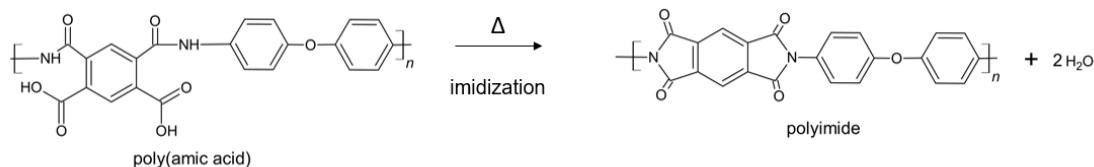


Figure 6.1: Imidization reaction of a poly(amic acid) to a polyimide

This chapter deals with the monitoring of the imidization reaction of polyimides and illustrates the development and verification for a novel LIBS based method as well as several application examples. Furthermore, in-situ measurements of the reaction process using an in-house designed heatingstage are presented. Part of this chapter has been published in *Analytical and Bioanalytical Chemistry* [78]. Still, additional information is provided in chapters 6.2.1 regarding the imaging and depth-profiling of artificial samples, chapter 6.3 presenting in-situ measurements in a heating chamber and chapter 6.4 on the transferability of the proposed LIBS method.

6.1 Method development

Although LIBS has been successfully used for polymer analysis [16–19], it has not yet been applied to track a specific reaction of polymers where only the reaction process of the educts is observed. In this study, the aim was to follow a specific reaction step, more precisely the cyclodehydration of a poly (amic acid) (see figure 6.1) during the fabrication of a polyimide and exploit the LIBS depth profiling and imaging capability for the investigation of thin films. Besides, a quantitative measure to characterize material properties was searched for.

In the following chapters, the implementation of the LIBS method and its verification using IR spectroscopy is explained step by step and the differences, strengths and weaknesses of the individual methods are discussed. Furthermore, application examples on model polyimides as well as commercial products are presented.

6.1.1 Sample preparation

Self-synthesized polyimide based on PMDA and ODA was used to fashion calibration standards for the method development. A detailed overview of the sample synthesis can be found in chapter 5.2.

Polymer thin films were prepared by drop casting a 7 m% poly (amic acid) precursor solution onto a gold coated silicon wafer ($10 \times 10 \text{ mm}^2$) functioning as the substrate. $50 \mu\text{l}$ of the precursor were evenly dispersed, so that the substrate surface was completely covered. Subsequently, the solvent (NMP) was removed at $80 \text{ }^\circ\text{C}$ in a vacuum dryer for 120 min. Finally, the samples were cured under nitrogen gas flow in a tube furnace. For each set of samples, a predefined curing temperature T_c and a specific curing time t_c were chosen. All in all, five different temperatures ranging from $160 \text{ }^\circ\text{C}$ to $400 \text{ }^\circ\text{C}$ and six curing times between 5 and 120 min were selected. The times and temperatures were chosen according to literature [42, 47, 49], in order to obtain different conversion rates of the amic acid group into the corresponding imide, resulting in samples exhibiting different degrees of imidization. To check the reproducibility of the developed method later on, 4 replicates were produced for each set of conditions. Combined with ten samples who solely exhibited the solvent evaporation step at $80 \text{ }^\circ\text{C}$, a total of 130 samples with a final thickness of about $18 \mu\text{m}$ (based on profilometer measurement with a DektakXT from Bruker) were produced. Depending on the thermal treatment applied, the color of the polyimide thin film varied from transparent to dark yellow, already indicating a different evaluation of the imidization reaction based on the curing parameter. An overview of the prepared samples and names is given in table 6.1.

Curing temperature T_c [°C]	Curing time t_c [min]	Sample name
80	120	PAA-80-120-1 to 10
160	5, 10, 15, 20, 60, 120	PI-160-tc-1 to 4
180	5, 10, 15, 20, 60, 120	PI-180-tc-1 to 4
200	5, 10, 15, 20, 60, 120	PI-200-tc-1 to 4
300	5, 10, 15, 20, 60, 120	PI-300-tc-1 to 4
400	5, 10, 15, 20, 60, 120	PI-400-tc-1 to 4

Table 6.1: Overview of calibration samples with different degrees of imidization

In addition, polyimide films containing commercially available polymer additives were prepared to test the practicability of LIBS for the monitoring of the imidization process. The additives were chosen based on their solubility in NMP and the presence of aromatic structures in the molecule. Approx. 2 m% (based on the polymer content) of either butylated hydroxytoluene or 2,4-dibromophenol were added to the PAA solution. Butylated hydroxytoluene is commercially used as an antioxidant while 2,4-dibromophenol serves as a flame retardant in real-live polymer products. Structures of both additives are illustrated in figure 6.2.

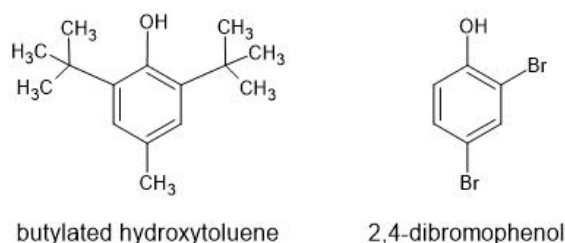


Figure 6.2: Chemical structure of used polymer additives

To prepare the spiked precursor solutions, small amounts of the additives were placed in a vial (0.0033 g butylated hydroxytoluene and 0.0022 g 2,4-dibromophenol) and mixed with a defined amount of an approx. 10 m% precursor solution (1.4217 g for butylated hydroxytoluene and 1.4101 g for 2,4-dibromophenol). The PAA solutions including the additives were homogenized using a vortex mixer and applied onto a gold coated silicon wafer, analog to the pristine samples. The polyimide films were then subjected to solvent evaporation at 80 °C for 120 min and used as is, or further exposed to thermal curing at either 200 °C for 30 min or 400 °C for 60 min. 4 samples were prepared per additive and exposure conditions resulting in 24 samples in total.

6.1.2 IR as a reference method

To characterize the fabricated polyimide samples a reference technique was needed. IR spectroscopy is commonly used to monitor the reaction process of various polyimides and quick and easy to carry out. Additionally, the calculation of the degree of imidization based on certain absorption bands is state-of-the art and well discussed in literature. [42,47,49]

FT-IR measurements have been performed in ATR mode, with a rectangular sampling area exhibiting a diameter of 1.0 mm. All 130 polymer thin films, exposed to different curing parameters and therefore displaying different imidization degrees, were measured. The samples were placed approximately centered on the specimen holder and an average of 6 scans was collected from the same position. Every spectrum was recorded in the range from 550 - 4000 cm^{-1} with a resolution of 4 cm^{-1} but all the relevant bands to trace the imidization reaction can be found between 550 - 2500 cm^{-1} . An overview of the important bonds for imide characterization according to literature [42,47,48] is shown in table 6.2.

C=O stretch (imide I) (symmetric)	1770 - 1780 cm^{-1}
C=O stretch (imide I) (asymmetric)	1720 - 1740 cm^{-1}
C-N stretch (imide II)	1360 - 1380 cm^{-1}
C-H bend (imide III)	1070 - 1140 cm^{-1}
C=O bend (imide IV)	720 - 740 cm^{-1}
C=C aromatic ring stretching	1500 - 1520 cm^{-1}

Table 6.2: Assignment of IR absorption bands [42,47,48]

Since IR measurements were performed on various samples exhibiting different imidization temperatures T_c and imidization times t_c , the advancement of the imidization reaction was visible within the recorded spectra and assigned bonds in table 6.2. The IR spectra of 3 representative polyimides subjected to different curing conditions illustrate the spectral changes and therefore the advancing reaction process in figure 6.3. The spectrum of a hardly imidized film (PI-160-005-1) is shown in red and was compared to a semi-imidized film (PI-200-030-1, green) and a completely cured polyimide (PI-400-120, yellow). With the increase of the imidization temperature, a general increase of all imide absorption peaks became clear. The signals were particularly intense for the imide I band around 1720 cm^{-1} as well as the imide II between 1360 and 1380 cm^{-1} . Also, the aromatic ring stretching around 1500 - 1520 cm^{-1} remained unaffected by the reaction. This signal was used for normalization purposes during the following data evaluation. By comparing the IR spectra of different polyimide samples it became also clear, that that polyimides with

the intended properties, meaning different imidization rates have indeed been created.

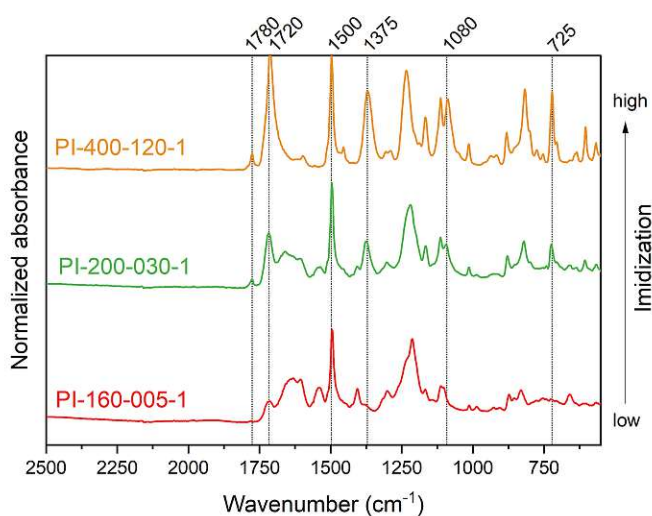


Figure 6.3: Representative FT-IR spectra of sample polyimides in the region from 550 - 2500 cm^{-1} ; the polymer thin films were cured at different temperatures T_c and with different curing times t_c [78]

Besides monitoring the reaction process, the magnitude of the imide absorption bands has been used to calculate a quantitative measure for the reaction process, named the degree of imidization. In general, this indicator represents the percent conversion of the amic acid group into imide. A formula, based on the most commonly used IR band, the C-N stretching between 1360 and 1380 cm^{-1} is depicted in equation 6.1. [42, 47, 48]

$$\text{Imidization degree (\%)} = \frac{A_{1375}/A_{1500}}{A'_{1375}/A'_{1500}} \quad (6.1)$$

where A is the peak area or height of the measurement sample and A' is the peak area or height of the maximum cured sample. The wavenumbers of the according absorption bands are shown as subscript numbers. This formula shows that the imide band height or area has to be normalized to the aromatic ring stretching at 1500 cm^{-1} . Furthermore, this ratio has to be referenced to the values obtained from a thoroughly cured film.

In this work, data evaluation was carried out using Epina ImageLab (Version 4.09, Epina GmbH, Austria) and the peak area was used for the analysis of all IR spectra. The respective peak area was subjected to baseline subtraction and the band limits were adjusted in the event of slight peak shifts. Also, the polyimide cured at a temperature of 400 °C for 120 min was set as the maximum cured sample.

The extent of the imidization reaction for the 130 piece calibration standards is illus-

trated in figure 6.4. The degree of imidization is displayed as a function of the curing temperature T_c and time t_c and was calculated based on equation 6.1.

After solvent evaporation at 80 °C practically no conversion from the amic acid group in the imide group has occurred based on the recorded IR spectra. These samples served as the zero point and the average is depicted as a dotted line in figure 6.4. All other polymer films exhibited different degrees of imidization based on the curing parameter. The displayed values in the graph represent an average of 4 samples per exposure. In general, higher T_c and longer t_c resulted in a higher degree of imidization. In the present study, the maximum curing time was set to 120 min. Therefore, for each selected curing temperature, the progression over these 120 min is displayed in figure 6.4. Curing temperatures below 200 °C, namely 160 and 180 °C, led to medium imidized samples even after the maximum curing time. Depending on the time t_c , polyimide films with imidization degrees between 1 and 43 % were preserved. At higher temperatures, the reaction took place more rapidly, leading to conversion rates of 87 ± 13 % at 200 °C and 97 ± 0.7 % at 300 °C after 120 min. Figure 6.4 also shows, that exposure to 300 °C and 400 °C, led to imidization degrees above 95 % even after 5 min of thermal treatment.

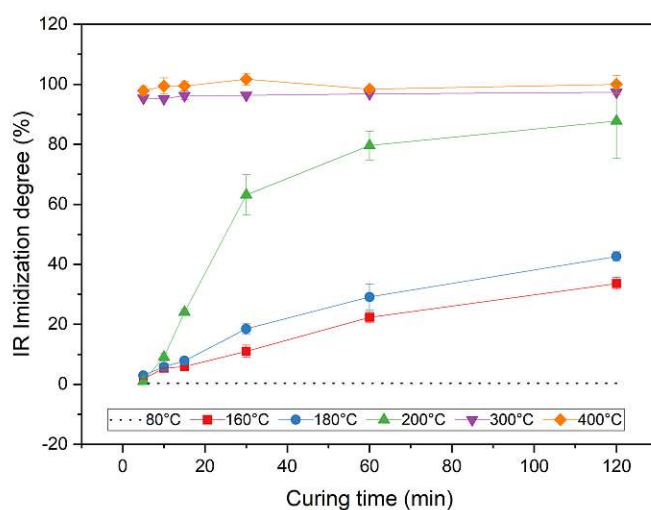


Figure 6.4: Degree of imidization for the self-synthesized sample set based on IR absorption bands (average of 4 samples per exposure)

Furthermore, the sample used as a reference in equation 6.1 has a considerable effect on the calculated values of the degree of imidization. In this study, the reference film was selected based on the curing program, using the highest temperature ($T_c = 400$ °C and longest curing time $t_c = 120$ min). But, the real conversion of these samples (PI-400-120-1 to 4) is not known. It is assumed, that the imidization reaches 100 % but it is unlikely that this is really the case. Therefore, the equation rather states the percent conversion

based on the maximum achievable amount. This can then result in calculated imidization degrees $> 100\%$, which was also the case for samples PI-400-030-1 to 4 with a calculated imidization degree of $102 \pm 2\%$.

6.1.3 LIBS method development

During method development, the 130-piece calibration samples of self-synthesized PMDA-ODA, which were previously investigated by FT-IR, were analyzed using LIBS. An overview of the measurement parameter is given in table 6.3, while the instrument configuration can be found in table 5.4 in chapter 5.4. Every sample was measured using three parallel linescans with a length of 8 mm and a stage scan speed of 2 mm/s, almost covering the entire width of the specimen. As a result, a representative area of 2.4 mm^2 was sampled for each film. Each line produced 80 shots, adding up to 240 shots in total per sample. Then, 20 shots each were accumulated for the further data evaluation, using Epina ImageLab (Version 4.09, Epina GmbH, Austria) resulting in 12 spectra per sample. Each accumulated spectrum was normalized to constant sum of squares to compensate for shot-to-shot variations.

Laser wavelength	266 nm
Laser energy	3.2 mJ
Laser spotsize	100 μm
Sample fluence	10.2 J/cm^2
Frequency	20 Hz
Atmosphere	Argon
Spectrometer	Czerny-Turner
Detector	6 channel CCD
Gate delay	0.3 μs
Gate width	1.05 ms
Covered wavelength range	188 - 1048 nm

Table 6.3: Measurement parameter for J200 LIBS instrument during method development

After the measurement, polymer specific emission signals were assigned and are listed in table 6.4 including atomic emission lines and molecular bands.

Three representative LIBS spectra of different polyimide samples (same as in figure 6.3 for IR measurements) are displayed in figure 6.5 and emission signals from major polymeric components are earmarked in the figure. Varying intensities were observed, depending on the thermal treatment of the samples: while a decrease of the H(I) emission line was apparent when comparing a hardly imidized sample (PI-160-005-1, red) with a

fully cured polymer film (PI-400-210-1, yellow), the C_2 emission bands as well as the C(I) emission line at 247 nm increased with the advancing reaction process.

C(I)	193.1 nm
C(I)	247.8 nm
CN violet band	388.3 nm
C_2 swan band $\Delta v -1$	473.7 nm
C_2 swan band $\Delta v 0$	516.5 nm
C_2 swan band $\Delta v +1$	563.5 nm
H(I)	656.3 nm
O(I) triplet	777.2 / 777.4 / 777.5 nm
C(I)	833.5 nm

Table 6.4: Assignment of LIBS emission signals - according to [20,79]

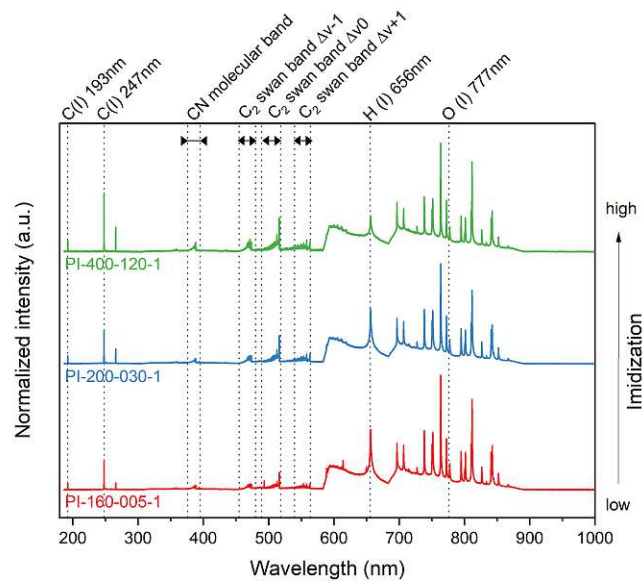


Figure 6.5: Representative LIBS spectra (average of 20 spectra, normalized to constant sum of squares) of sample polyimides in the region from 180 - 1000 nm; the polymer thin films were cured at different temperatures T_c and with different curing times t_c [78]

However, no further information, e.g. about how strongly the individual signals were influenced by the imidization reaction or whether the intensities of individual signals depend on each other, could be obtained solely by comparing the LIBS spectra. To learn about the data structure and the effects of each signal, the whole dataset (all 130 samples with 12 spectra per sample) was subjected to a principal component analysis

(PCA). For this purpose, the background-corrected and integrated emission signals from all components listed in table 6.4 were used as variables in the PCA. All input values were mean-centered and the PCA was calculated using Epina ImageLab (Version 4.09, Epina GmbH, Austria).

The variance explained by each principal component (PC) was as follows: 85.01 % for PC1, 9.20 % for PC2, 4.06 % for PC3 and < 1 % for the remaining PC. Since most of the variance in the dataset was explained by PC1 and PC2, the score plot showing those two principal components is displayed in figure 6.6a. It is noticeable that the datapoints were fanned out along the x-axis which represent PC1. This arrangement also corresponds to the thermal treatment, namely the curing temperature T_c , which was used to color code the data. Based on this representation, it seemed possible to track the imidization reaction using LIBS. To reveal the influence of the input variables on PC1, the weighting was analyzed based on the loadings plot, depicted in figure 6.6b. As already visible in the LIBS spectra, the hydrogen signal as well as the C_2 swan band $\Delta v 0$ had the most effect on PC1. While the hydrogen signal shifted the value of PC1 into a positive direction, the C_2 swan band $\Delta v 0$ had the most negative effect. It should be noted that with mean-centering, the data is scaled in such a way that the mean of each item becomes zero but the magnitude of the individual input variables still has an influence on the outcome of the PCA (in comparison to standardizing used for scaling). Since the aim of this work was to gather information from possibly single LIBS spectra, the actual signal height was important and this approach made sense in this context.

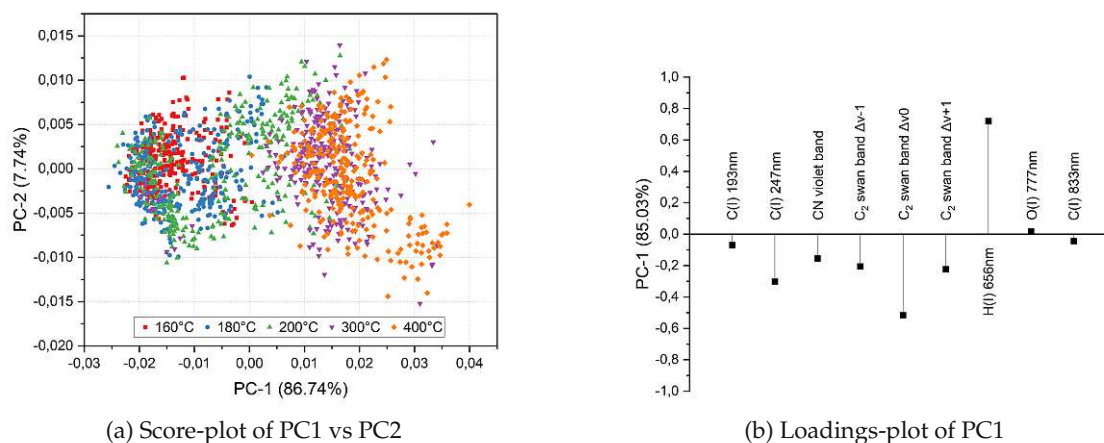


Figure 6.6: Principal Component Analysis of all LIBS spectra obtained from the 130 piece self-synthesized polymer samples; the dataset was colored based on the curing temperature [78]

Based on these findings, the LIBS signal trends for both, the hydrogen emission line at 656 nm as well as the C_2 molecular emission around 515 nm were further investigated.

First of all, the mean signal intensity and standard deviation were calculated for each exposure condition by averaging all spectra per sample (12 in total). This mean value was then used as the initial value for each specimen. With 4 samples per curing temperature T_c and curing time t_c , this resulted in 4 values per parameter set. With this procedure, IR data and LIBS data were treated equally.

The trend for both LIBS signals, H and C_2 is depicted in figure 6.7. The data is summarized and color coded by the curing temperature T_c and presented as a function of the curing time t_c . A clear trend indicated the increase of the C_2 molecular emission, while the hydrogen signal decreased with more intense curing conditions. Other than IR spectroscopy, the LIBS signals did not directly show the bond formation happening during the imidization reaction. Nevertheless, emission signals corresponded with the ongoing process since the curing of a polyimide precursor at temperatures $> 150\text{ }^\circ\text{C}$ involves dehydration and the evaporation of residual solvent as well as imide bond formation and crystallization. [49] Consequently, the loss of hydrogen signal intensity could be attributed to the evaporation of water and solvent in the course of the imidization reaction. Furthermore, structural changes within the forming polyimide film e.g. the formation of the imide bond as well as increasing chain rigidity might be the source of the increase in the C_2 molecular emission.

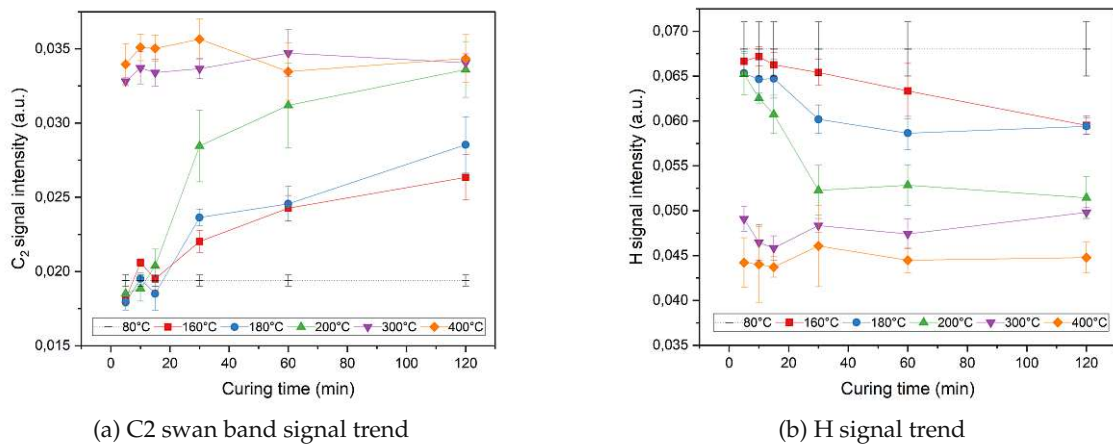


Figure 6.7: LIBS signal trends based on the curing temperature T_c and time t_c [78]

After monitoring the reaction process itself using LIBS, the next step was to implement a quantitative measure analog to the imidization degree from IR spectroscopy. To set up an equation based on LIBS spectral emission data, it was important that the parameter chosen are easily determined. Based on the presented details, it was possible to monitor the course of the imidization reaction by analyzing the hydrogen line as well as the C_2 molecular emission signal of a recorded LIBS spectrum. To resolve the reaction process as

precisely as possible, the ratio of the C_2 intensity to the H emission signal was introduced. Also, a reference value for a fully-imidized film was necessary for the calculation, similar to the formula based on IR data (see equation 6.1). Because the H as well as C_2 molecular emission are also recorded from non-imidized samples, the equation had to be adapted further and a non-cured polymer film was introduced for additional scaling. This resulted in the final equation for the degree of imidization based on LIBS data as following:

$$\text{Imidization degree (\%)} = \frac{C_2/H - C_{2,min}/H_{min}}{C_{2,max}/H_{max} - C_{2,min}/H_{min}} \quad (6.2)$$

In equation 6.2, C_2 and H represent the background-corrected, integrated LIBS signal intensities calculated according to table 6.4 for the C_2 swan band and the H atomic line of the sample. $C_{2,min}$ and H_{min} are the same emission signals coming from a merely dried, non-imidized sample. $C_{2,max}$ and H_{max} on the other hand, derive from a maximum-imidized polyimide. In this work, $C_{2,min}$ and H_{min} were obtained from the polymer films merely exposed to solvent evaporation at 80 °C (PAA-080-120-1 to 10). $C_{2,max}$ and H_{max} were extracted from the maximum cured specimen, which were all samples exposed to 400 °C for 120 min (PI-400-120-1 to 4), the same samples chosen as reference for IR based calculations.

A graphical representation of the calculated LIBS imidization degrees based on the self-synthesized polyimide samples is illustrated in figure 6.8.

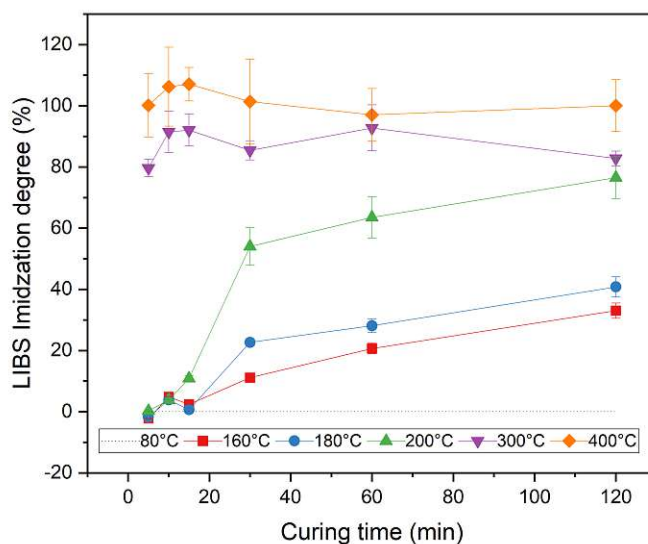


Figure 6.8: Degree of imidization for the self-synthesized sample set based on LIBS signal ratios (average of 4 samples per exposure) [78]

For temperatures below 200 °C, only medium-imidized thin films were obtained even

after the maximum curing time of 120 min. For samples cured at 160 °C this resulted in a maximum imidization degree of 33 ± 7.5 % ($n = 4$) and 41 ± 8.1 % ($n = 4$) for polymer films exposed to 180 °C for 120 min. Exposure to higher temperatures led to higher imidized samples due to enhanced reaction rates and resulted in a degree of imidization of 69 ± 9.9 % ($n = 4$) after 120 min at 200 °C. Exposure to 300 °C and 400 °C, led to imidization degrees > 80 % even after 5 min of curing time and conversion rates remained nearly constant. The degree of imidization calculated for samples treated with 400 °C and varying curing times ranged from 97 - 107 % with RSD from 5.1 - 13.6 %.

6.1.4 Comparison of both techniques

The data presented in the previous chapters demonstrates, that it is possible to monitor the imidization reaction of a polyimide with LIBS by selecting certain emission signals (see figure 6.7a and 6.7b). Also, the calculation of a quantitative measure named the degree of imidization was demonstrated based on LIBS spectral information (see figure 6.8). The method development was based on a set of self-synthesized polyimide films exhibiting different conversion rates of the amic acid into imide and IR spectroscopy was implemented as a reference to characterize the in-house prepared standards.

Since the two analytical methods used, IR and LIBS differ in several aspects, a comparison of results based on both techniques was necessary. The calculated imidization degrees of all 130 samples based on IR spectroscopy as well as LIBS data are compared in figure 6.9.

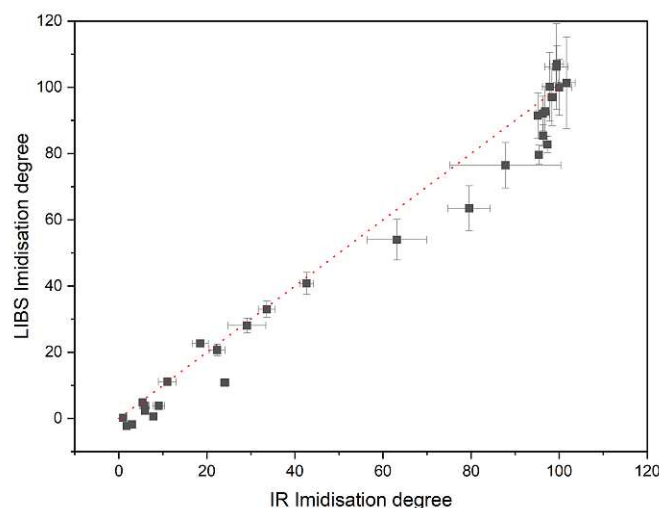


Figure 6.9: Comparison of imidization degrees based on IR spectroscopy and LIBS [78]

Both techniques yielded very similar outputs, especially when considering the the red line indicates exactly the same value for both methods. It is also apparent, that up to an

imidization degree of 50 %, the calculated values were almost the same for LIBS and IR. At later stages of the reaction process, LIBS tended to provide lower results compared to IR spectroscopy. Nevertheless, the course of the reaction was depicted with both methods.

Regarding the error, IR and LIBS behaved slightly differently as well: IR had a relative standard deviation of 6 % on average for all polymer films and curing conditions, while LIBS exhibited a relative standard deviation of 8 % for the same set of samples. Additionally, using IR spectroscopy, the error decreased at higher imidization degrees (8 % at 160 °C, 2 % at 400 °C). This was probably due to the fact that imide absorption bands used for the calculation all increase with the ongoing imidization and the error during spectrum evaluation became smaller. For LIBS on the other hand, the error increased with increasing imidization (5 % at 160 °C, 10 % at 400 °C). This behavior could be attributed to the active sampling area analyzed with LIBS. First, the ATR-IR penetration depth is dependent on the wavenumber and is approximately 1.3 μm at 1500 cm^{-1} . LIBS ablation craters were around 1 μm deep. But more importantly, in ATR-IR the active sampling area is the size of the ATR crystal. In the instrument used, this corresponded to an area of 0.5 mm^2 and all 6 scans were measured and averaged at the same spot in the middle of the polymer film. As a result, the IR data reflected only deviations resulting from sample measurement and between samples but not variations in film homogeneity. Using LIBS, a total area of 2.4 mm^2 was sampled, covering the entire width of the specimen and variations in the reaction process due to sample preparation were included. Inhomogeneity in film thickness and reaction rate could therefore attribute to the increased error at later stages of the imidization reaction based on LIBS data.

Finally, the two analytical methods differ in the basic information that is collected. With IR spectroscopy, characteristic vibrations of functional groups within a molecule are measured and the calculation of the degree of imidization is based on the ratio of two vibrational bands. Using this technique the direct observation of the imide bond formation during the imidization reaction is possible and the imide absorption bands are used for the calculation (see equation 6.1). In contrast, LIBS is a method used for elemental analysis and no information about the molecular structure or the formation (or breaking) of bonds is observed directly. Instead, the determination of the degree of imidization is based on the ratio of emission signals: the C_2 swan band and the H atomic line of the sample. Both signals are probably related to processes occurring during the thermal treatment of a polyimide precursor, like the evaporation of water and solvent or the structural changes due to imidization and chain ordering. But the bond formation cannot be followed directly in the form of an emission line as with IR spectroscopy.

All of this must be taken into account when comparing reaction processes and calculat-

ing the degree of imidization using two different analytical techniques. Still, monitoring the imidization reaction is possible using LIBS as well as IR spectroscopy and both techniques can be used to calculate comparable degrees of imidization.

6.2 Application examples

6.2.1 Imaging and depth-profiling of artificial samples

In this section, two applications highlighting the imaging and depth-profiling capabilities of the proposed LIBS method to monitor the imidization reaction of polyimides are presented. First, the mapping of an artificially prepared sample, exhibiting areas with differently imidized polyimide films is shown. In the second case, stacked samples were prepared and the degree of imidization was investigated via the sample thickness.

Imaging

Figure 6.10 displays an artificially prepared polyimide sample and the corresponding LIBS map, representing the degree of imidization of the analyzed polymer film. In order to achieve areas with different imidization degrees, the self-synthesized PAA solution was applied sequentially on a gold coated silicon wafer. The inner circle was thermally cured for 30 min, in contrast to the outer area which was only imidized for 15 min at approximately 180 °C. Parallel linescans featuring the measurement parameter listed in table 6.3 were used to analyze the cured polyimide film, whereat a total number of 7500 pixels covering an area of 15 mm × 5 mm was recorded. Each pixel in the displayed mapping represents an average of 5 spectra. Data evaluation was carried out using the integrated emission signals previously introduced in table 6.4 during LIBS method development. The completely cured samples (PI-400-120-1 to 4) and merely dried polyimide films (PAA-080-120-1 to 10) were measured as reference points and the LIBS imidization degree of each pixel was calculated according to the proposed equation 6.2. As can be seen in figure 6.10, a clear distinction between the two areas with different imidization degrees using the proposed LIBS method was possible. Additionally, the calculated values of the degree of imidization corresponded well with the values obtained during method development. The inner circle, which was cured at 180 °C for approx. 30 min, exhibited an imidization degree of 25 to 30 % while the self-synthesized films used for method development exposed to a similar heat treatment (PI-180-030-1 to 4) exhibited a mean value of 23 ± 1 %. At shorter imidization times, the calibration standards (PI-180-005 to PI-180-015) possessed degrees of imidization < 5 %, which was also measured for the sample in figure 6.10.

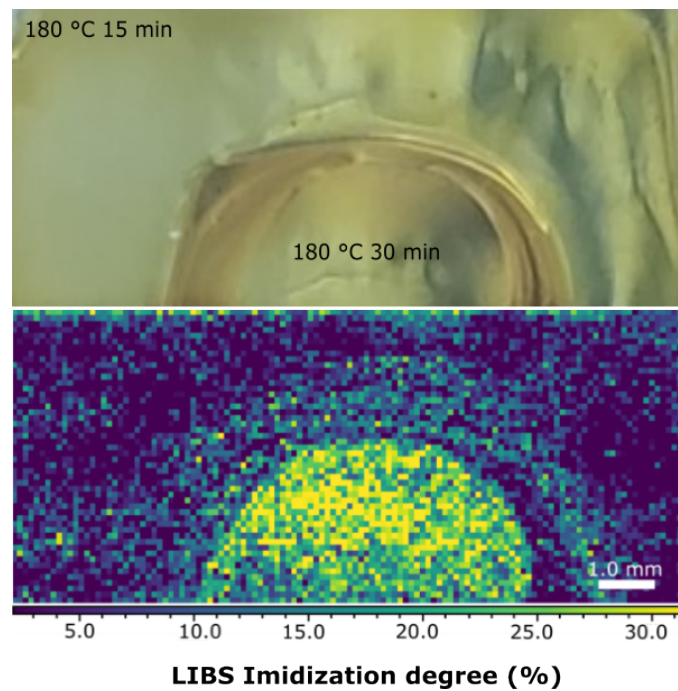


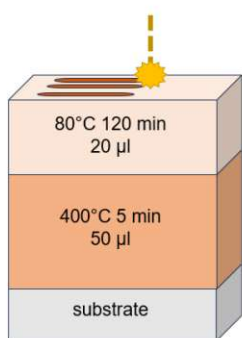
Figure 6.10: LIBS imidization degree of a model sample with areas exposed to different thermal treatment (accumulation of 5 spectra per pixel)

Depth-profiling

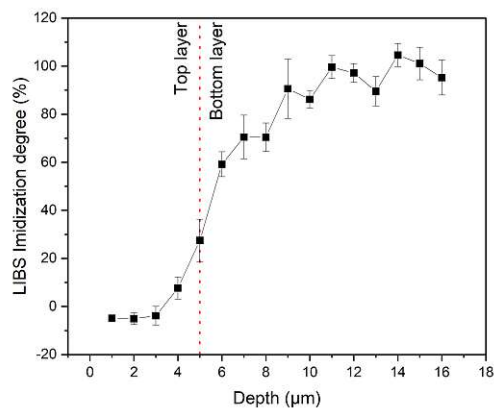
Several stacked model samples were prepared from PAA solution to follow the course of the imidization degree via the sample thickness and demonstrate the applicability of the proposed LIBS method for depth-profiling of layered structures.

A schematic of the first model sample is shown in figure 6.11a. In this case, a first layer of PAA precursor solution was thermally cured for 5 min at 400 °C to obtain a fully cured polyimide film as a base. Subsequently, another layer of poly(amic acid) was added on top and dried for 120 min at 80 °C in a vacuum oven. This resulted in a layered polyimide structure with a completely imidized part, topped with a non-imidized film and an overall film thickness of approx. 16 μm .

Depth profiling was done starting from the top layer down to the base until the substrate was reached, resulting in 16 single layers each representing 1 μm of sample thickness (see figure 6.11b). The recorded LIBS spectra were then normalized and signal intensities for the C_2 swan band and the H line were extracted and averaged per layer. In order to calculate the degree of imidization according to equation 6.2, samples fabricated for method development served as reference points. The completely cured polyimides (PI-400-120-1 to 4) were used to sustain $\text{C}_{2,max}$ and H_{max} while the merely dried films (PAA-080-120-1 to 10) accounted for $\text{C}_{2,min}$ and H_{min} .



(a) Schematic of the model sample [78]



(b) Depth profile of the LIBS imidization degree of the model sample [78]

Figure 6.11b shows the signal trend of the LIBS imidization degree of the layered sample. Starting with a degree of imidization of approx. 0 %, a value of 100% was reached after a steep increase around 4 μm sample depth. This trend corresponded well with the sample structure: we can assume that the top layer was hardly imidized while the fabricated bottom layer should be completely imidized after curing at 400 °C.

Regarding the signal course depicted in figure 6.11b, the ratio of top layer to bottom layer corresponded to the applied quantities of PAA (20 μl for the top versus 50 μl for the base). Also, the signal trend in the transition region could be influenced by intermixing and solvent effects when applying the top layer as a dissolved precursor solution on a cured polyimide. Another influencing factor on the signal sequence could be the ablation behavior, precisely the generated crater shapes derived from a Gaussian laser beam profile.

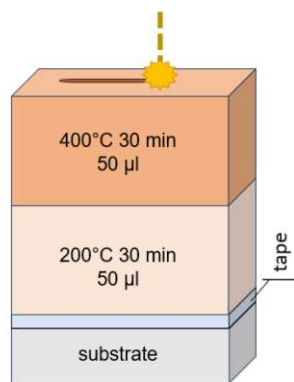
A second depth profile using LIBS was recorded, but in this case the top layer was supposed to exhibit a higher degree of imidization as the following film. For this purpose, a first layer of PAA precursor solution was cast on a substrate and cured at 400 °C for 30 min. Then, a second layer of poly(amic acid) was put on top and the whole sample was cured at 200 °C for another 30 min. Subsequently, the fabricated polyimide film was detached from the substrate using a sharp razor blade and fixated upside down using commercial tape. A schematic of the final film is illustrated in figure 6.11c.

Depth-profiling was done starting with the former bottom layer cured at 400 °C down to the less imidized layer solely cured at 200 °C. 25 Layers, each layer representing approx. 1 μm of film thickness were obtained during measurement. The signal trend of the degree of imidization is illustrated in figure 6.11d.

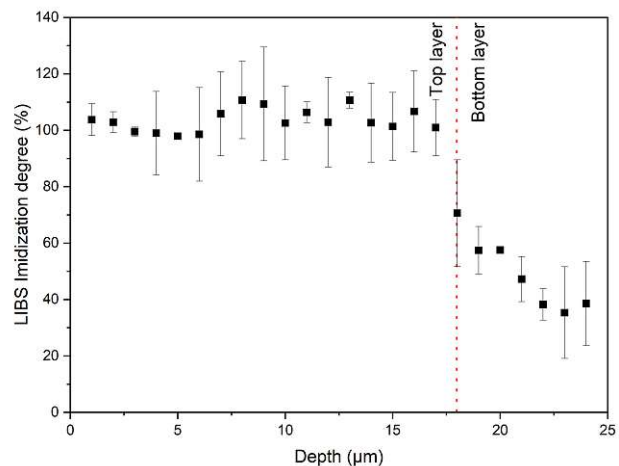
Since only one linescan covering the entire sample width was measured during LIBS

analysis, 4 average values representing the average of 20 spectra each were available. The two areas in the middle were chosen for data evaluation to exclude the edge where the degree of imidization may be influenced by thinner layer thicknesses. The selected spectra were normalized and signal intensities for the C_2 swan band and the H line were extracted and averaged per layer ($n=2$).

The same samples (PI-400-120-1 to 4 and PAA-080-120-1 to 10) were used as reference values for $C_{2,max}$, H_{max} , $C_{2,min}$ and H_{min} and the degree of imidization was calculated according to 6.2. The signal curve showed the transition from a completely imidized film to a layer with a medium degree of imidization, matching the expected trend based on the sample preparation.



(c) Schematic of the model sample



(d) Depth profile of the LIBS imidization degree of the model sample

Regarding the signal course, an average degree of imidization of $103 \pm 10 \%$ was calculated for the first 16 layers, presumably within the completely cured layer imidized at $400 \text{ }^\circ\text{C}$. Afterwards a sharp decrease to an average value of $46 \pm 9 \%$ was recorded, representing the transition from one layer to another. The transition between the two layers is also recognizable with a degree of imidization of $70 \pm 18 \%$, probably due to intermixing effects and the ablation profile as already discussed with the previous sample. Again, the calculated imidization degrees corresponded well with the values obtained during method development when compared to the average degree of imidization of $54 \pm 6 \%$ for PI-200-030-1 to 4.

6.2.2 Investigation of industry samples

To test the robustness of the developed LIBS method, the following measurements were conducted under more realistic circumstances. First, the influence of additives on the

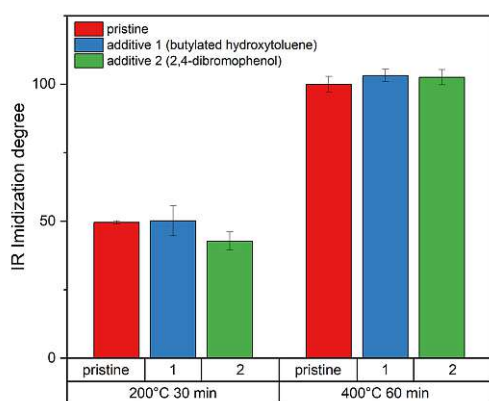
measurement method was examined, since it is very unlikely, that a commercially available polyimide might only consist of pure polymer. Second, polyimide films from industry applications were analyzed using IR spectroscopy and LIBS and the degree of imidization was calculated using self-synthesized polymer films as reference.

Influence of additive addition

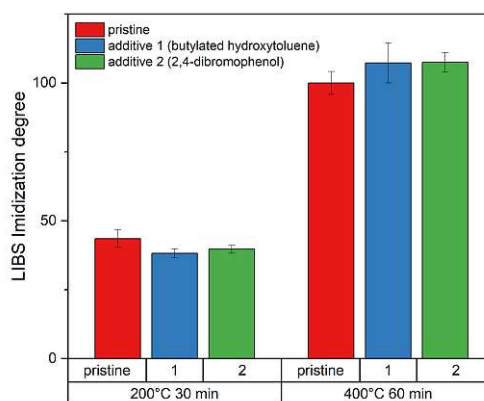
As described in chapter 6.1.1, 24 samples containing commercially available polymer additives were prepared in total. 12 samples contained approx. 2 m % of butylated hydroxytoluene, while the other 12 films included approx. the same amount of 2,4-dibromophenol. Four replicates were fabricated per exposure condition including solvent evaporation only, curing at 200 °C for 30 min and and imidization at 400 °C for 60 min. Thus, not only samples with different additives but also degrees of imidization were available.

The sample set was analyzed with both IR spectroscopy as well as LIBS. The calculation of the degree of imidization was done for both techniques and was carried out using suitable self-synthesized polyimide standards as reference points. For IR spectroscopy, the pristine film cured at 400 °C for 60 min (PI-400-060-1 to 4) was used according to equation 6.1. In the case of LIBS, non-cured (PAA-80-120-1 to 10) as well as maximum-cured (PI-400-060-1 to 4) polymer films were measured based on equation 6.2.

A comparison of imidization degrees of additive doped vs pristine polyimide films is illustrated in figure 6.11e for IR spectroscopy and 6.11f for LIBS. The calculation of the imidization degree was feasible using both techniques and similar results were obtained.



(e) IR Imidization degree of self-synthesized polyimides with commercial additives



(f) LIBS Imidization degree of self-synthesized polyimides with commercial additives

The pristine films cured at 400 °C represented 100 % imidization because they served as reference points for the calculation. Compared to that, the samples doped with additives

exhibited IDs of $103 \pm 2 \%$ (additive 1, $n = 4$) and $103 \pm 3 \%$ (additive 2, $n = 4$) based on IR spectroscopy. The same polyimide films displayed degrees of imidization of $107 \pm 7 \%$ (additive 1, $n = 4$) and $108 \pm 4 \%$ (additive 2, $n = 4$) using LIBS. For all films cured at $200 \text{ }^\circ\text{C}$, the degree of imidization was calculated based on the dedicated formula for each technique. Results from IR spectroscopy showed medium-imidized samples: $50 \pm 1 \%$ (pristine, $n = 4$), $50 \pm 4 \%$ (additive 1, $n = 4$) and $43 \pm 4 \%$ (additive 2, $n = 4$). Similar results were obtained from LIBS spectra, with medium-imidized samples exhibiting IDs of $44 \pm 3 \%$ (pristine, $n = 4$), $38 \pm 2 \%$ (additive 1, $n = 4$) to $40 \pm 2 \%$ (additive 2, $n = 4$).

These experiments showed, that the calculation of the degree of imidization was successful for both, IR and LIBS, in the presence of polymer additives and that the results for each method were consistent. Similar to the observations discussed in chapter 6.1.4, when comparing results from both techniques, slightly different values for the medium-imidized films were recorded: $50 \pm 1 \%$ (pristine, $n = 4$) for IR and $44 \pm 3 \%$ (pristine, $n = 4$) for LIBS. Again, this could be attributed to the physically different spectra that are recorded as well as different cross-sections and sampling areas covered by each technique. When comparing the absolute values between IR and LIBS, the selection of standards must also be taken into account. Because the selection of appropriate standards used as minimum and maximum imidized films is crucial for the calculation of the imidization degree. Choosing a different set of reference films might shift the calculated values accordingly.

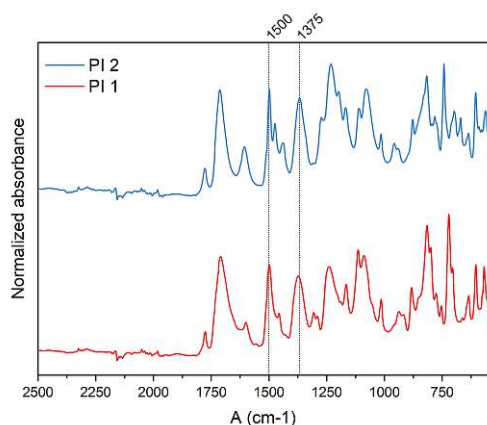
However, the calculated imidization degrees within one technique were consistent and the influence of additives on the evaluation was negligible.

Application on commercial products

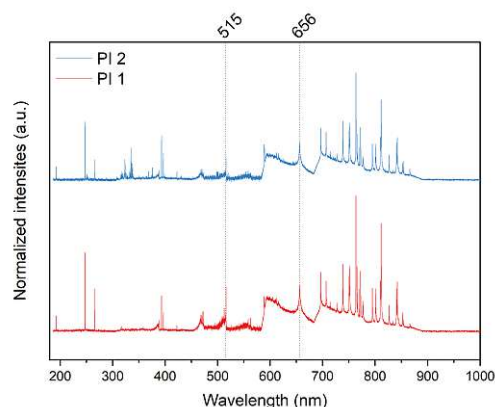
Since the addition of common polymer additives had no effect on the determination of the degree of imidization, the applicability of the developed LIBS method was demonstrated on two industry relevant polyimides. The two commercially available thin films were named PI1 and PI2. PI1 represented a general-purpose polyimide film used for applications in fiber optics, insulation tubings or as diaphragms sensors and manifolds in the automotive industry. The second polymer, PI2 was based on a photosensitive precursor commonly used in the electronics industry. The exact structures of the two polyimides are unknown, although PI1 is most likely a PMDA-ODA polyimide [75,76].

Both samples were first analyzed using IR spectroscopy. The recorded ATR-IR spectra for both products are displayed in figure 6.11g. Subsequently LIBS spectra were recorded with the established measurement parameter according to table 6.3 and representative spectra of both polyimides are shown in figure 6.11h. The spectral information used to trace the imidization reaction and ultimately calculate the degree of imidization are

emarked in the spectra for both cases. For IR spectroscopy this was the imide II absorption band between $1360 - 1380 \text{ cm}^{-1}$ and the $\text{C}=\text{C}$ aromatic ring stretching around 1500 cm^{-1} which was used for referencing. LIBS spectra were evaluated by extracting the peak area of the H emission line at 656 nm and the C_2 molecular band around 515 nm .



(g) Representative FT-IR spectra of two commercially available polyimides [78]



(h) Representative LIBS spectra of two commercially available polyimides

Based on the recorded raw data, the degree of imidization was calculated based on equation 6.1 for IR respectively equation 6.2 for LIBS. Self-synthesized polyimide films which were prepared for method development were used as reference material in this application as well. Polyimides subjected to $400 \text{ }^\circ\text{C}$ for 120 min (PI-400-1201 to 4) served as a fully cured polymer while PAA-080-120-1 to 10 was used as a hardly-imidized sample. The resulting degrees of imidization for both techniques are shown in figure 6.11.

It was clearly visible, that the results from IR spectroscopy and LIBS in the case of commercial polymer samples differ. Determining the degree of imidization based on IR spectroscopy worked for PI 1 but failed for the other product. The ATR-IR spectra in figure 6.11g revealed, that for PI 2 (blue line) the band of the aromatic ring stretching ($\text{C}=\text{C}$) around 1500 cm^{-1} was disturbed by another peak appearing on the right shoulder. Since this absorption band was used as a reference in IR spectroscopy based calculations, the determination of the peak area was affected and an unnaturally high degree of imidization was calculated for PI 2. Nevertheless, this effect could be circumvented by using an appropriate reference material instead of self-synthesized films which might differ in polymer structure. Figure 6.11 also revealed, that both samples were accessible for analysis and calculation of the degree of imidization using self-synthesized standards and LIBS, resulting in IDs of $99 \pm 8 \%$ for PI 1 and $89 \pm 7 \%$ for PI 2.

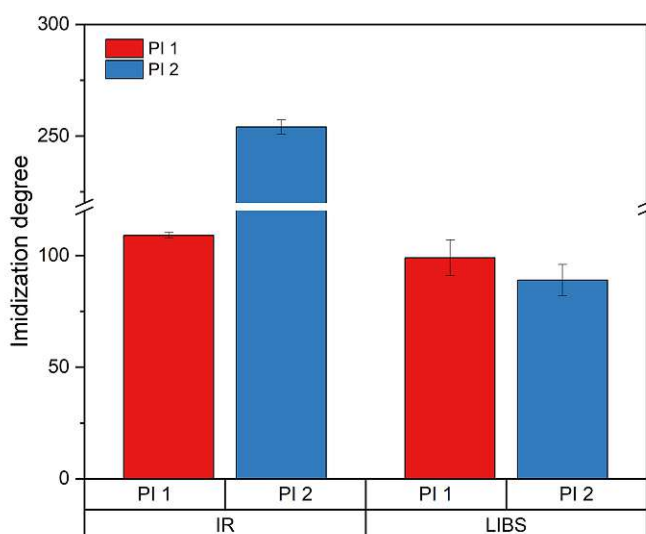


Figure 6.11: Calculated degrees of imidization for both polyimides based on IR and LIBS data [78]

6.3 In-situ monitoring of the imidization reaction

As described in the previous chapters, the thermal curing parameter had a major influence on the final properties, in this case the degree of imidization of the polymer film. To study the effect of elevated temperatures, laboratory tests with ex-situ analysis are state of the art and were also carried out during the method development for determining the degree of imidization. This included the preparation of 130 single samples, subjected to different curing temperatures and times before the method development could start. The oven program alone lasted several hours (5 x 120 min), and the curing procedure had to be carried out several times after individual optimization steps.

Before starting with the sample preparation process, however, it would be useful to test and optimize certain parameters, e.g. layer thickness, temperatures and holding times in an easy and fast way. In this case, an in-situ LIBS study would be an option. In addition, the same sample would be analyzed throughout the heating cycle, reducing the influence of sample preparation steps e.g. heat distribution in the oven or storage and reducing the overall sample preparation time. Finally, the development of the polyimide film over the sample geometry, including the thickness of the layer, could be monitored by exploiting LIBS depth-profiling capabilities.

For this reason, a feasibility test was carried out to observe the degree of imidization using an in-situ heating platform. The aim was to determine whether the imidization reaction could also be monitored with this newly developed instrumental setup and whether the influence of increased temperature on the plasma dynamics had a negative

effect on the calculation of the degree of imidization. For this purpose, in-situ (measurements at elevated temperature) and ex-situ (measurements at room temperature) tests were carried using self-synthesized polyimide samples.

The only sample preparation step necessary beforehand was the application of 50 μl of poly(amic)acid precursor solution on a gold coated silicon wafer ($10 \times 10 \text{ mm}^2$) and a drying step in a vacuum dryer (80 $^{\circ}\text{C}$ for 120 min). Afterwards, a single sample was placed in the LIBS heating chamber. A detailed description of the system configuration can be found in chapter 5.4.1. For this study, only the heating option by means of a controlled heating coil were used. The temperature program for both experiment runs, in-situ and ex-situ is illustrated in figure 6.12. The temperature was measured using a type S thermoelement adjusted between the heating coil and the sample placed above it. The accuracy of the temperature measurement was checked beforehand using test measurements with a dummy wafer and a thermocouple placed on top.

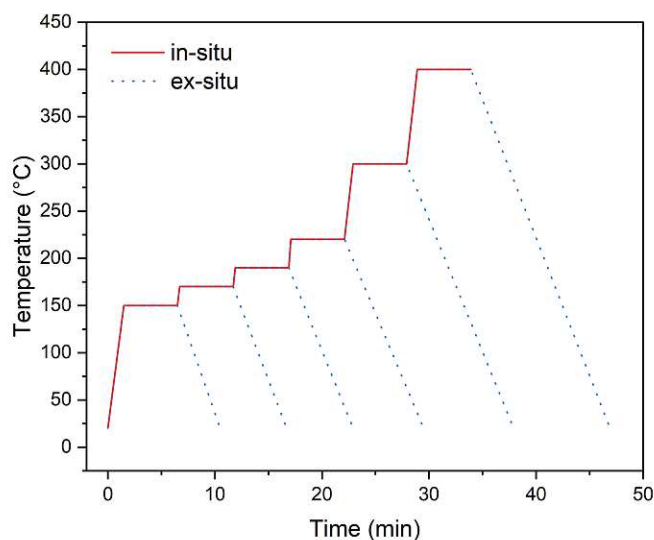
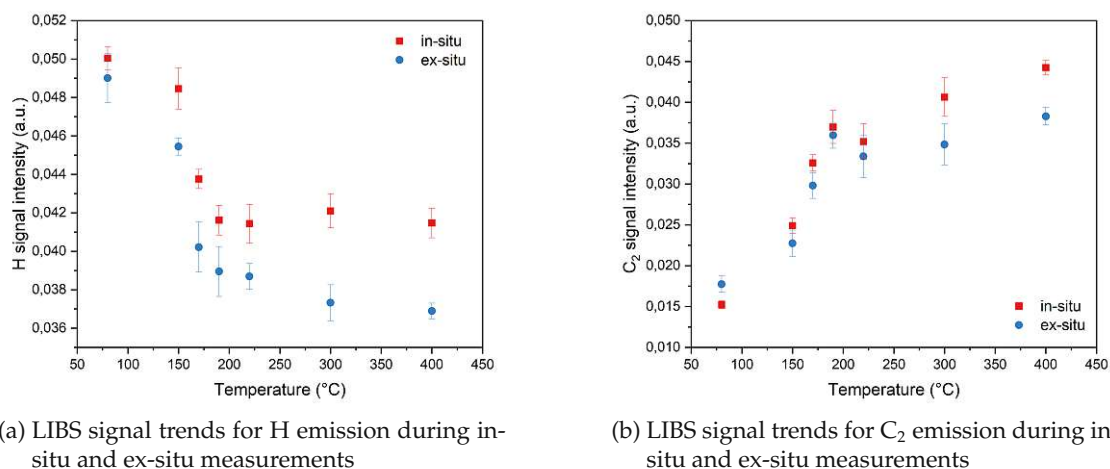


Figure 6.12: Temperature program for in-situ and ex-situ experiments

The in-situ LIBS measurement procedure and data evaluation strategy was similar to the steps performed during method development. First, the LIBS measurements were executed with parameters chosen according to the settings used during method development and are listed in table 6.3. Each sample was analyzed using three parallel linescans with adjacent, non-overlapping laser shots with a total of 60 shots per line. 20 shots each were accumulated and normalized (constant sum of squares) resulting in 9 spectra per sample. The signal areas for all polymer specific emission signals listed in table 6.4 were extracted using Epina ImageLab. In order to monitor the imidization reaction, the trends for the H emission line at 656 nm and the C₂ molecular emission around 517 nm

were plotted and are displayed in figures 6.13a and 6.13b.



Similar to the signal trends observed during method development, the H signal decreased with the advancing imidization reaction while the C₂ emission increased. Furthermore, a difference in signal intensity was determined between in-situ and ex-situ measurements, as the ongoing temperature increase during the in-situ procedure affected the overall signal level. For in-situ experiments, the signal intensities for both emission signals were higher than for measurements at room temperature.

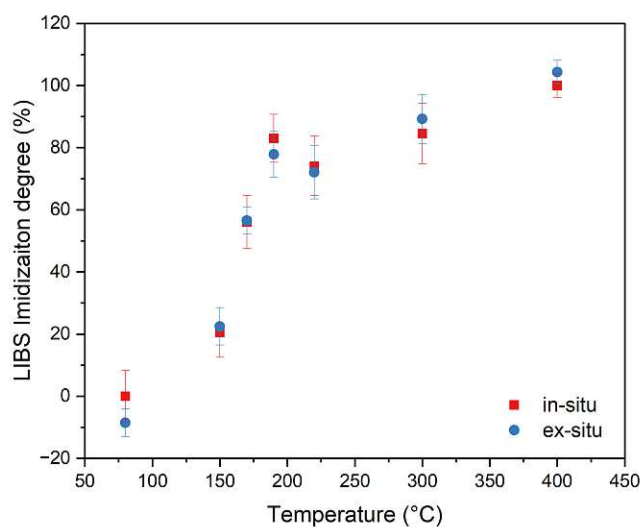


Figure 6.13: Calculated Degrees of imidization for in-situ and ex-situ imidization experiments of self-synthesized polyimides

However, to determine the degree of imidization using LIBS (see equation 6.2), the ratio C₂/H is formed and used for calculation. Thus, the increased signal intensities in

the in-situ measurements did not pose a problem and the degree of imidization could be calculated using the ex-situ sample cured at 400 °C and the ex-situ sample solely subjected to vacuum drying as reference points. The imidization degree trend measured in-situ vs. ex-situ is illustrated in figure 6.13 whereby very similar results were achieved in both cases.

This feasibility study for in-situ monitoring of the degree of imidization showed, that the instrumental setup could be successfully applied for in-situ polymer studies. For the in-situ measurement run, only one sample was needed and analyzed throughout the whole heating cycle thus decreasing the overall number of samples and preparation time necessary for an imidization study. Also, the reaction progress could be tracked continuously on the same sample avoiding alteration due to sample storage or variations due to the sample preparation steps. In the future, this method could be used for screening purposes or depth-profiling and imaging applications during elevated temperatures to study the film development in more detail.

6.4 Transferability of the proposed LIBS method

One key factor in improving the applicability of LIBS to determine the degree of imidization was the transferability of the proposed measurement procedure to different instrumental settings with different laser wavelengths. To ensure that the degree of imidization based on LIBS spectra could be determined when changing the instrumental setup, comparative measurements to the method development presented in the previous sections are shown in the following passage.

Therefore, a selection of the 130-piece calibration samples of self-synthesized PMDA-ODA were analyzed using a 193 nm laser source (imageGEO193^{LIBS}) coupled to a 5-channel spectrometer (ESLumen), equipped with a CMOS camera. An overview of the measurement parameter is given in table 6.5, while the instrument configuration can be found in section 5.4.1 in chapter 5.4. Five lines each including 80 shots, resulting in a total number of 400 spectra, were recorded per sample covering the entire width of the specimen. Subsequent data evaluation, including averaging of 80 spectra per sample and the specification of spectral descriptors was done using Iolite.

Representative LIBS spectra of a solely dried, not cured polyimide (PAA-080-120-1 to 10) and a maximum cured film (PI-400-120-1 to 4) are illustrated in figure 6.14. The C₂ swan emission band around 517 nm as well as the H(I) emission line at 656.3 nm are marked in the spectra. When comparing the two spectra, it became clear that the C₂ band increased with higher temperatures, while the H line slightly decreased. This trend was in accordance with the previous LIBS investigations regarding the monitoring of the

imidization reaction, using a LIBS system with a 266 nm laser (J200).

Laser wavelength	193 nm
Laser energy	1.2 mJ
Laser spotsize	100 μm
Sample fluence	12 J/cm^2
Frequency	100 Hz
Atmosphere	Helium
Spectrometer	Czerny-Turner
Detector	5 channel CMOS
Gate delay	0.1 μs
Gate width	3 ms
Covered wavelength range	188 - 1097 nm

Table 6.5: Measurement parameter for LIBS setup based on the imageGEO193^{LIBS} and ESLumen during method development

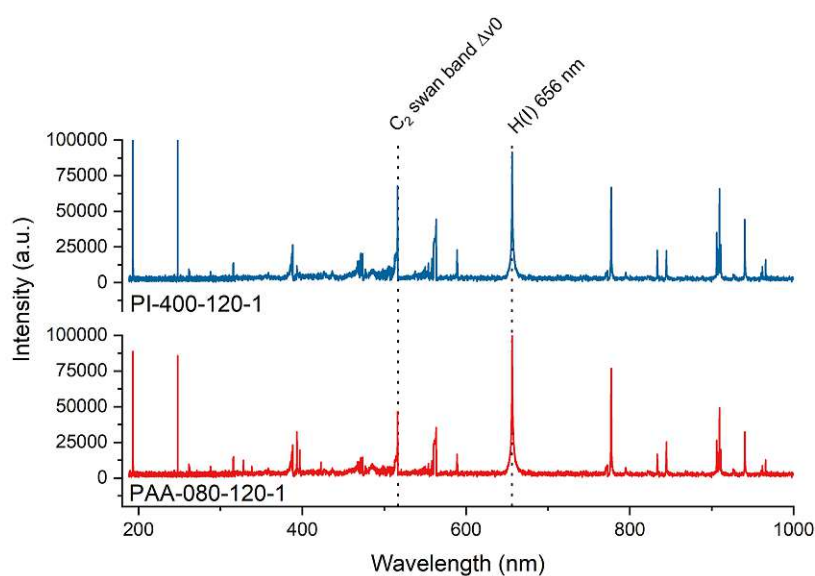


Figure 6.14: Representative LIBS spectra (average of 80 spectra, not normalized) of sample polyimides in the region from 180 - 1000 nm

The ratio of the C₂ band to the H emission served as an indicator for the imidization reaction and the signal trend for samples cured at 180°C, 300°C and 400°C is displayed in figure 6.15. The polyimide precursor solely dried at 80°C for 120 min represented the starting point of the reaction and is depicted as a dotted line. To calculate the degree of imidization according to equation 6.2, the background-corrected, integrated LIBS signal

intensities of the C_2 band and the H emission line were necessary not only from the sample but from two reference samples as well: a merely dried, non-imidized film and a maximum-imidized polyimide. Polyimides subjected to 400°C for 120 min (PI-400-120 1 to 4) served as a fully cured reference, while PAA-080-120-1 to 10 was used as a hardly-imidized sample. The calculated degrees of imidization for the analyzed sample set is shown in figure 6.15 (right y-axis) as well.

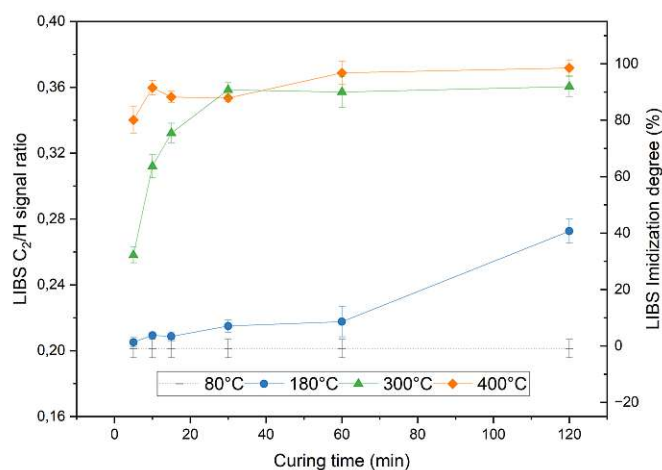


Figure 6.15: C_2/H signal trend and imidization degree for self-synthesized calibration samples exhibiting different thermal curing cycles

When comparing the data from this measurement using a 193 nm laser source (imageGEO193^{LIBS}) with the results of the method development where a different LIBS instrument (J200) was applied, a good agreement of the results emerges: the signal trend for all samples indicate an increase in C_2/H respectively imidization degree with increasing curing time and curing temperature. Also, PI-400-120-1 to 4 which was exposed to 400°C for 120 min exhibited the highest degree of imidization. At curing times of 300°C, the imidization reaction proceeded slower but imidization degrees > 80 % were reached after 120 min (imageGEO193^{LIBS}: 93 ± 2 %, J200: 83 ± 2 %) while curing at 180 °C led to medium imidized samples (imageGEO193^{LIBS}: 42 ± 1 %, J200: 41 ± 3 %).

Thus, the determination of the degree of imidization using LIBS is transferable to other instrument setups, especially the presented 193 nm laser source and dedicated spectrometer. Therefore, this system was used to further investigate structural alterations in commercial polyimide films.

7 Polymer films exposed to migration cell experiments

The chemical structure of polyimide significantly affects ion diffusion and migration through its influence on the polymer's morphological and microstructural properties. Therefore, analytical techniques which do not only provide information about one or the other are of great interest. The capability of LIBS to monitor structural changes within the polyimide network in the form of the imidization reaction were demonstrated in the previous chapter.

In this chapter, a procedure to determine the uptake and distribution of ions as well as changes within the polymer structure of stressed polyimide samples is presented. For this purpose, commercially available polyimide films were put in a migration cell setup under varying conditions, e.g. electrolyte composition, voltage or duration to simulate electrochemical migration. Subsequently, the specimen were examined using LIBS to obtain information about the lateral and depth resolved distribution of harmful analytes. Furthermore, the existence of structural variations based on the previously implemented measurement method to determine the degree of imidization were applied. In the case of migrating substances, K and Cl were the analytes of interest and thorough method development was undertaken to reach optimum sensitivity for both elements. In the case of LIBS, reducing the ambient pressure by using a self-build heating and vacuum chamber was one strategy to increase sensitivity for Cl determination. The other option was, switching to LA-ICP-MS altogether and utilizing lower detection limits.

Finally, the laser based methods were expanded to traditional polymer analysis to learn more about structural variations and increase surface sensitivity by introducing IR spectroscopy or contact angle measurements.

7.1 LIBS investigations of exposed polymer films

In the course of migration cell experiments, a variety of tested polyimide films has been produced, which were examined both in terms of ion absorption and changes in polymer structure. The migration cell experiments were conducted with varying electrolytes but the main focus during this work was to investigate the distribution of K and Cl within a

polyimide thin film. Besides that, changes in polymer structure due to the migration cell exposure were of great interest. Since it was successfully demonstrated to monitor the imidization reaction of polyimides using LIBS, it should be possible to detect the reverse reaction, the hydrolysis of an imide bond with this technique, as well.

All investigations at this point were performed on fully cured, commercially available polyimide films. After the migration cell exposure, the films were rinsed using deionized water and stored in plastic bags covered in lint-free cloth. In the case of free standing films, the polyimide was first split in half using a scalpel and then fixated on a 30 x 30 mm² silicon wafer using double sided tape. To obtain images from both stressed sides (anodic and cathodic), the two halves were secured with the desired side at the top. Polymer films subjected to the single sided setup were used as is, since they were already attached to a suitable substrate for analysis.

7.1.1 J200

First, the polyimide films subjected to migration cell exposure were investigated using a commercially available LIBS instrument (J200), equipped with an additional optical spectrometer (SpectraPro HRS-750 with PI-MAX-4) for amplification of the Cl(I) emission line at 837.6 nm. An overview of the measurement parameter is given in table 7.1. In general, the fixated films were analyzed using adjacent linescans covering the entire stressed area and the recorded maps were evaluated using Epina ImageLab (Version 4.09, Epina GmbH).

The elemental maps of K, Cl, H and C₂ of a representative polyimide film are displayed in figure 7.1. The presented sample was measured using 60 parallel linescans with a diameter of 100 100 μm, covering a total area of 18 x 6 mm² resulting in 10 800 single spectra. Both maps, recorded with the broadband spectrometer from the J200 as well as with the additional optical spectrometer for Cl detection were imported into Epina ImageLab for normalization (constant sum of squares) and the selection of spectral descriptors. To analyze the lateral distribution of K and Cl, the K(I) emission lines at 766.5 nm and 769.9 nm and the Cl(I) emission at 837.6 nm were selected and displayed as elemental maps in the figure below. Additionally, the C₂ emission band around 517 nm as well as the H(I) emission line at 656.3 nm were selected based on previous LIBS investigations of polyimide structures (see chapter 6 presenting a LIBS measurement technique to determine the degree of imidization based on the C₂ and H emissions).

As can be seen in figure 7.1, the area where the polyimide film was in contact with the aqueous KCl was clearly visible. It could also be shown, that the analytes K and Cl seemed to be evenly distributed within the exposed area. Also, small wholes, originated from previous test measurements were visible in the Cl distribution pattern.

J200

Laser wavelength	266 nm
Laser energy	3.2 mJ
Laser spotsize	100 μm
Sample fluence	10.2 J/cm ²
Frequency	10 Hz
Atmosphere	Helium
Spectrometer	Czerny-Turner
Detector	6 channel CCD
Gate delay	0.3 μs
Gate width	1.05 ms
Covered wavelength range	188 - 1048 nm

SpectraPro HRS-750 with PI-MAX-4

Slit width	200 μm
Grating	1800 g/mm
Center wavelength	837 nm
Covered wavelength range	833 - 841 nm
Gate delay	0.3 μs
Gate width	5 μs
Intensifier gain	10

Table 7.1: Measurement parameter for the mapping of polyimide films exposed to migration cell experiments

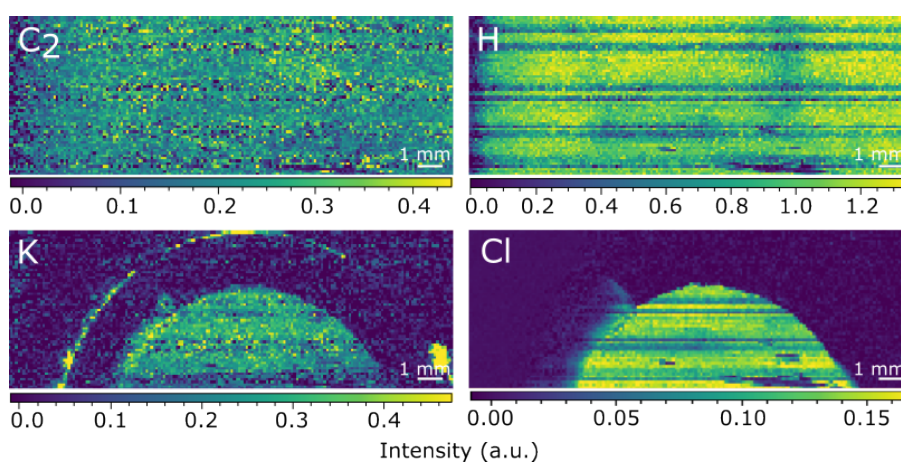


Figure 7.1: LIBS mapping of exposed polyimide thin film (PI2-mig-double-KCl-20220429, anodic side) using the J200 and an additional optical spectrometer equipped with an iccd camera

All in all, the sensitivity of the LIBS setup (J200 + additional ICCD spectrometer) appeared sufficient to investigate the distribution of K and Cl within a polymer film after migration cell experiments with a certain exposure period (whereby quantification has not yet been carried out).

In contrast, no changes in the C₂ or H signal could be detected, indicating no or not sufficient changes in the imidization degree. It must be noted that the polyimide film displayed here (PI2-mig-double-KCl-20220429) was subjected to the migration cell experiment in the double-sided configuration, where a freestanding polyimide film was tested. Therefore, an anodic as well as a cathodic side of the film was available for investigation (more details concerning the migration cell setup can be found in chapter 5.3). On the anodic side, it was assumed that due to the consistent pH level during the exposure probably no hydrolysis of the polyimide occurred.

Besides sensitivity for elemental detection and structural investigations, the ablation behavior as well as time expenditure were considered. Especially the beam profile, achievable depth-resolution and measurement time were important performance indicators since the aim was to provide a fast and easy measurement method for routine analysis of stressed polymer films.

Regarding the depth-resolution, an ablation depth of 1 - 2 μm depending on the type of polymer (self-synthesized, commercial) and curing parameter was achieved when using a sample fluence of approx. 10.2 J/cm² and adjacent shots with the 266 nm laser. However, the ablation craters are not flat but have a Gaussian beam profile, typical for the type of laser used.

Another important performance indicator was the overall measurement time. Every recorded line comprised of 100 warm up and 180 measurement shots, resulting in a total of 16 800 laser shots. With a repetition rate of 10 Hz, the total measurement time was approx. 45 min, whereat only half of the exposed film was investigated. Since it was necessary to implement a method for routine analysis of the tested polymer films, switching to a faster laser system for LIBS analysis became necessary.

7.1.2 imageGEO193

The combination of the imageGEO193^{LIBS} laser and the ESLumen was another option for LIBS analysis of the sampled polyimides facilitating higher depth resolution (ablation depth per laser pulse 150 - 180 nm for polymer films possible), a flat-top beam profile and faster measurement times (repetition rates of up to 100 Hz feasible). The measurement parameter frequently used for polyimide imaging are listed in table 7.2. Regarding the depth resolution, an overall ablation depth of 800 nm was achieved when working with the listed sample fluence of 12.2 J/cm² and the measurement time for mapping half

an exposed polyimide film was reduced to approximately 3 min. All subsequent data analysis was done using Iolite.

Laser wavelength	193 nm
Laser energy	1.2 mJ
Laser spotsize	100 μm
Sample fluence	12.2 J/cm ²
Frequency	100 Hz
Atmosphere	Helium
Spectrometer	Czerny-Turner
Detector	5 channel CMOS
Gate delay	0.1 μs
Gate width	3 ms
Covered wavelength range	188 - 1097 nm

Table 7.2: Measurement parameter for LIBS setup based on imageGEO193^{LIBS} and ESLumen mapping of migration cell samples

Figure 7.2 and 7.3 show the elemental maps of an exemplary polyimide sample exposed to the migration cell stress test in the double sided configuration. Images were obtained from both, the anodic as well as the cathodic side from the fixated films. LIBS images were recorded using the measurement parameter listed in table 7.2, whereat the samples were scanned line by line resulting in 228 x 71 spectra each. Important for the interpretation of the migration cell experiment were the K (766.5 nm) and Cl (837.6 nm) distribution, as well as differences in the C₂ (516.5 nm) and H (656.3 nm) signal between the stressed and non-stressed area to assess the imidization. Figure 7.2 represents the anodic side of the measurement setup. Similar to sample PI2-mig-double-KCl-20220429, which was presented in the previous chapter, the stressed area was clearly recognizable by the occurrence of K and Cl and both analytes were evenly distributed. In the case of K, accumulation on the outside of the sealing ring was also noticeable. Based on the applied voltage during the migration test, only K should have penetrated into the polymer from this side. During the experiment, however, Cl₂ was formed on the anodic side, which was presumably the source of the detected Cl. Regarding the distribution of C₂ and H, no difference between the stressed and non-stressed zone was visible, similar to the previous sample and probably due to the constant pH value.

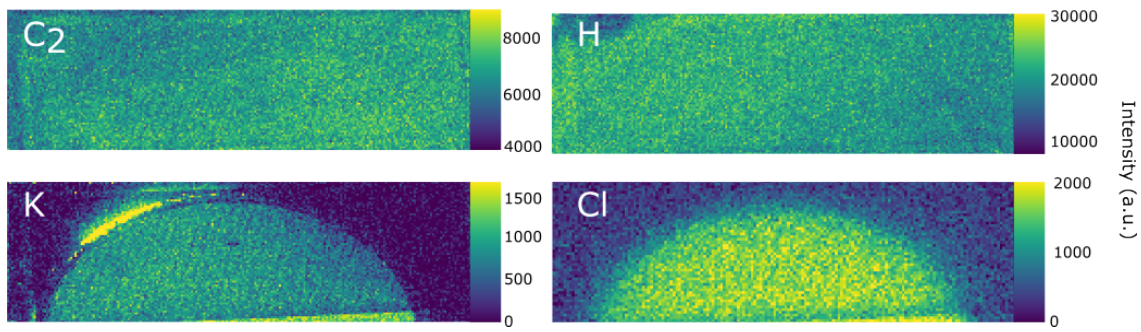


Figure 7.2: LIBS mapping of exposed polyimide thin film (PI2-mig-double-KCl-20220719, anodic side) using the imageGEO193^{LIBS} system

Regarding the cathodic side in figure 7.3, no uniform uptake of K or Cl could be detected. Solely, deposits of K were present in the first layer visible as a bright band in the top area of the elemental map. Also, no Cl uptake could be determined using the selected instrumental setup. As for the polymer-based signals C₂ and H, again no difference between the stressed and non-stressed area was apparent, although the pH value should increase in the course of the experiment and thus hydrolysis of the polyimide would be possible. Meaning, that either the proposed method is not sensitive enough to detect any changes within the polymer or no hydrolysis has taken place.

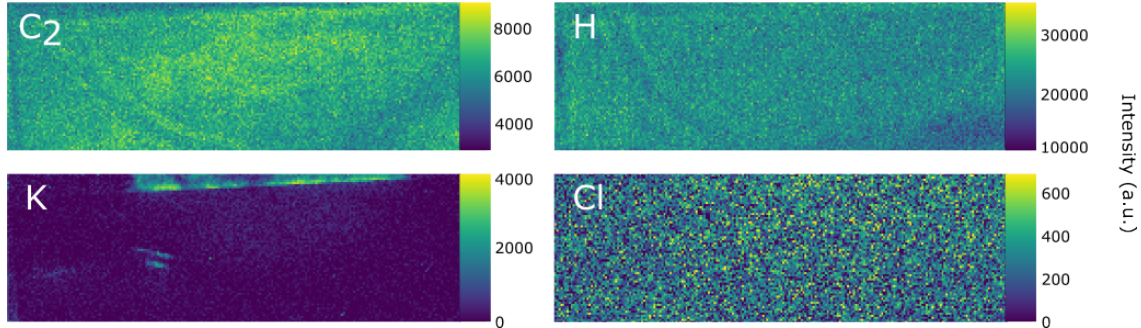


Figure 7.3: LIBS mapping of exposed polyimide thin film (PI2-mig-double-KCl-20220719, cathodic side) using the imageGEO193^{LIBS} system

In order to find out more about the processes taking place in the course of the migration cell experiment, e.g. at what point in time the uptake of K and Cl occurs, and also to optimize the measurement setup to the specifications needed, time-limited experiments were carried out. For this purpose, several polyimide films were subjected to the same set of parameters regarding electrolyte concentration and voltage but the experiment was interrupted after different times, in particular the time after a sharp increase of current was set to 0 h, 2 h, 4 h, 8 h and 16 h. The measurement parameter for the LIBS setup (imageGEO193^{LIBS} laser and ESLumen) were slightly optimized (Laser energy: 2.7 mJ,

Laser spotsize: 150 μm) to obtain higher sensitivity and increase depth-resolution but were still based on the initial parameter from table 7.2.

Figures 7.4 and 7.5 show the elemental mappings of the Cl and K uptake of the anodic side after the specified exposure time. Cl (I) at 837.6 nm and K (I) at 766.5 nm were chosen for the representation. In both cases, the signal intensity increased with increasing exposure time.

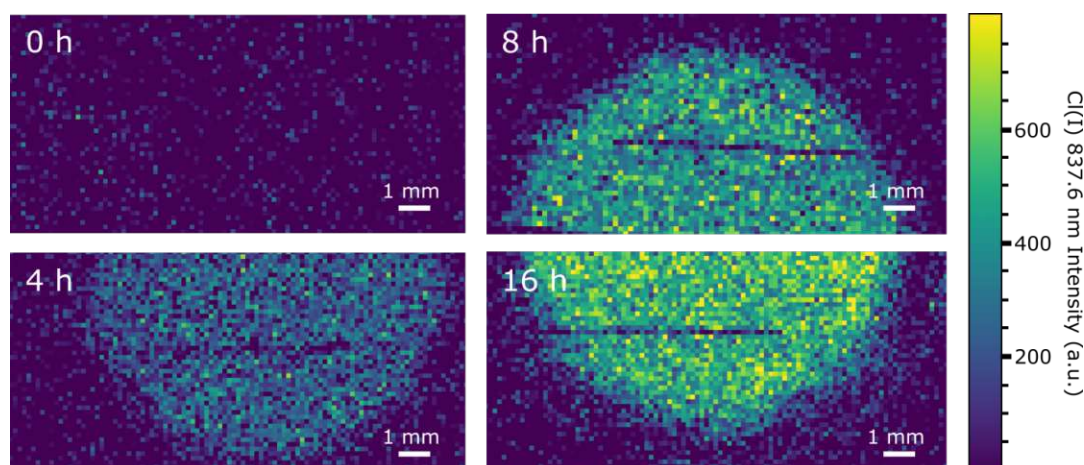


Figure 7.4: LIBS mapping of Cl distribution within exposed polyimide thin films (PI1-mig-double-KCl with exposure times from 0 h - 16 h, anodic side) using the imageGEO193^{LIBS} system

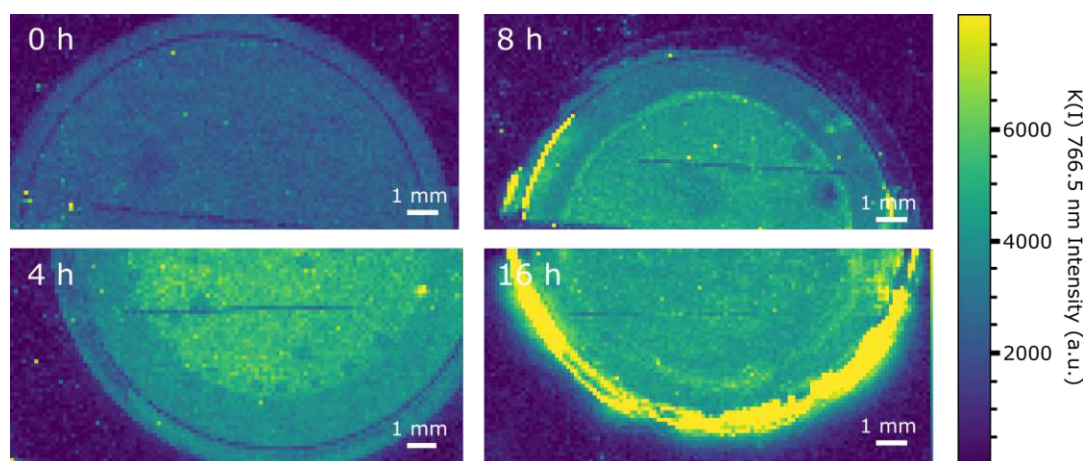


Figure 7.5: LIBS mapping of K distribution within exposed polyimide thin films (PI1-mig-double-KCl with exposure times from 0 h - 16 h, anodic side) using the imageGEO193^{LIBS} system

In addition to the lateral information collected from the polymer surface, the uptake and distribution over the polymer thickness was equally important. Figure 7.6 shows

the LIBS depth profile, recorded in the form of subsequent, 2-dimensional layers of an exemplary sample (PI1-mig-double-KCl-2h). A depth resolution of 800 nm was achieved using the same system parameter as for the maps presented above, covering a total of 4 μm from an 12 μm thick film. Another set of maps showing the subsequent 4 μm (5 layer) is available but no changes in intensity or distribution were recorded and the graphical representation was therefore omitted.

Besides the distribution of K and Cl, images of the H emission signal and C_2 molecular band were evaluated but no changes between stressed and non-stressed areas or within the polymer depth were measured.

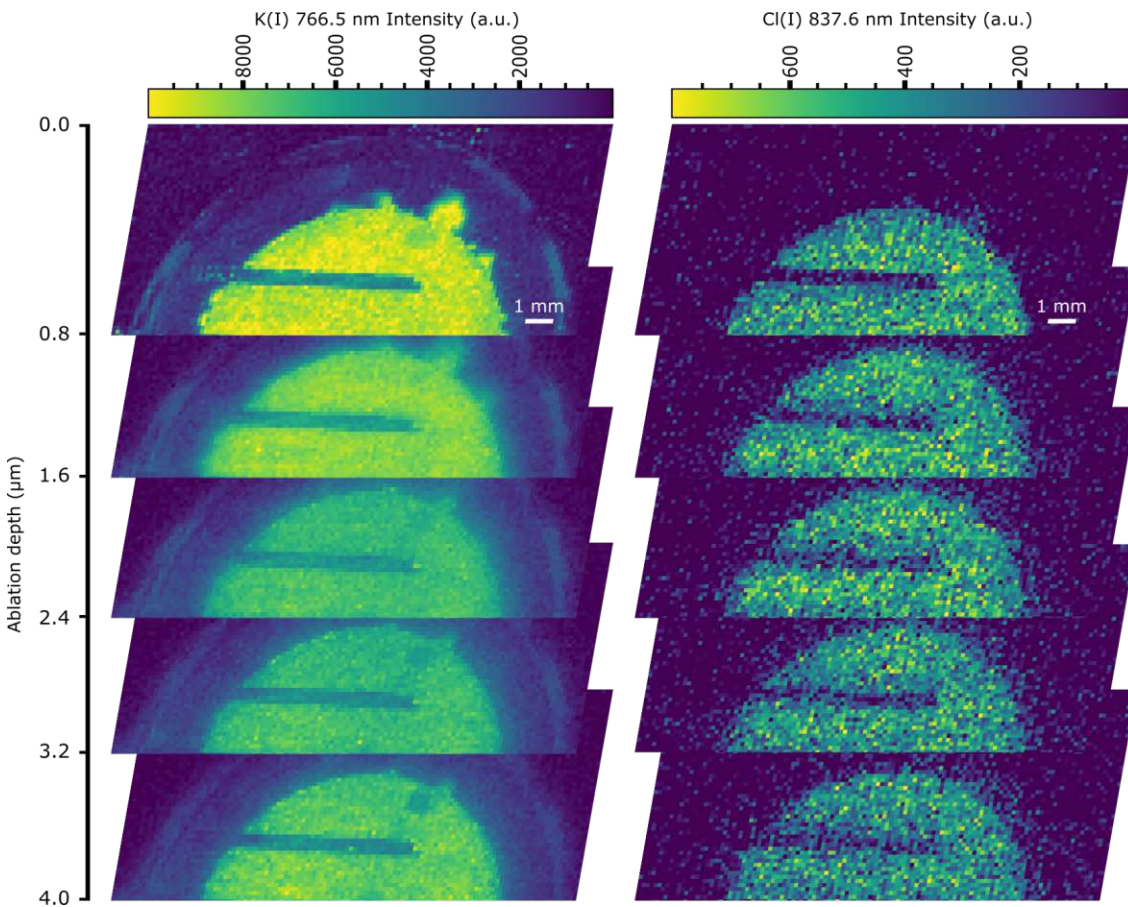


Figure 7.6: Depth-resolved visualization of the K and Cl distribution within an exposed polyimide thin film (PI1-mig-double-KCl-2h, anodic side) using the imageGEO193^{LIBS} system

The images in figure 7.6 show, that both analytes were evenly distributed throughout the investigated depth of the polymer film. The darker lines in the stressed area were due to previous test measurements for parameter optimization, but besides that a homogeneous distribution was visible. Also, it seemed as if the signal intensity was

highest in the outermost layers, especially for the K uptake. To investigate the matter further and save measurement time at the same time, depth profiling based on subsequent linescans with a diameter of 100 μm covering the width of the stressed sample area (approx. 8 mm) was introduced. Based on instrument availability and also to increase sensitivity for Cl detection, the imageGEO193^{LIBS} was coupled to an additional optical spectrometer with an ICCD camera (SpectraPro HRS-750 with PI-MAX-4, see chapter 5.4). The measurement parameters listed in table 7.3 were chosen for LIBS depth profiling. To increase depth-resolution, the sample fluence was decreased and 20 subsequent layers were measured from each side (anodic, cathodic) with an average removal depth of 200 nm. Also quantification of the measured depth profiles was done using in-house calibration standards prepared from polymer films and powder compacts. More details on the preparation of the standards is available in section 5.3.3.

imageGEO193^{LIBS} laser system

Laser wavelength	193 nm
Laser energy	0.6 mJ
Laser spot size	100 μm
Sample fluence	5.0 J/cm ²
Frequency	100 Hz
Atmosphere	Helium
Spectrometer	not available

SpectraPro HRS-750 with PI-MAX-4

Slit width	200 μm
Grating	1800 g/mm
Center wavelength	836 nm
Covered wavelength range	832 - 840 nm
Gate delay	0.2 μs
Gate width	1 μs
Intensifier gain	100

Table 7.3: Measurement parameters for the mapping of polyimide films exposed to migration cell experiments

The results of the depth profiling measurements are illustrated in figure 7.7 representing the same polyimide as in the previous mappings (figures 7.4 and 7.6). Figure 7.7a shows the calibration curve for the LIBS measurements using solid, polymer-based standards with a Cl content ranging from 0.4 - 10 m%. The limit of detection (LOD) for Cl was calculated using the formula

$$LOD = 3.3 * \frac{S_y}{S} \quad (7.1)$$

based on the standard deviation of the response S_y and the slope S of the calibration curve. The signal trends of the measured depth profiles is depicted in figure 7.7b, indicating that the amount of Cl taken up by the polymer does depend on the selected exposure time. The data points and error bars in the graph were calculated from two different samples exposed to the same conditions by averaging the linescan from both samples from the same sample depth. The ablation depth of the each single layer was determined by profilometer measurements (DektakXT, Bruker) and was approximately 200 nm per linescan.

The calculated LOD is also shown in the diagram and calculations based on the equation 7.1 resulted in a value of 0.71 m% Cl. Although the chosen LIBS setup fulfilled the desired requirements regarding speed and depth resolution, the sensitivity of the method was not satisfactory for further investigations.

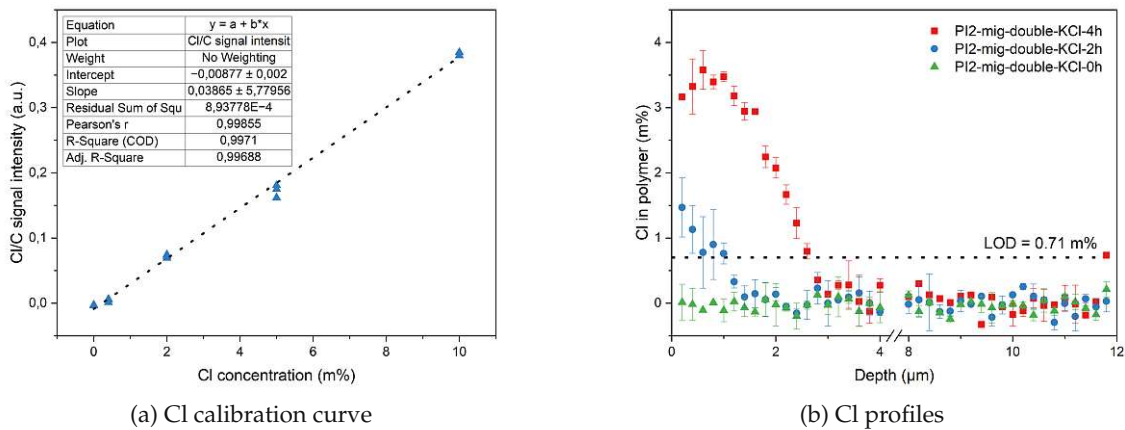


Figure 7.7: Cl depth profiling of exposed polyimide films using LIBS

7.2 Increasing sensitivity to detect ion migration

Based on the LIBS measurements presented in the previous sections, it could be shown that the analytes of interest, K and Cl, enter the polymer after a certain period of time and from a certain side within the course of the migration cell exposure. Furthermore, both species were evenly distributed throughout the stressed area of the polymer film. In order to increase sensitivity, especially for the determination of Cl two alternative approaches were implemented: switching from LIBS to LA-ICP-MS and LIBS under reduced pressure. Results based on both methods will be presented in the following chapters.

7.2.1 Depth-profiling using LA-ICP-MS

LA-ICP-MS measurements were conducted using the imageGEO193^{LIBS} laser system, coupled to an iCap Qc ICP-MS system, using PTFE tubing and a Dual Concentric Injector (DCI) interface. More details regarding the individual components can be found in chapter 5.4. Same as for LIBS measurements, LA-ICP-MS experiments were conducted on solid polyimide thin films attached to a wafer. No prior sample preparation aside from sectioning and fixation using double sided tape was necessary in the case of free standing films. Samples already attached on a suitable substrate were used as is.

The optimized measurement parameter applied for depth profiling of exposed polyimide thin films are displayed in table 7.4. The profiles were recorded using 25 consecutive line scans on the same sample location covering the entire width of the stressed sample area, which is approx. 8 mm. Each line scan resulted in one transient ICP-MS signal per isotope which was averaged over the entire duration of around 1.5 s. For each film, depth profiles were sampled at 3 different locations, separated by 100 μm . All ICP-MS measurements were conducted in KED mode to minimize polyatomic interferences of the isotopes chosen for Cl and K determination. For data evaluation, the K and Cl analyte signals were normalized by the recorded C-signal.

imageGEO193^{LIBS} laser system	
Laser wavelength	193 nm
Laser energy	0.24 mJ
Laser spotsize	100 μm
Sample fluence	2.0 J/cm ²
Frequency	100 Hz
Carrier gas flow rate	800 ml/min He

Thermo Fisher iCAP Qc	
Plasma power	1500 W
Auxiliary gas flow rate	0.8 l/min
Cool gas flow rate	13 l/min
KED gas flow rate	3 ml/min (10% H ₂ in He)
Isotopes	¹³ C, ³⁵ Cl, ³⁹ K
Dwell times	10 ms (¹³ C, ³⁹ K), 50 ms (³⁵ Cl)

Table 7.4: Measurement parameter for depth-profiling of polyimide films using LA-ICP-MS

Quantification was done using in-house calibration standards based on doped polyimide thin films in the concentration range from 0.02 – 0.37 m% for K and 0.04 – 1.5 m%

for Cl. More information on the preparation of the standards is given in section 5.3.3. The calibration curves for both Cl and K are displayed in figures 7.8a and 7.8b.

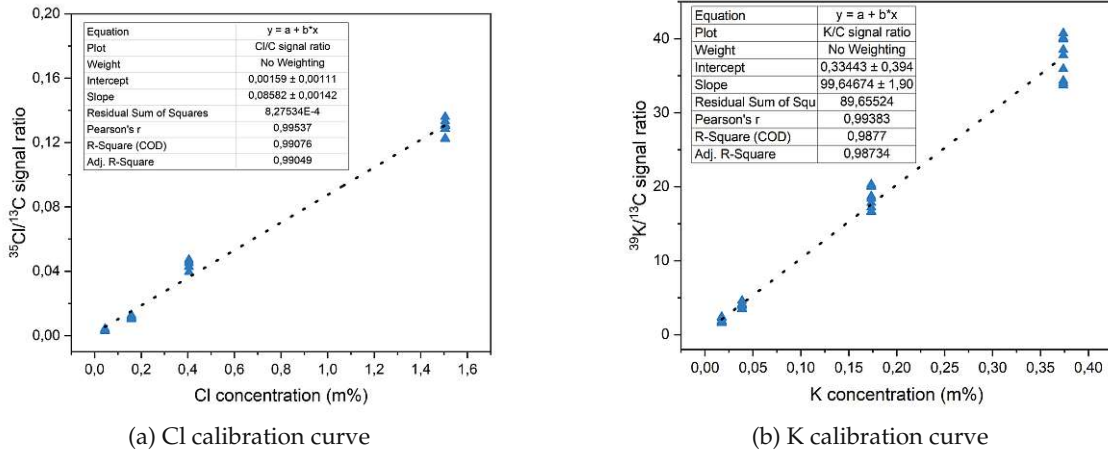


Figure 7.8: calibration curves for Cl and K determination using LA-ICP-MS based on doped polyimide films

The quantified depth profiles for 3 samples, exposed to the migration cell treatment for different amounts of time (same as in figure 7.7 for LIBS analysis) are illustrated in figure 7.9. The data points and error bars in the graph were calculated from the averages of the 3 lines scans from the same sample depth. The ablation depth of the each single layer was determined by profilometer measurements (DektakXT, Bruker) and was approximately 220 nm per linescan. The LOD was calculated in the same way as in the previous section, based on equation 7.1 using the standard deviation of the response and the slope of the calibration curve.

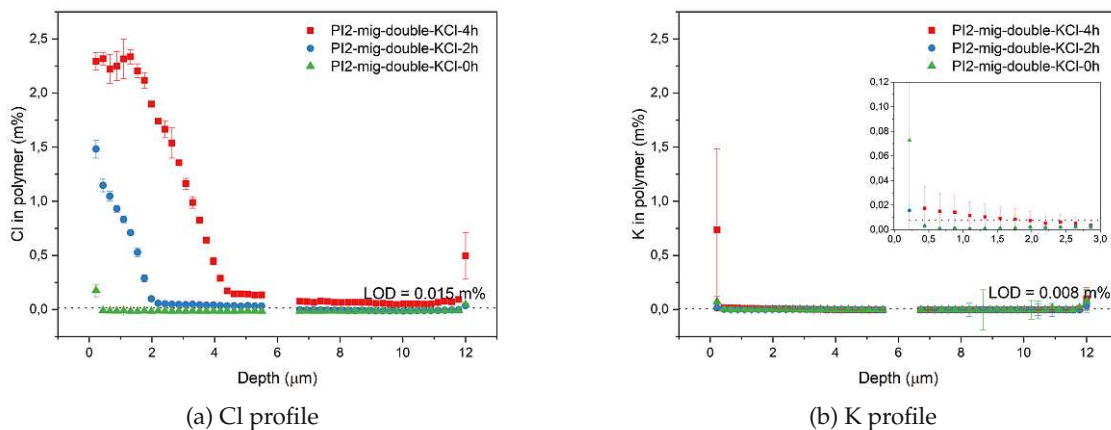


Figure 7.9: Depth profiles for Cl and K uptake of exposed polyimide films using LA-ICP-MS

The signal trends for the Cl and K uptake for three samples including the calculated LOD values illustrated in figures 7.9a and 7.9b represent exemplary depth-profiling trends regarding the total of samples investigated. The presented samples depict standards exposure conditions with varying experiment times to investigate the influence of the exposure time. Regarding the Cl distribution, both LIBS (see figure 7.7) and LA-ICP-MS provided significant insight into the distribution of the element. But LA-ICP-MS provided better sensitivity and thus a lower LOD (0.71 m% LIBS vs. 0.015 m% LA-ICP-MS) for Cl detection. Therefore, it was possible to decrease laser energy and improve depth-resolution from 800 nm to 200 nm. Compared to the Cl uptake, the amount of K detected inside the polymerfilm was lower, in the ppm range instead of m% and only detectable after a certain exposure period.

Besides the double chamber setup, used for the samples discussed in previous sections, commercial polymer films deposited on a gold coated silicon wafer were investigated using the single chamber setup. The measurement procedure to determine the Cl and K distribution was the same for both experimental conditions, but the Cl and K profiles were only obtained from one side since the polymer film stayed attached to the substrate. Therefore, a total number of 50 layers was ablated and a depth resolution of approx. 150 nm was achieved. Also, a different ICP-MS system was used but similar conditions adjusted as far as possible. An overview of the measurement parameter is given in table 7.5.

imageGEO193^{LIBS} laser system	
Laser wavelength	193 nm
Laser energy	0.26 mJ
Laser spotsize	150 μm
Sample fluence	1.2 J/cm ²
Frequency	100 Hz
Carrier gas flow rate	800 ml/min He
Thermo Fisher iCAP TQ	
Plasma power	1550 W
Auxiliary gas flow rate	0.89 l/min
Cool gas flow rate	14 l/min
KED gas flow rate	3.5 ml/min (He)
Isotopes	¹³ C, ³⁵ Cl, ³⁹ K
Dwell times	10 ms

Table 7.5: Adapted measurement parameter for depth-profiling of polyimide films using LA-ICP-MS with a different MS system

The exemplary signal trends for the K and Cl uptake of the exposed samples are shown in figures 7.10a and 7.10b and again the amount of both analytes within the film seemed to be dependent on the total exposure time. Also, due to the applied voltage and experiment conditions in general, significantly less Cl migrated into the polyimide.

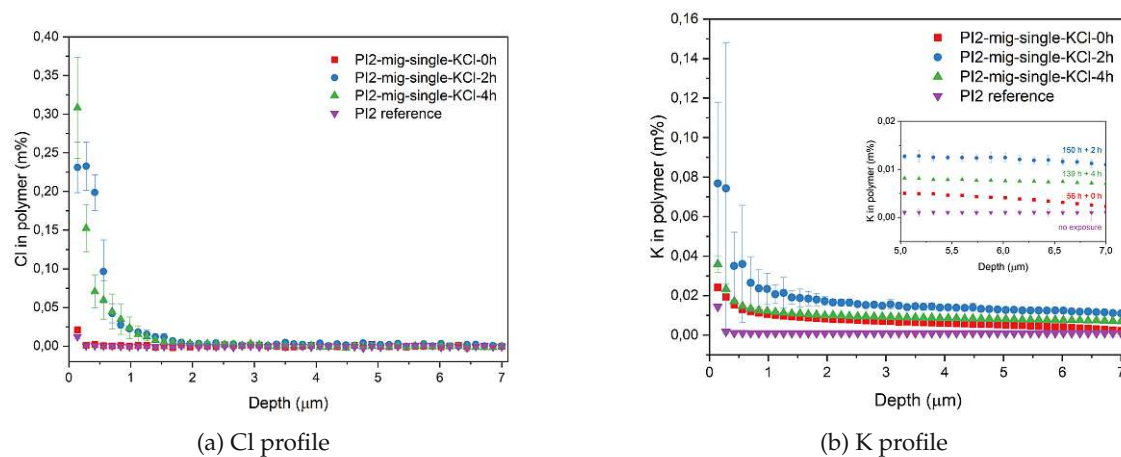


Figure 7.10: Depth profiles for Cl and K uptake of exposed polyimide films in the single sided setup using LA-ICP-MS

In conclusion, using LA-ICP-MS a significant improvement in sensitivity and depth-resolution compared to LIBS measurements could be achieved. But in contrast to LIBS, LA-ICP-MS was only used for depth-profiling using subsequent linescans and not applied for imaging due to severe problems regarding the wash-out behaviour of C and Cl. Especially for Cl, high wash-out times > 100 ms were observed based on the amount of material that needed to be transported for sufficient sensitivity. Also contributing, Cl has to be transported as a gas and therefore generally exhibits poorer wash-out behavior than other elements present in the form of particles.

7.2.2 LIBS under reduced pressure

Another approach to increase the sensitivity for the detection of Cl within a polymer matrix while still offering imaging and depth-profiling applications was the application of reduced pressure during LIBS measurements. Based on changing plasma dynamics, this should result in enhanced sensitivity for certain elements. In order to achieve LIBS measurement under defined pressure conditions, a self-built sample chamber, also applicable for in-situ heating experiments (more details see 5.4.1) was integrated into a commercial LIBS system (for more details on the J200 see chapter 5.4.1). The sample chamber was flushed with a small He or Ar stream (0.2 l/min) during measurement and the exhaust was connected to a laboratory pump (Welch IImvacTM LVS-laboratory vacuum system)

for pressure control. Furthermore, an additional optical spectrometer (for more details on the SpectraPro HRS-750 with PI-MAX-4 see chapter 5.4.1) was connected to the LIBS instrument for amplification of the Cl(I) emission line at 837.6 nm. An overview of the instrumental setup is shown in figure 7.11.

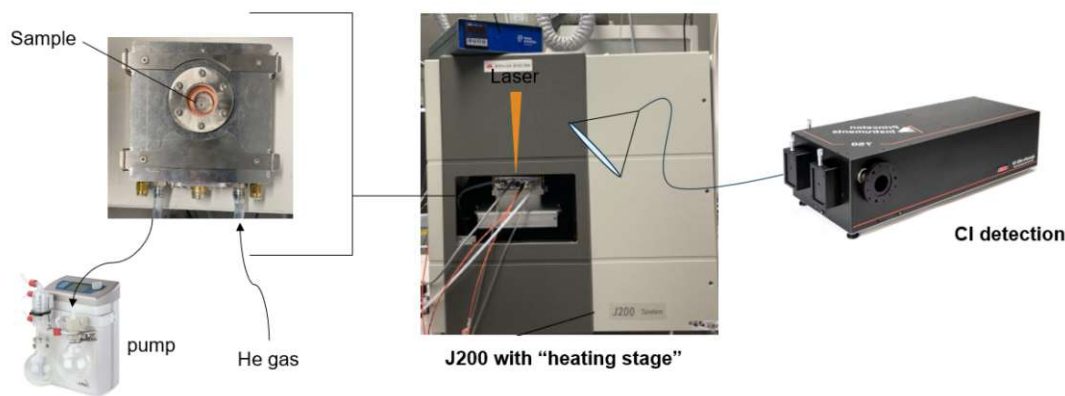


Figure 7.11: Setup for in-situ LIBS measurements

First, different measurement parameter like atmosphere, pressure and gate delay were optimized using a polymer based standard with a Cl content of 0.4 m% (polymer thin film based on P84 doped with 4-Chlorobenzoic acid, more details on the preparation of in-house standards are available in chapter 5.3.3). The sample was placed in the ablation chamber and purged with either He or Ar for approx. 2 min before starting the measurements. For analysis under atmospheric pressure, the He or Ar flow rate was set to 1 l/min, during reduced pressure measurements, the flow was decreased to 0.2 l/min. The spectrometer was set to a central wavelength of 836 nm to record the Cl(I) emission line at 837.6 nm as well as the C(I) emission at 833.5 nm. The gate delay was held constant at 0.1 μ s during all measurements and the gain was set to 10. Finally, a total of 100 spectra was averaged per recording. The results for the Cl determinations with different pressures applied is illustrated in figure 7.12a for Ar and in figure 7.12b for He atmosphere.

The figures 7.12a and 7.12b clearly show that He atmosphere was generally preferable for the detection of Cl at 837.6 nm. In Ar atmosphere, the Cl emission line was barely visible even at low pressures while in He atmosphere 0.4 m% Cl could be detected even under atmospheric pressure. With decreasing pressure, the emission intensity and peak shape changed resulting in higher intensities and narrower peaks. For the depicted Cl standard the peak height for the Cl emission increased from an average of 700 counts (1013 mbr He) to 1200 counts (100 mbar He) and the background (average between 836 - 836.5 nm) decreased from approx. 7600 counts to 4100 counts. Therefore, a pressure

7 Polymer films exposed to migration cell experiments

of 100 mbar under a light He flow was chosen as the optimum condition for further investigations.

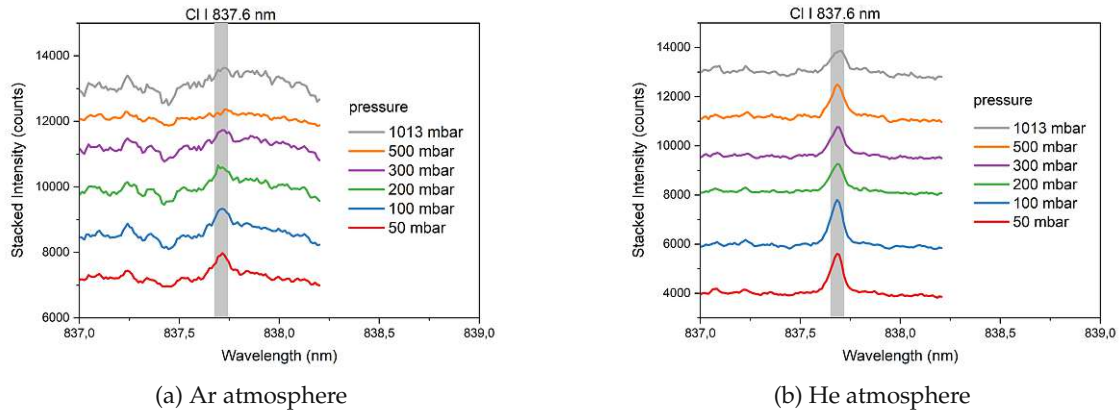


Figure 7.12: Stacked LIBS spectra ($n = 100$) of a Cl-doped polymer thin film (0.4 m% Cl) in different atmospheres and pressures; the scaling only applies to the red line, all other signals are shifted for display purposes.

Subsequently, the influence of the gate delay was studied at a constant pressure of 100 mbar He using the same polymer standard. Gate delay variations from 0.1 μs to 1 μs were applied while all other measurement parameters were held constant. The results are depicted in figure 7.13, clearly indicating that a shorter gate delay resulted in enhanced signal intensity.

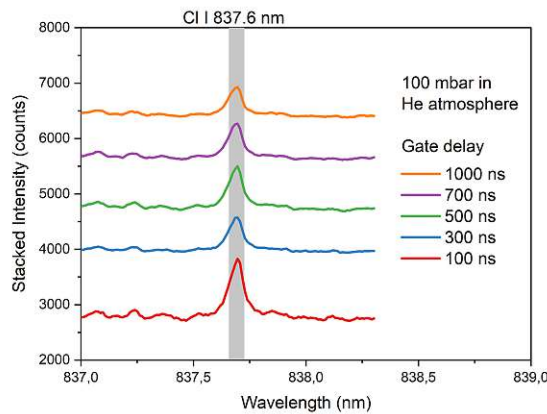


Figure 7.13: Optimization of the gate delay for Cl detection (0.4 m% Cl in polymer) in He atmosphere at 100 mbar (stacked LIBS raw spectra - scaling only applicable for the red signal, $n = 100$)

After the parameter optimization, the optimum conditions were set for all further measurement. An overview of these settings is depicted in table 7.6.

J200	
Laser wavelength	266 nm
Laser energy	7.0 mJ
Laser spotsize	100 μm
Sample fluence	7 J/cm ²
Frequency	20 Hz
He flow rate	0.2 ml/min
Pressure	100 mbar
Spectrometer	not used

SpectraPro HRS-750 with PI-MAX-4	
Slit width	200 μm
Grating	1800 g/mm
Center wavelength	836 nm
Covered wavelength range	832 - 840 nm
Gate delay	0.1 μs
Gate width	10 μs
Intensifier gain	20

Table 7.6: Optimized measurement parameter for Cl detection under reduced pressure

Employing the optimized measurement parameter from table 7.6, a calibration curve using doped polymer thin films was recorded. The Cl content within the samples ranged from 0.16 to 1.5 m% (see chapter 5.3.3) and each sample was measured using 3 parallel linescans. The raw spectra of each linescan were averaged ($n = 100$) to obtain a total of 3 values per standard.

The raw spectra of both, the highest and lowest calibration standard while measuring in atmospheric pressure as well as with reduced pressure, are displayed in figure 7.14 a) to d). The C(I) emission line at 833.5 nm was recorded as well as the Cl (I) emission line at 837.6 nm. Figures 7.14a and 7.14b show the spectra collected under atmospheric pressure. The Cl emission line was clearly visible when investigating the highest standard with a Cl content of 1.5 m%. As for the lowest calibration sample with a Cl content of 0.16 m%, the Cl line was only vaguely distinguishable from the background. In figures 7.14c and 7.14d, the same samples were measured under reduced pressure and a clear increase in signal intensity was observed. Even for the lowest standard a small Cl peak was apparent in the spectrum ranging from 833 - 841 nm, shown in the magnified image area.

As a next step, calibration curves for the same samples measured under different atmospheric conditions were recorded and are illustrated in the following figures: figure 7.15a shows the Cl signal to background ratio for atmospheric pressure while figure

7.15b shows the same trend for 100 mbar He atmosphere. The calibration curve could be recorded in both configurations, but the slope was clearly higher under reduced pressure (100 mbar He: 2.7 vs. 1013 mbar He: 0.8) although LODs calculated from the calibration curves based on the standard deviation of the response (see equation 7.1) were nearly the same (100 mbar He: 0.12 m% vs. 1013 mbar He: 0.11 m%).

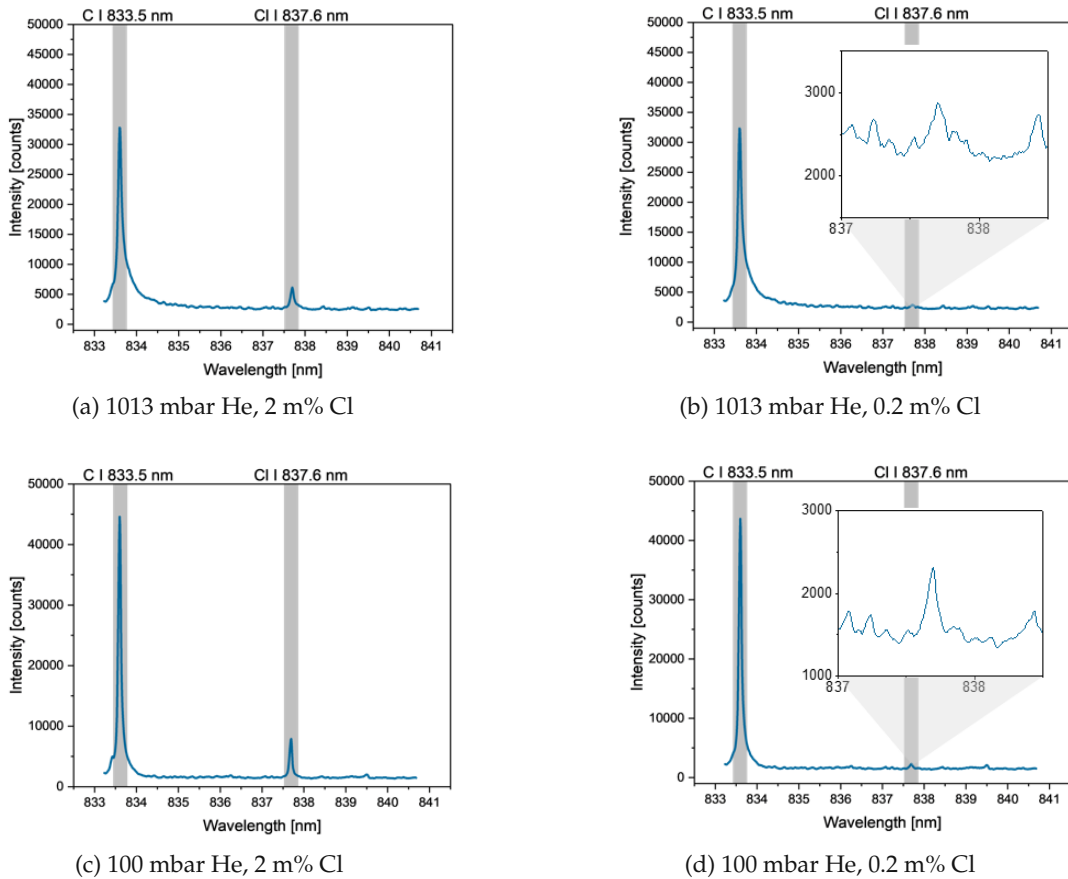


Figure 7.14: Representative LIBS spectra of Cl-doped polymer pellets in He atmosphere and different pressures

All of the results presented in this section were obtained from an average of 100 spectra. Although this is possible for bulk measurements, imaging while averaging 100 spectra with a beam diameter of 100 μm is very impracticable. Ideally, the measurement should also be possible using single spectra which was the goal for the imaging experiment presented in figure 7.16. Employing the optimized measurement conditions listed in table 7.6, a commercial polyimide film was investigated. First, the sample was exposed to a migration cell experiment. Afterwards the polymer film (sample PI2-mig-double-KCl-20230719) was cut into quarters and attached to a silicon wafer using double sided tape with the anodic side up.

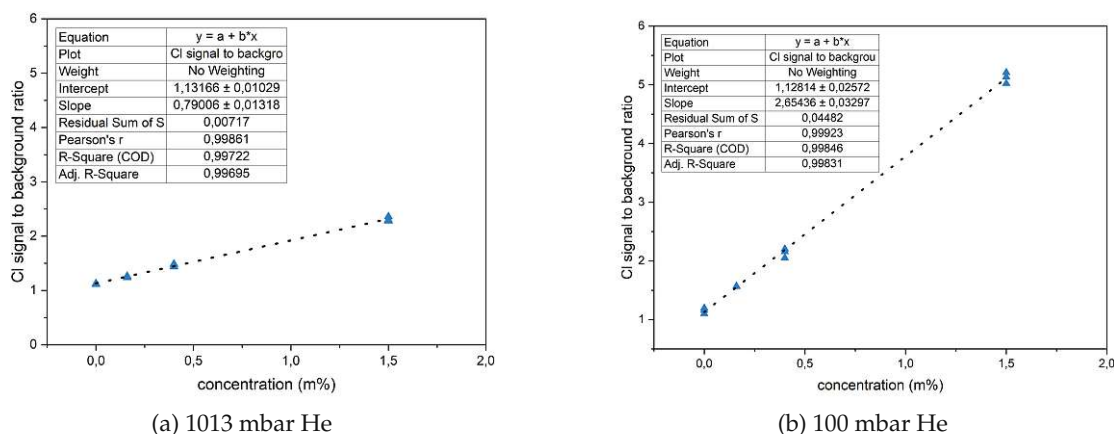
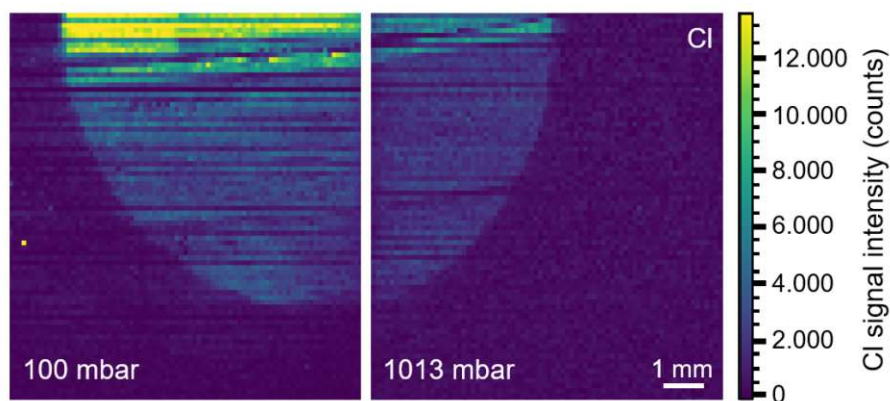


Figure 7.15: Cl (I) line signal to background ratio

Both images were recorded using consecutive linescans with no overlapping of laser shots, resulting in 100×80 pixels in the left figure and 80×80 pixels in the right picture. No spectral post-treatment was applied and solely the signal intensity in counts was evaluated. The map, representing the Cl signal intensity of the Cl(I) emission line at 837.6 nm of one quarter of the sampled film using different pressure conditions is shown in the presented figure. In both cases, the Cl uptake could be detected using a single spectra. But the image also shows, that the signal enhancement due to reduced pressure can be exploited during imaging even when single spectra are collected.

Figure 7.16: LIBS map of stressed, commercial polyimide film [75] (Cl signal height, $n = 1$, Gate delay = 300 ns)

7.3 Detection of polymer alterations

Besides the uptake and distribution of ions, the detection of structural changes after migration cell experiments was another important piece of information to understand

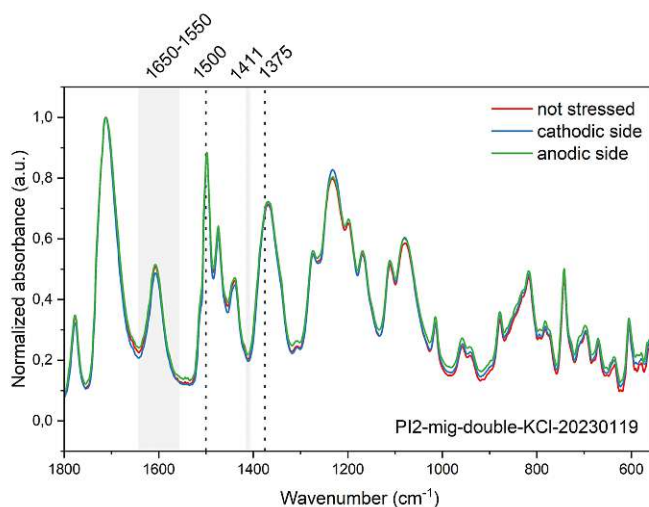
the migration behaviour of harmful substances within a polymer matrix. In this context, the detection of different degrees of imidization of model polyimides using LIBS has successfully been demonstrated within this work. Nevertheless, applied to commercial products after migration cell exposure, no changes in the LIBS emission of the C₂ molecule band and H signal could be detected, even with with different instrumental setups.

As an alternative, IR spectroscopy as a common tool to analyze the structure of polymers was applied to the stressed films. The FT-IR measurements were performed in ATR-mode, covering an area of approx. 0.5 mm². 6 scans covering the range from 550 - 4000 cm⁻¹ and a resolution of 4 cm⁻¹ were recorded per position. To compare the pristine and stressed polymer, a non-stressed area of the film at the edge of the sample was measured as reference. The stressed spectra were recorded from the middle section of the exposed area from the cathodic as well as the anodic side.

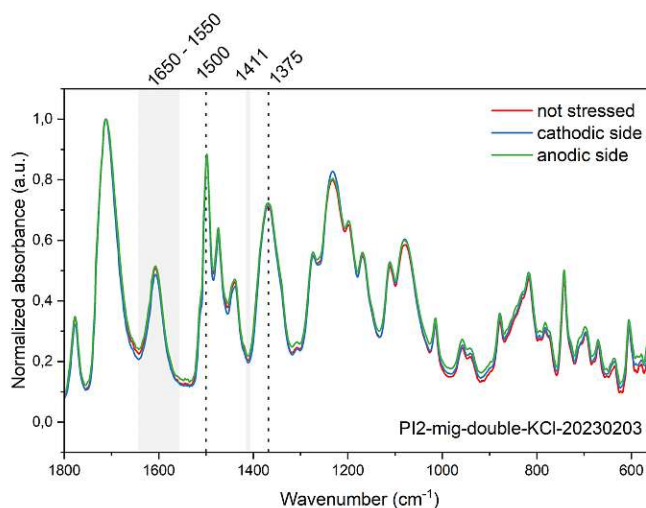
Figure 7.17 shows exemplary data from two different polyimide films. In both cases the spectra were normalized to the maximum signal height and important IR absorption bands to characterize evolution of the degree of imidization were earmarked. Besides the C=C aromatic ring stretching between 1500 - 1520 cm⁻¹ and the C-N stretch (imid II) around 1360 - 1380 cm⁻¹ useful to calculate the degree of imidization, spectral regions indicating the hydrolysis of a polyimide were included: amid I and amid II at 1652 cm⁻¹ and 1558 cm⁻¹ and the C=O stretching at 1600 cm⁻¹ (indicated as a gray area from 1650 - 1550 cm⁻¹) as well as a shoulder appearing at 1411 cm⁻¹ due to the COOH deformation [80].

For both polyimide samples, no difference between non-stressed and stressed areas or between the cathodic and anodic side could be detected, confirming the presented results from the LIBS investigations. One explanation being that simply no hydrolysis of the polyimide surface had taken place under the chosen exposure conditions. Alternatively, the hydrolysed layer was too thin to be detect with ATR-IR were the penetration depth depends on the wavenumber and was calculated to be approximately 1.3 μm at 1500 cm⁻¹.

Therefore, a more surface sensitive approach was applied and the exposed polyimide films were subjected to contact angle measurements. As the films were flushed with deionised water after the exposure cell treatment and stored in small plastic bags between lint-free cloths, they were solely cleaned with compressed air before measurement. To provide a flat measuring surface, a perforated sample holder with suction was used with the DSA 30 (detailed instrument information is provided in chapter 5.4.2).



(a) sample PI-mig-double-KCl-20230119 mounted in cell 2



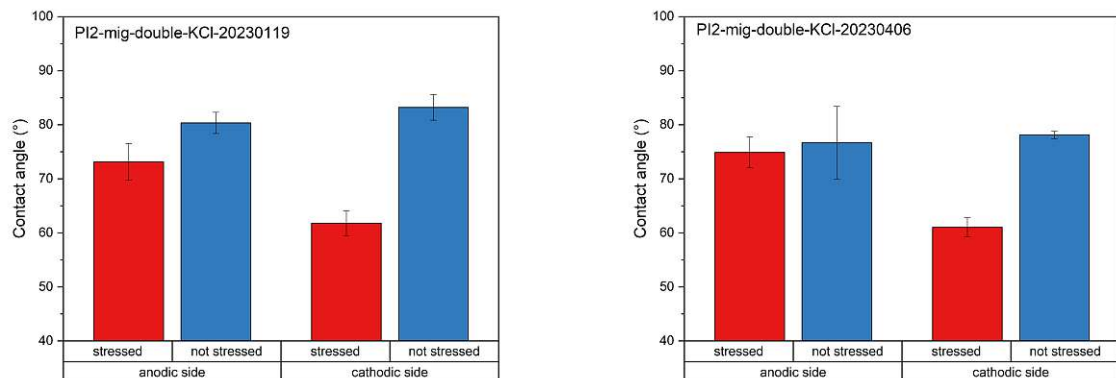
(b) sample PI-mig-double-KCl-20230203 mounted in cell 4

Figure 7.17: Comparison of IR spectra of polyimide films exposed to migration cell experiments from the anodic and cathodic side as well as from a reference point

All measurements were conducted with distilled water in 'sessile drop' mode with automatic baseline correction and the Young Laplace fitting method. A volume of 4 μm was applied per drop and a total of 3 - 5 measurements on different areas of the sample were conducted per exposure area. On each side of the polyimide film, the stressed as well as the non-stressed area was tested. Exemplary results of two polyimide films are displayed in figure 7.18. In general, the highest contact angle values were recorded from the non-stressed areas, regardless of which side was measured. For the anodic side, the results were inconclusive - in some cases lower contact angles were achieved, in other cases no decrease was observed. In contrast, a clear change could be measured on the

7 Polymer films exposed to migration cell experiments

cathodic side where the contact angles from the stressed area were smaller than on the anodic side or reference area.



(a) sample PI-mig-double-KCl-20230119 mounted in cell 2

(b) sample PI-mig-double-KCl-20230406 mounted in cell 4

Figure 7.18: Comparison of contact angle measurements on polyimide films exposed to migrations cell experiments (average of 3-5 measurements per area)

Unfortunately, the measurement of the contact angle does not provide any information about the type of change that has occurred in this area. It could be that hydrolysis has occurred on the surface and/or a low contact angle has developed due to the change in roughness [80]. However, it is also possible that the contact angle has changed due to other processes that have not yet been identified. Further, alternative investigations would therefore be necessary to resolve this issue, e.g. XPS or organic mass spectrometry.

8 Summary and Outlook

The aim of this work was to implement new analytical techniques to study the behavior of polyimides as a protective layer. Therefore, it was necessary to develop measurement methods which provide structural information about the polymer itself but also enable multi-element analysis to detect and track the uptake of harmful species within a polymer thin film.

Since LIBS is a prominent laser based technique for elemental analysis, exhibiting mapping and depth-profiling capabilities and furthermore, specific parts of a polymer LIBS spectrum can be used to obtain molecular information, it has the potential to become a viable tool for polyimide testing and failure analysis. In the course of this work, structural investigations and elemental analysis were initially considered separately and measurement procedures to track structural changes as well as harmful substances within a polyimide network were developed individually and thoroughly optimized.

First, the capabilities to track changes within the polymer structure were investigated using LIBS and the imidization reaction was chosen as an illustrative and industry-oriented example. A set of self-synthesized polyimide films was prepared and served as standards with different thermal curing parameters. It has been demonstrated that LIBS is able to monitor the imidization reaction based on the C_2 molecular band and the H atomic emission of the polymer spectrum. IR spectroscopy was used as the reference method for method development. Besides tracking the reaction, the degree of imidization was calculated as a quantitative measure. This parameter describes the percentage of imide bonds formed in the polymer during thermal or chemical curing. In IR spectroscopy, this value is calculated based on certain IR absorption bands distinctive of the imide bond. Using the IR based equation as a template, a formula based on the C_2 and H LIBS emission signals was introduced. In both equations, reference values are needed to calculate a percent value. For LIBS, a fully cured polyimide sample as well as a non-imidized polymer film were necessary for scaling the data. The degrees of imidization based on IR spectroscopy and LIBS were in quite good agreement, with deviations due to differences in ablation depth and sampling area. Additionally, both techniques are based on different principles: IR tracks bond formation based on vibrational lines providing direct information about changes in molecular structure, while LIBS is traditionally used

for elemental analysis. However, changes observed in the LIBS spectrum could be attributed to the ongoing imidization reaction, such as solvent evaporation and changes in polymer density and orientation. As a result, the degree of imidization calculated from different techniques did not provide exactly the same numerical value, but relative comparisons within a sample set based on IR as well as LIBS were possible. Method improvements using additional spectral information or by selecting alternative standards as reference values, etc. would be possible but the scope of this work was to provide the simplest formula possible for easy and practicable application.

Besides method development, the applicability and versatility of the LIBS method was tested by depth profiling and imaging applications on stacked model samples prepared from PAA solution. Imaging of different degrees of imidization was possible based on 5 accumulated spectra only with a spatial resolution of 100 μm . While depth profiling with a depth resolution of approx. 1 μm , the calculated imidization degrees corresponded well with the sample structure indicating no influence of laser-matter interaction on subsequent layers. Such investigations are not possible with conventional techniques like IR spectroscopy, demonstrating the benefits of the developed LIBS procedure.

Furthermore additive-doped polyimide films based on the self-synthesized PAA solution as well as commercially available polymers were investigated and the determination of the imidization degree using LIBS was feasible in both cases. Especially in the case of the commercial samples, where polyimide structure was unknown LIBS was able to provide a more universal approach.

As a next step, the implemented LIBS method was transferred to other instrumental setups including in-situ studies in a heating chamber as well as different laser wavelengths.

To investigate certain failure mechanisms of electronic devices, the uptake and distribution of harmful substances is equally important as changes in polymer structure. Monitoring the imidization reaction and determining the degree of imidization based on LIBS was an important step in uncovering device deterioration and possible breakdown. Subsequently the LIBS methodology was optimized and applied to quantify the Cl and K uptake in a polyimide matrix as exemplary, corrosion-inducing substances. To simulate certain environmental conditions and force electrochemical migration, commercially available polyimide films were exposed to aqueous solution containing K and Cl and voltage in a migration cell setup leading to the uptake of those elements. A particular challenge was to establish an analytical technique to investigate the prepared sample films in a fast and simple way while applying the newly developed method for determining the degree of imidization.

Based on different LIBS setups, elemental maps and depth profiles of the stressed

polymers were recorded with a spatial resolution of 100 - 150 μm and a depth resolution ranging from 800 nm - 2 μm based on laser wavelength, fluence and beam profile. The investigations revealed a uniform, lateral distribution of K and Cl throughout the exposed area of the polyimide film and a decreasing amount over the film thickness. The amount of Cl and K within the polyimide was dependent on the applied conditions during the migration cell experiment, especially the overall exposure time.

Quantification was achieved using in-house calibration standards based on doped polyimide films or pressed powder pellets and a LOD of 0.71 m% was calculated for the determination of Cl using LIBS.

Especially the investigation of halogens poses a challenge in elemental analysis due to weak transition probability in the LIBS spectral range. Therefore, optimization in terms of sensitivity were undertaken by changing the measurement atmosphere during LIBS analysis as well as implementing a suitable LA-ICP-MS measurement method. Using LA-ICP-MS, the LOD for Cl detection was decreased to 0.015 m% while increasing depth resolution to 200 nm. Unfortunately, imaging applications were not feasible due to severe problems regarding the sample transport resulting in image blurring.

Alternatively, LIBS measurements under reduced pressure were conducted using a self-built heating chamber. Thorough method optimization regarding the measurement atmosphere, pressure conditions and gate delay were conducted and a reduced He atmosphere at 100 mbar turned out to provide the best results. With decreasing pressure, the emission intensity and peak shape changed resulting in higher intensities, narrower peaks and lower background signals. Calibration curves of the same set of standard samples with a Cl content ranging from 0.16 -1.5 m% were recorded in atmospheric as well as reduced pressure. Although similar LODs were obtained (100 mbar He: 0.12 m% vs. 1013 mbar He: 0.11m%), the calibration curve slopes were significantly different and higher for measurements under reduced pressure. Also imaging applications based on single spectra were feasible with this approach.

Regarding changes in the polymer structure, no effect on the the LIBS C_2 molecular emission or H atomic line could be observed when analysing stressed polyimide films. Either depth-resolution or sensitivity being a problem or simply, no changes in structure occurred during the migration cell exposure. Therefore, alternative methods like IR spectroscopy and CA measurements were conducted on the polyimide films. No differences in the IR spectra of stressed and non-stressed polymer films were obtained, confirming the findings based on LIBS. Only CA measurements showed differences between the exposed areas but could not provide any chemical information about the type of change that had happened. Further, alternative investigations based on XPS or organic mass spectrometry would probably be necessary to solve this task.

Since the commercially available polyimides turned out to be extremely stable under the exposure conditions applied in the migration cell setup, investigations based on the self-synthesized polyimides might be helpful in uncovering structural alterations in the future. Unfortunately, the polyimides prepared in the lab were not sufficiently stable to withstand such drastic conditions (exposure up to 800 V for > 24 h) and polyimides with higher molecular weight may be necessary.

As for the analytical techniques developed, LIBS and LA-ICP-MS proved to be a useful tool for the investigation of polyimide samples facilitating information about ion migration and the imidization reaction. With regard to LIBS, the sensitivity for Cl detection could be further improved: the application of reduced pressure led to an enhancement but needs to be further investigated. Alternative approaches like double pulse LIBS or the detection of Cl in the form of molecular bands would be possible in the future.

Bibliography

- [1] “Plastics - the Facts 2022 • Plastics Europe,” <https://plasticseurope.org/knowledge-hub/plastics-the-facts-2022/>.
- [2] A. C. C. de Leon, Í. G. M. da Silva, K. D. Pangilinan, Q. Chen, E. B. Caldon, and R. C. Advincula, “High performance polymers for oil and gas applications,” *Reactive and Functional Polymers*, vol. 162, p. 104878, May 2021.
- [3] L. W. McKeen, “Polyimides,” in *Film Properties of Plastics and Elastomers (Fourth Edition)*, ser. Plastics Design Library, L. W. McKeen, Ed. William Andrew Publishing, Jan. 2017, pp. 147–185.
- [4] J. A. Kreuz and J. R. Edman, “Polyimide Films,” *Advanced Materials*, vol. 10, no. 15, pp. 1229–1232, 1998.
- [5] C. P. Constantin, M. Aflori, R. F. Damian, and R. D. Rusu, “Biocompatibility of Polyimides: A Mini-Review,” *Materials*, vol. 12, no. 19, p. 3166, Jan. 2019.
- [6] I. Gouzman, E. Grossman, R. Verker, N. Atar, A. Bolker, and N. Eliaz, “Advances in Polyimide-Based Materials for Space Applications,” *Advanced Materials*, vol. 31, no. 18, p. 1807738, 2019.
- [7] A. Sezer Hicyilmaz and A. Celik Bedeloglu, “Applications of polyimide coatings: A review,” *SN Applied Sciences*, vol. 3, no. 3, p. 363, Feb. 2021.
- [8] W. M. Edwards, “Aromatic polyimides and the process for preparing them,” US Patent US3 179 634A, Apr., 1965.
- [9] —, “Polyamide-acids, compositions thereof, and process for their preparation,” US Patent US3 179 614A, Apr., 1965.
- [10] A. L. Endrey, “Aromatic polyimide particles from polycyclic diamines,” US Patent US3 179 631A, Apr., 1965.
- [11] —, “Aromatic polyimides from meta-phenylene diamine and para-phenylene diamine,” US Patent US3 179 633A, Apr., 1965.

- [12] —, “Process for preparing polyimides by treating polyamide-acids with lower fatty monocarboxylic acid anhydrides,” US Patent US3 179 630A, Apr., 1965.
- [13] F. W. Mercer and T. D. Goodman, “Effect of Structural Features and Humidity on the Dielectric Constant of Polyimides,” *High Performance Polymers*, vol. 3, no. 4, pp. 297–310, Aug. 1991.
- [14] L. Varain, “Electrochemical investigation and modeling of ion- and water transport through polymer membranes,” Thesis, Technische Universität Wien, 2022.
- [15] L. Varain, S. Larisegger, M. Nelhiebel, and G. Fafilek, “Simultaneous measurement and ODE-modeling of ion- and water permeability through ion exchange membranes,” *Journal of Membrane Science*, vol. 684, p. 121847, Oct. 2023.
- [16] K. Liu, D. Tian, C. Li, Y. Li, G. Yang, and Y. Ding, “A review of laser-induced breakdown spectroscopy for plastic analysis,” *TrAC Trends in Analytical Chemistry*, vol. 110, pp. 327–334, Jan. 2019.
- [17] Z. Gajarska, L. Brunnbauer, H. Lohninger, and A. Limbeck, “Advanced Polymer Characterization,” in *Laser-Induced Breakdown Spectroscopy in Biological, Forensic and Materials Sciences*, 1st ed. Springer Cham, Dec. 2022, p. 313.
- [18] S. J. Mousavi, M. Hemati Farsani, S. M. R. Darbani, A. Mousaviazar, M. Soltanolkotabi, and A. Eslami Majd, “CN and C2 vibrational spectra analysis in molecular LIBS of organic materials,” *Applied Physics B*, vol. 122, no. 5, p. 106, Apr. 2016.
- [19] J. Moros and J. Laserna, “Laser-Induced Breakdown Spectroscopy (LIBS) of Organic Compounds: A Review,” *Applied Spectroscopy*, vol. 73, no. 9, pp. 945–1106, Sep. 2019.
- [20] I. Chamradová, P. Pořízka, and J. Kaiser, “Laser-Induced Breakdown Spectroscopy analysis of polymers in three different atmospheres,” *Polymer Testing*, vol. 96, p. 107079, Apr. 2021.
- [21] Z. Gajarska, L. Brunnbauer, H. Lohninger, and A. Limbeck, “Identification of 20 polymer types by means of laser-induced breakdown spectroscopy (LIBS) and chemometrics,” *Analytical and Bioanalytical Chemistry*, vol. 413, no. 26, pp. 6581–6594, Nov. 2021.
- [22] S. Grégoire, M. Boudinet, F. Pelascini, F. Surma, V. Detalle, and Y. Holl, “Laser-induced breakdown spectroscopy for polymer identification,” *Analytical and Bioanalytical Chemistry*, vol. 400, no. 10, pp. 3331–3340, Jul. 2011.

- [23] S. Grégoire, V. Motto-Ros, Q. L. Ma, W. Q. Lei, X. C. Wang, F. Pelascini, F. Surma, V. Detalle, and J. Yu, "Correlation between native bonds in a polymeric material and molecular emissions from the laser-induced plasma observed with space and time resolved imaging," *Spectrochimica Acta Part B: Atomic Spectroscopy*, vol. 74–75, pp. 31–37, Aug. 2012.
- [24] L. Brunnbauer, M. Mayr, S. Larisegger, M. Nelhiebel, L. Pagnin, R. Wiesinger, M. Schreiner, and A. Limbeck, "Combined LA-ICP-MS/LIBS: Powerful analytical tools for the investigation of polymer alteration after treatment under corrosive conditions," *Scientific Reports*, vol. 10, no. 1, p. 12513, Jul. 2020.
- [25] J. Willner, L. Brunnbauer, C. Derrick Quarles, M. Nelhiebel, S. Larisegger, and A. Limbeck, "Development of a simultaneous LA-ICP-MS & LIBS method for the investigation of polymer degradation," *Journal of Analytical Atomic Spectrometry*, vol. 38, no. 10, pp. 2028–2037, 2023.
- [26] T. Völker, G. Wilsch, I. B. Gornushkin, L. Kratochvilová, P. Pořízka, J. Kaiser, S. Millar, G. Galbács, D. J. Palásti, P. M. Janovszky, S. Eto, C. Langer, G. Kapteina, M. Illguth, J. Götz, M. Licht, M. Raupach, I. Elhamdaoui, M. Sabsabi, P. Bouchard, L. Nagli, M. Gaft, Y. Raichlin, L. J. Fernández-Menéndez, C. Méndez-López, N. Bordel, C. Gottlieb, C. Bohling, R. Finotello, D. L'Hermite, C. Quéré, and M. B. Lierenfeld, "Interlaboratory comparison for quantitative chlorine analysis in cement pastes with laser induced breakdown spectroscopy," *Spectrochimica Acta Part B: Atomic Spectroscopy*, vol. 202, p. 106632, Apr. 2023.
- [27] T. Dietz, J. Klose, P. Kohns, and G. Ankerhold, "Quantitative determination of chlorides by molecular laser-induced breakdown spectroscopy," *Spectrochimica Acta Part B: Atomic Spectroscopy*, vol. 152, pp. 59–67, Feb. 2019.
- [28] L. J. Fernández-Menéndez, C. Méndez-López, C. González-Gago, J. Pisonero, and N. Bordel, "Improving Cl determination in cements by molecular LIBS using noble gas-enriched atmospheres and new approaches for interference removal," *Journal of Analytical Atomic Spectrometry*, vol. 38, no. 2, pp. 325–332, Feb. 2023.
- [29] C. E. Sroog, "Polyimides," *Progress in Polymer Science*, vol. 16, no. 4, pp. 561–694, Aug. 1991.
- [30] M. T. Bogert and R. R. Renshaw, "4-Amino-o-phthalic acid and some of its derivatives," *Journal of the American Chemical Society*, vol. 30, no. 7, pp. 1135–1144, Jul. 1908.
- [31] J. Li, W. Zhao, C. Zhao, T. Qi, P. Ma, D. Ning, C. Yang, and W. Li, "A comparison

- study of high thermal stable and resistant polyimides," *AIP Advances*, vol. 12, no. 9, p. 095301, Sep. 2022.
- [32] P. Ma, C. Dai, H. Wang, Z. Li, H. Liu, W. Li, and C. Yang, "A review on high temperature resistant polyimide films: Heterocyclic structures and nanocomposites," *Composites Communications*, vol. 16, pp. 84–93, Dec. 2019.
- [33] J. A. Cella, "Degradation and stability of polyimides," *Polymer Degradation and Stability*, vol. 36, no. 2, pp. 99–110, Jan. 1992.
- [34] Yu. N. Sazanov, L. A. Shibaev, and T. A. Antonova, "Comparative thermal analysis (CTA) of thermally-stable polymers and model compounds. Polyimides and model compounds," *Journal of thermal analysis*, vol. 18, no. 1, pp. 65–75, Feb. 1980.
- [35] M. M. Koton and Yu. N. Sazanov, "Thermal degradation of polypyromellitimides," *Polymer Science U.S.S.R.*, vol. 15, no. 7, pp. 1857–1863, Jan. 1973.
- [36] R. A. Dine-Hart and W. W. Wright, "Effect of structural variations on the thermo-oxidative stability of aromatic polyimides," *Die Makromolekulare Chemie*, vol. 153, no. 1, pp. 237–254, 1972.
- [37] B. Alston and R. Gratz, "3F Condensation Polyimides Review and Update," NASA, Maui, Hawaii, Technical Memorandum 102353, Dec. 1989.
- [38] C. Zeng, J. Li, T. Chen, J. Chen, and C. Chen, "Dynamic sorption and transport of water vapor in dense polyimide membranes," *Journal of Applied Polymer Science*, vol. 102, no. 3, pp. 2189–2198, 2006.
- [39] J. Melcher, Y. Deben, and G. Arlt, "Dielectric effects of moisture in polyimide," *IEEE Transactions on Electrical Insulation*, vol. 24, no. 1, pp. 31–38, Feb. 1989.
- [40] J. Seo and H. Han, "Water sorption behaviour of polyimide thin films with various internal linkages in the dianhydride component," *Polymer Degradation and Stability*, vol. 77, no. 3, pp. 477–482, Jan. 2002.
- [41] F. W. Harris, "Synthesis of aromatic polyimides from dianhydrides and diamines," in *Polyimides*, D. Wilson, H. D. Stenzenberger, and P. M. Hergenrother, Eds. Dordrecht: Springer Netherlands, 1990, pp. 1–37.
- [42] H.-T. Kim and J.-K. Park, "Effect of Imidization Temperature and Spinning Condition on Structure of Polyimide Film Derived from Cyclobutanedianhydride and 2,2-Bis(4-aminophenoxyphenyl)propane," *Polymer Journal*, vol. 29, no. 12, pp. 1002–1006, Dec. 1997.

- [43] R. Li, Z. Lu, Y. Liu, K. Zeng, J. Hu, and G. Yang, "The retarding effects and structural evolution of a bio-based high-performance polyimide during thermal imidization," *Journal of Applied Polymer Science*, vol. 136, no. 3, p. 46953, Jan. 2019.
- [44] T. Miwa, Y. Okabe, and M. Ishida, "Effects of precursor structure and imidization process on thermal expansion coefficient of polyimide (BPDA/PDA)," *Polymer*, vol. 38, no. 19, pp. 4945–4949, Jan. 1997.
- [45] T. Nishino, M. Kotera, N. Inayoshi, N. Miki, and K. Nakamae, "Residual stress and microstructures of aromatic polyimide with different imidization processes," *Polymer*, vol. 41, no. 18, pp. 6913–6918, Aug. 2000.
- [46] N. C. Stoffel, E. J. Kramer, W. Volksen, and T. P. Russell, "Solvent and isomer effects on the imidization of pyromellitic dianhydride-oxydianiline-based poly(amic ethyl ester)s," *Polymer*, vol. 34, no. 21, pp. 4524–4530, Nov. 1993.
- [47] S. Diahm, M. L. Locatelli, T. Lebey, and D. Malec, "Thermal imidization optimization of polyimide thin films using Fourier transform infrared spectroscopy and electrical measurements," *Thin Solid Films*, vol. 519, no. 6, pp. 1851–1856, Jan. 2011.
- [48] C. A. Pryde, "IR studies of polyimides. I. Effects of chemical and physical changes during cure," *Journal of Polymer Science Part A: Polymer Chemistry*, vol. 27, no. 2, pp. 711–724, 1989.
- [49] W. Chen, W. Chen, B. Zhang, S. Yang, and C.-Y. Liu, "Thermal imidization process of polyimide film: Interplay between solvent evaporation and imidization," *Polymer*, vol. 109, pp. 205–215, Jan. 2017.
- [50] M. Kotera, T. Nishino, and K. Nakamae, "Imidization processes of aromatic polyimide by temperature modulated DSC," *Polymer*, vol. 41, no. 10, pp. 3615–3619, May 2000.
- [51] D. E. Herr, N. A. Nikolic, and R. A. Schultz, "Chemistries for High Reliability in Electronics Assemblies," *High Performance Polymers*, vol. 13, no. 3, pp. 79–100, Sep. 2001.
- [52] S. Krumbein, "Metallic electromigration phenomena," *IEEE Transactions on Components, Hybrids, and Manufacturing Technology*, vol. 11, no. 1, pp. 5–15, Mar. 1988.
- [53] R. Ambat, "A review of Corrosion and environmental effects on electronics," 2006.
- [54] R. E. Russo, "Laser ablation research and development: 60 years strong," *Applied Physics A*, vol. 129, no. 3, p. 168, Feb. 2023.

- [55] G. Galbács, "A critical review of recent progress in analytical laser-induced breakdown spectroscopy," *Analytical and Bioanalytical Chemistry*, vol. 407, no. 25, pp. 7537–7562, Oct. 2015.
- [56] J. Koch and D. Günther, "Review of the state-of-the-art of laser ablation inductively coupled plasma mass spectrometry," *Applied Spectroscopy*, vol. 65, no. 5, pp. 155–162, May 2011.
- [57] S. Musazzi and U. Perini, *Laser-Induced Breakdown Spectroscopy Theory and Applications*, 1st ed., ser. Springer Series in Optical Sciences. Heidelberg: Springer Berlin, 2014, vol. 182.
- [58] L. Brunnbauer, Z. Gajarska, H. Lohninger, and A. Limbeck, "A critical review of recent trends in sample classification using Laser-Induced Breakdown Spectroscopy (LIBS)," *TrAC Trends in Analytical Chemistry*, vol. 159, p. 116859, Feb. 2023.
- [59] G. Galbács, Ed., *Laser-Induced Breakdown Spectroscopy in Biological, Forensic and Materials Sciences*. Cham: Springer International Publishing, 2022.
- [60] D. W. Hahn and N. Omenetto, "Laser-Induced Breakdown Spectroscopy (LIBS), Part II: Review of Instrumental and Methodological Approaches to Material Analysis and Applications to Different Fields," *Applied Spectroscopy*, vol. 66, no. 4, pp. 347–419, Apr. 2012.
- [61] L. Brunnbauer, V. Zeller, Z. Gajarska, S. Larisegger, S. Schwab, H. Lohninger, and A. Limbeck, "Classification of epoxy molding compounds by Tandem LA-ICP-MS/LIBS to enhance the reliability of electronic devices," *Spectrochimica Acta Part B: Atomic Spectroscopy*, vol. 207, p. 106739, Sep. 2023.
- [62] L. Brunnbauer, S. Larisegger, H. Lohninger, M. Nelhiebel, and A. Limbeck, "Spatially resolved polymer classification using laser induced breakdown spectroscopy (LIBS) and multivariate statistics," *Talanta*, vol. 209, p. 120572, Mar. 2020.
- [63] L. Pagnin, L. Brunnbauer, R. Wiesinger, A. Limbeck, and M. Schreiner, "Multivariate analysis and laser-induced breakdown spectroscopy (LIBS): A new approach for the spatially resolved classification of modern art materials," *Analytical and Bioanalytical Chemistry*, vol. 412, no. 13, pp. 3187–3198, May 2020.
- [64] L. St-Onge, R. Sing, S. Béchar, and M. Sabsabi, "Carbon emissions following 1.064 Mm laser ablation of graphite and organic samples in ambient air," *Applied Physics A*, vol. 69, no. 1, pp. S913–S916, Dec. 1999.

- [65] J. Guezenoc, A. Gallet-Budynek, and B. Bousquet, "Critical review and advices on spectral-based normalization methods for LIBS quantitative analysis," *Spectrochimica Acta Part B: Atomic Spectroscopy*, vol. 160, p. 105688, Oct. 2019.
- [66] P. Pořízka, J. Klus, A. Hrdlička, J. Vrábek, P. Škarková, D. Prochazka, J. Novotný, K. Novotný, and J. Kaiser, "Impact of Laser-Induced Breakdown Spectroscopy data normalization on multivariate classification accuracy," *Journal of Analytical Atomic Spectrometry*, vol. 32, no. 2, pp. 277–288, Feb. 2017.
- [67] P. Pořízka, J. Klus, E. Képeš, D. Prochazka, D. W. Hahn, and J. Kaiser, "On the utilization of principal component analysis in laser-induced breakdown spectroscopy data analysis, a review," *Spectrochimica Acta Part B: Atomic Spectroscopy*, vol. 148, pp. 65–82, Oct. 2018.
- [68] R. Thomas, *Practical Guide to ICP-MS: A Tutorial for Beginners, Third Edition*, 3rd ed. Boca Raton: CRC Press, May 2013.
- [69] D. Günther and B. Hattendorf, "Solid sample analysis using laser ablation inductively coupled plasma mass spectrometry," *TrAC Trends in Analytical Chemistry*, vol. 24, no. 3, pp. 255–265, Mar. 2005.
- [70] R. E. Russo, X. Mao, H. Liu, J. Gonzalez, and S. S. Mao, "Laser ablation in analytical chemistry—a review," *Talanta*, vol. 57, no. 3, pp. 425–451, May 2002.
- [71] B. Hattendorf and D. Günther, "Laser Ablation Inductively Coupled Plasma Mass Spectrometry (LA-ICPMS)," in *Handbook of Spectroscopy*. John Wiley & Sons, Ltd, 2014, ch. 17, pp. 647–698.
- [72] D. Günther, I. Horn, and B. Hattendorf, "Recent trends and developments in laser ablation-ICP-mass spectrometry," *Fresenius' Journal of Analytical Chemistry*, vol. 368, no. 1, pp. 4–14, Aug. 2000.
- [73] W. Volksen and P. M. Cotts, "The Synthesis of Polyamic-Acids with Controlled Molecular Weights," in *Polyimides: Synthesis, Characterization, and Applications. Volume 1*, K. L. Mittal, Ed. Boston, MA: Springer US, 1984, pp. 163–170.
- [74] N. L. Dygert, "Model polyimide films: Synthesis, characterization and deposition by resonant infrared laser ablation," Ph.D. dissertation, Vanderbilt University, Nashville, 2008.
- [75] DuPont de Nemours, Inc., "DuPont™ Kapton® HN Data Sheet."

- [76] M. McAlees, "Raw material challenges and new technology innovations in pressure sensitive tape," DuPont, Tech. Rep., May 2012.
- [77] C. Paton, J. Hellstrom, B. Paul, J. Woodhead, and J. Hergt, "Iolite: Freeware for the visualisation and processing of mass spectrometric data," *Journal of Analytical Atomic Spectrometry*, vol. 26, no. 12, pp. 2508–2518, Dec. 2011.
- [78] B. Achleitner, L. Girault, S. Larisegger, M. Nelhiebel, P. Knaack, and A. Limbeck, "LIBS as a novel tool for the determination of the imidization degree of polyimides," *Analytical and Bioanalytical Chemistry*, vol. 416, no. 7, pp. 1623–1633, Mar. 2024.
- [79] AtomTrace a.s., "Elements Database| AtomTrace," <https://www.atomtrace.com/elements-database/>.
- [80] J. Barrera Calderón, "Oberflächenmodifizierung und -analytik von Polyimid," Ph.D. dissertation, Rheinisch-Westfälische Technischen Hochschule Aachen, Karlsruhe, Jun. 2005.

Curriculum Vitae

 Birgit Achleitner
 birgit.achleitner@tuwien.ac.at
 +43 1 58801 15142



Education

- 03/2021 - recent **Doctoral thesis**
TU Wien
- Research area: Laser based material analysis to characterize ion mobility and structural changes within polyimides
 - Awards: 'Best Oral Communication by a Young Researcher' at Colloquium Spectroscopicum Internationale XLII, Gijon 2022
 - Teaching: Environmental and process analytics (lab course, 2023W)
- 11/2013 – 12/2015 **Master's program in Technical Chemistry**
TU Wien
- Focus area: Sustainable technologies and environmental engineering
 - Master thesis: '*Development of a LA-ICP-MS procedure for the spatially resolved analysis of fly ash particles*'
 - Other: Participation in TUtheTOP 2014/2015
- 10/2009 – 10/2013 **Bachelor's degree in Technical Chemistry**
TU Wien
- Bachelor thesis: '*Makrozellulare mullitbasierte Keramiken aus präkeramischen Polymeren*'
- 09/2002 – 06/2007 **A-levels**
Höhere Technische Lehranstalt Braunau / Inn
- Focus on computer science and electronics

Employment

03/2021 - recent

Project assistant

TU Wien

- Research area: Laser based material analysis to characterize ion mobility and structural changes within polyimides
- Preparation of project applications
- Coordination with external project partners
- Active participation in FemChem and group management

03/2016 – 04/2021

Chemist in R & D

Smart Minerals GmbH, 1030 Wien

- Research area: Cement chemistry and analysis, corrosion of steel in concrete
- Preparation of project applications (FFG, ACR) and cost plans
- Dissemination of project results (presentations and publications) and exchange with company partners
- Establishment of the 'Inorganic Trace Analysis' division and accreditation in accordance with EN ISO 17294-2

10/2007 – 09/2009

Software development

cts GmbH, D-84508 Burgkirchen

- Programming and commissioning of process control systems
- On-site customer support

Further education

- Summer school: **LEADable: Leadership and management skills for researchers**, Ludwig Boltzmann Gesellschaft, 2023
- Uvex academy: **Laser safety officer for technical applications**, 2022
- EdX Online Course: **'Cement Chemistry and Sustainable Cementitious Materials'**, EPFL, 2020
- Rilem – PhD Course: **'Corrosion Science and Corrosion Control for Infrastructure'**, TU Delft – Microlab, 2019

Other skills

Languages German (native), English very good in writing and speech (C2), Spanisch basics (A1)
IT MS-Office, OriginPro, basic programming skills in Python, WordPress

Dissemination

Peer-reviewed articles

Birgit Achleitner, Laurie Girault, Silvia Larisegger, Michael Nelhiebel, Patrick Knaack, and Andreas Limbeck. LIBS as a novel tool for the determination of the imidization degree of polyimides. *Analytical and Bioanalytical Chemistry*, 416(7):1623–1633, February 2024. [doi:10.1007/s00216-024-05163-6](https://doi.org/10.1007/s00216-024-05163-6)

Awards

Best Oral Communication by Young Researchers, Colloquium Spectroscopicum Internationale XLII (CSI XLII), Gijon, Spain, June 2022.

Conference contributions

Oral presentations

Three talks were actively presented as the first author at conferences and contributions to the presented work was given to one additional talk. The presenting author is underlined in the following listing.

Birgit Achleitner, Silvia Larisegger, Michael Nelhiebel, Patrick Knaack, and Andreas Limbeck. Investigation of high-performance polymer degradation using laser induced breakdown spectroscopy (LIBS). In Colloquium Spectroscopicum Internationale XLII (CSI XLII), Gijon, Spain, June 2022.

Birgit Achleitner, Silvia Larisegger, Michael Nelhiebel, Patrick Knaack, and Andreas Limbeck. Investigation of the imidization degree of polyimides using laser induced breakdown spectroscopy (LIBS). In European Workshop on Laser Ablation (EWLA 2022), Bern, Switzerland, July 2022.

Birgit Achleitner, Jakob Willner, Maximilian Podsednik, Silvia Larisegger, Michael Nelhiesel, Tobias Huber, Patrick Knaack, and Andreas Limbeck. In-situ LIBS study of temperature induced processes in material analysis. In 12th Euro-Mediterranean Symposium on Laser-induced Breakdown Spectroscopy (EMSLIBS), Porto, Portugal, September 2023.

Maximilian Podsednik, Birgit Achleitner, Jakob Willner, Ahmed Bahr, Helmut Riedl, Paul Mayrhofer, Tobias Huber, Silvia Larisegger, Michael Nelhiesel, and Andreas Limbeck. Application of an in-situ LIBS heating stage for material characterization. In 2024 Winter Conference on Plasma Spectrochemistry (WCPS), Tucson, Arizona, January 2024.

Poster presentations

Eight posters were presented as first author at conferences and contributions were given to additional three posters. The presenting author of each work is underlined in the following listing.

Birgit Achleitner, Lars Varain, Michael Nelhiesel, Günter Fafilek, Silvia Larisegger, and Andreas Limbeck. Determination of ion diffusion in polyimides using LA-ICP-MS. In European Workshop on Laser Ablation (EWLA 2022), Bern, Switzerland, July 2022.

Birgit Achleitner, Silvia Larisegger, Michael Nelhiesel, Patrick Knaack, and Andreas Limbeck. Realisation of a LIBS method to determine the degree of imidization of polyimides. In European Symposium on Analytical Spectrometry, Brno, Czech Republic, September 2022.

Birgit Achleitner, Aida Fazlic, Davide Ret, and Andreas Limbeck. Determination of K and N within functionalized polystyrene beads for glycan purification. In European Symposium on Analytical Spectrometry, Brno, Czech Republic, September 2022.

Maximilian Podsednik, Birgit Achleitner, Jakob Willner, Silvia Larisegger, Michael Nelhiesel, Tobias Huber, and Andreas Limbeck. Time-resolved investigation of copper scaling at different temperatures by in-situ LIBS measurements. In European Winter Conference on Plasma Spectrochemistry (EWCPs), Ljubljana, Slovenia, January 2023.

Jakob Willner, Maximilian Podsednik, Birgit Achleitner, Tobias Huber, Michael Nelhiesel, Silvia Larisegger, and Andreas Limbeck. Implementation of a new heating stage for in-situ LIBS analysis of temperature induced processes. In European Winter Confer-

ence on Plasma Spectrochemistry (EWCPs), Ljubljana, Slovenia, January 2023.

Birgit Achleitner, Lars Varain, Michael Nelhiebel, Guenter Fafilek, Silvia Larisegger, and Andreas Limbeck. A 3D approach to visualize ion diffusion in polymers using LA-ICP-MS and LIBS. In European Winter Conference on Plasma Spectrochemistry (EWCPs), Ljubljana, Slovenia, January 2023.

Birgit Achleitner, Maximilian Podsednik, Jakob Willner, Silvia Larisegger, Michael Nelhiebel, Tobias Huber, Patrick Knaack, and Andreas Limbeck. In-situ study of temperature related changes in polymers using LIBS. In European Winter Conference on Plasma Spectrochemistry (EWCPs), Ljubljana, Slovenia, January 2023.

Birgit Achleitner, Maximilian Podsednik, Jakob Willner, Silvia Larisegger, Michael Nelhiebel, Tobias Huber, Patrick Knaack, and Andreas Limbeck. In-situ investigation of the thermal behaviour of polymers using laser induced breakdown spectroscopy. In ANAKON, Vienna, Austria, April 2023.

Maximilian Podsednik, Birgit Achleitner, Jakob Willner, Silvia Larisegger, Michael Nelhiebel, Tobias Huber, and Andreas Limbeck. Time-resolved analysis of copper scaling by in-situ LIBS measurements at elevated temperatures in different oxygen partial pressures. In ANAKON, Vienna, Austria, April 2023.

Birgit Achleitner, Lars Varain, Michael Nelhiebel, Günter Fafilek, Silvia Larisegger, and Andreas Limbeck. Determination of chlorine migration in polymers using LIBS. In 12th Euro-Mediterranean Symposium on Laser-induced Breakdown Spectroscopy (EM-SLIBS), Porto, Portugal, September 2023.

Birgit Achleitner, David Ken Gibbs, Silvia Larisegger, Michael Nelhiebel, and Andreas Limbeck. Employing reduced pressure to analyze challenging elements in LIBS. In 2024 Winter Conference on Plasma Spectrochemistry (WCPS), Tucson, Arizona, January 2024.